8-8-2013 12:00 AM

Amine Functionalization of Bacterial Cellulose for Targeted Delivery Applications

Justin Cook
The University of Western Ontario

Supervisor
Dr. Wankei Wan
The University of Western Ontario

Graduate Program in Biomedical Engineering
A thesis submitted in partial fulfillment of the requirements for the degree in Master of Engineering Science

AMINE FUNCTIONALIZATION OF BACTERIAL CELLULOSE FOR TARGETED DELIVERY APPLICATIONS

(Thesis format: Monograph)

by

Justin R. Cook

Graduate Program in Biomedical Engineering

A thesis submitted in partial fulfillment
of the requirements for the degree of
Master of Engineering Science

School of Graduate and Postdoctoral Studies
The University of Western Ontario
London, Ontario, Canada

Abstract

Bacterial cellulose (BC), produced by acetic acid bacteria *Gluconacetobacter xylinus*, is ideal for delivery and related biomedical functions. It is FDA approved for wound dressings and internal applications, non-toxic to endothelial cells and has little effect on blood profiles. Conjugation of therapeutics to BC can be accomplished through the available alcohol groups of the anhydroglucose units (AGU), making targeted delivery possible. Amine was introduced to BC through a reaction involving epichlorohydrin and ammonium hydroxide. The chemical structure was analyzed using infrared spectroscopy and quantified through pH titration. Conjugation of amine to BC was demonstrated through fluorescein-5'-isothiocyanate (FITC) and bromocresol green (BCG) attachment. Due the its large molecular size, the protein horseradish peroxidise (HRP) was conjugated to aminated-BC through a bis(sulfosuccinimidyl)suberate (BS3) linker to reduce steric congestion on the BC surface. Hydrogen peroxide was used to hydrolyze BC to create nanocrystalline cellulose (NCC-BC) with dimensions capable of intracellular delivery. Amine was introduced to NCC-BC and the chemical structure was analyzed using infrared spectroscopy and quantified through pH titration. HRP was optimized to demonstrate protein attachment, while avidin-HRP was used to demonstrate the ability of maximizing protein loading. An avidin-biotin glucose oxidase and avidin-biotin β-galactosidase complex was conjugated to aminated NCC-BC to demonstrate the application of a drug carrier of therapeutic proteins.

Keywords: bacterial cellulose, aminated bacterial cellulose, nano-crystalline cellulose, protein conjugation, avidin-biotin complex, horseradish peroxidase, glucose oxidase, β-galactosidase, intracellular delivery, targeted delivery

Acknowledgments

I would like to express my genuine gratitude to my supervisor Dr. Wankei Wan for his support and intellectual guidance throughout my duration in his lab. His passion for research has allowed me to pursue my research interest, while exploring various ongoing projects. The diversity of his research made my learning experience more valuable and enjoyable, while developing the diversified knowledge needed to excel in a multidisciplinary field. His leadership and ambitious qualities provided me with the drive necessary to dominate any task I faced. The opportunity to attend and present at various conferences, as well as preparing and finishing manuscripts gave me the invaluable technical and communication skills needed to be superior in future endeavors.

Furthermore, I would like to thank all my colleagues in Dr. Wan's lab for their help and guidance in the completion of this work, not to mention the invaluable friendships developed along the way. Their technical and influential guidance in their area of expertise made me more knowledgeable in many components diverging from this work. I would like to send special thanks to Darcy Small and Marko Spaic for their valuable intellectual guidance and support throughout the many challenging times experienced during the completion of this work. Their critique and insightful guidance provided me with the knowledge needed to complete tasks with the highest precision and detail needed. Likewise, I would like to thank Roddick Shi for his contribution to some aspects of this work.

Finally, I would like to thank The University of Western Ontario, especially the Biomedical Engineering Graduate Program, for making this possible. Likewise, funding provided by the CIHR cardiovascular scholarship was greatly appreciated.

Table of Contents

List of Tables

List of Figures

List of Abbreviations

Name	Abbreviation
2,2,6,6-tetramethylpiperidine-1-oxyl	TEMPO
agitated bacterial cellulose culture	A-BC
alcohol/hydroxyl group	OH
anhydro-glucose unit	AGU
bacterial cellulose	BC
bis(sulfosuccinimidyl)suberate	BS3
bromocresol green	BCG
carbon-13 nuclear magnetic resonance	^{13}C-NMR
carcinoembryotic antigen	CEA
cellulose synthesis	CS
cetyl trimethylammonium bromide	CTAB
chlorocholine chloride-based solvent	ClChCl; ClCH2CH2N(Me)3Cl
degree of polymerization	DP
dry weight	D_w
dry weight percent	D_w %
epoxypropyltrimethylammonium chloride	EPTMAC
fluorescein-5'-isothiocyanate	FITC
fructokinase	FK
fructose-1-6-biophosphate phosphate	FBP
fructose-1-phosphate kinase	1-PFK
fructose-1,6-bi-phosphate	Fru-bi-P
fructose-6-P	Fru-6-P
Gluconacetobacter xylinus	*G. xylinus*
glucose-1-phosphate	Glc-α-1-P
glucose-6-phosphate	Glc-6-P
glucose-6-phosphate	Glc-6-P
glucose-6-phosphate dehydrogenase	G6PDH
horseradish peroxidase	HRP
human endothelial kidney	HEK
hydrobromic acid	HBr
hydrochloric acid	HCl
hydrogen peroxide	H_2O_2
nanocrystalline derived bacterial cellulose	NCC-BC
nanocrystalline cellulose	NCC

phosphoglucoisomerase	PGI
phosphoglucomutase	PGM
phosphoglucomutase	PMG
phosphogluconic acid	PGA
phosphoric acid	H_2PO_4
plant cellulose	PC
polyallylamine hydrochloride	PAH
polydiallydimethylammonium chloride	PDAD-MAC
polyethylenimine	PEI
polyvinyl alcohol	PVA
pyrophosphorylase	UGP
rhodamine B isothiocyanate	RBITC
sodium bromide	NaBr
sodium hydroxide	NaOH
sodium hypochlorite	NaClO
sodium phosphate dibasic	Na_2HPO_4
sodium phosphate monobasic	NaH_2PO_4
static bacterial cellulose culture	S-BC
sulfuric acid	H_2SO_4
system of phosphotransferases	PTS
terminal complex	TC
transmission electron microscopy	TEM
ultraviolet - visible spectroscopy	UV-Vis Spectroscopy
uridine diphospho-glucose	UDPGlc
uridine diphospho-glucose	UDPGlc
water retention value	WRV
wet weight	W_w
x-ray diffraction	XRD
zeta-potential	ζ - potential

CHAPTER 1 – INTRODUCTION

1.1 Overview

Bacterial cellulose (BC) is a biocompatible polymer, which can be used as a starting material for many biomedical applications. These applications include wound healing systems, biomimetic scaffolds, and drug delivery devices. BC is a biopolymer most efficiently produced in nanofibre form from the gram-negative, acetic acid bacteria *Gluconacetobacter xylinus*. It is ideal for delivery and related biomedical functions as it has been FDA approved for wound dressings and internal applications, as well as displaying non-toxic effects to endothelial cells and has little effect on blood profiles. The conjugation of therapeutic molecules to BC can be accomplished through the available surface alcohol groups (-OH) of the anhydroglucose units (AGU). However, in order to maximize surface area, control fibre aspect ratio and loading efficiency, nanocrystalline cellulose prepared by the hydrolysis of BC (NCC-BC) will generate fibre dimensions much smaller than that of native BC fibres. The hydrolysis of cellulose results in the removal of the amorphous regions, leaving highly ordered, nano-sized crystalline regions behind. Not only is NCC-BC beneficial for loading efficiency, due to its nano-sized dimensions (~150 nm in length, ~15 nm in diameter), cellular delivery of therapeutics can be achieved. Anionic chemical functionalization of cellulose has been investigated through the highly selective oxidation reaction involving 2,2,6,6-tetramethylpiperidine-1-oxyl (TEMPO) by converting the primary alcohol on the C_6 carbon to carboxylic acid. Studies have utilized this carboxylation reaction to functionalize the oxidized surface with cationic drugs to form ionic complexes. However, for this thesis the hydrolysis of BC with hydrogen peroxide (H_2O_2) will be used to create NCC-BC with narrow size distribution, to which amine functionalization of the NCC-BC surface will be achieved through a two-step reaction involving epichlorohydrin and ammonium hydroxide. The amine functionalization of BC can give rise to many pathways to which therapeutic drugs can be attached to this delivery system, including the use of an avidin-biotin complex.

The first section of this thesis will describe the preparation and characterization of aminated BC. This product will be functionalized with the fluorescent tag fluorescein-5'-isothiocyanate (FITC) and a pH indicator that changes colour as a function of pH,

bromocresol green (BCG). Subsequently, horseradish peroxidase (HRP) will be used to demonstrate protein conjugation and the versatility of using the aminated functionalized product for delivery applications.

The second portion of this work will outline the procedure used to create nano-sized, highly crystalline bacterial cellulose fibres for the intended use of intracellular delivery. The resulting NCC-BC fibre will be functionalized to create primary amines, to which HRP and avidin-HRP will be directly linked using the available N-terminal amino acid groups. Biotinylated glucose oxidase and biotinylated β-galactosidase will be complexed to avidin NCC-BC for the demonstration of protein conjugation through an avidin-biotin complex.

This thesis outlines the importance of developing a targeted therapeutics delivery system capable of targeting and treating the cells responsible for disease with the highest drug concentration possible while limiting the side effects and relative drug concentration in the surrounding tissue. It is known that only a small dose of therapeutic drug reaches the diseased area due to the non-selectivity of the delivery method. Therefore, it is assumed that the avidin-biotin complex can provide the system with the selectivity it needs to target and treat the diseased area at the site.

1.2 Objectives of Thesis

1. To functionalize the surface alcohol groups of BC and NCC-BC with amine and to determine the chemical and physical properties of the product.

2. To covalently attach and quantify the loading of a fluorescent tag (FITC), a pH indicator (BCG) and a model protein (HRP) to aminated BC for drug delivery applications.

3. To complex aminated NCC-BC with a model protein (HRP) and an avidin-biotin complex to quantify loading and demonstrate the efficiency of an avidin-biotin complex on the aminated NCC-BC surface.

CHAPTER 2 – LITERATURE REVIEW

2.1 Bacterial Cellulose (BC)

Due to its availability, sustainability and renewability, researchers are putting significant effort in utilizing cellulose for various applications. Cellulose provides many advantages including: low cost, low density, high specific strength and modulus, and reactive functional groups capable of surface modification. These advantages make it an attractive polymer for both industrial and biomedical applications.[1] To date, studies are being conducted in creating films (barrier, antimicrobial, transparent), reinforcement fillers for existing polymers, biomedical implants, fibres and textiles, and drug delivery applications from various sources of cellulose.[2] Cellulose has mechanical properties in the range of many reinforcement materials and its physical properties are ideal for biomedical applications. The following sections will outline the importance of the cellulose structure, production method, physical and mechanical properties, along with its current uses within the biomedical field.

2.1.1 Molecular and Supramolecular Structure of Cellulose

Cellulose is the most abundant natural polymer known to date.[3] The structure of cellulose is what provides it with its hydrophilicity, structure forming potential, chirality and biocompatibility.[4] Many source materials contain or produce cellulose, which include wood, plants (cotton, ramie, flax, wheat straw), tunicate, algae (green, gray, red, yellow-green), fungi and bacteria, each having its unique characteristics.[2] Six inter-convertible polymorphs of cellulose exist (I, II, III_I, III_{II}, IV_I, IV_{II}). Cellulose I is of main interest as it is the allomorphic form produced naturally by the organisms listed above. Even though cellulose I is considered to be the crystal structure with the highest axial elastic modulus,[5] it has two polymorphs (Iα & Iβ). Cellulose Iα is considered to be triclinic, prevalent in algae and bacteria (68%), where cellulose Iβ is referred to as monoclinic, which is more prevalent in higher plants (80%).[6] Cellulose I (Iα & Iβ), have parallel configurations, but differ in their hydrogen bonding patterns creating differences in its crystalline properties. Cellulose Iα can be converted from its meta-stable form to Iβ through annealing, making it more thermodynamically stable. Cellulose I,

arranged uniaxially having parallel packing, can be converted to cellulose II, arranged antiparallel, by regeneration (solubilization and recrystallization) or mercerization (treatments involving sodium hydroxide).[7, 8] Cellulose III can be created by liquid ammonia treated cellulose I or II, while cellulose III is thermally treated to create cellulose IV.

In general, cellulose is characterized as a polydiverse, high molecular weight homopolymer with a ribbon-like conformation. Each repeat unit consists of two anhydro-glucose units (AGU) bounded covalently through an oxygen from the C1 carbon of one ring to the C4 carbon on the other, also referred to as a β-1-4 glucosidic bound (Figure 2.1).[2] Cellulose adopts a linear conformation, as each chair-conformed AGU is rotated 180^{o}. The terminal ends of the cellulose structure have a reducing (open-ring aldehyde) and non-reducing (closed D-glucose ring) end, which creates a directional chemical asymmetry. The hydroxyl groups (-OH) are positioned in the equatorial direction on the ring, while the hydrogens are positioned in the axial direction.[9] The abundance of hydroxyl groups on the surface of cellulose provides the polymer with its hydrophilicity, and opportunity for functionalization.[1] It is also important to mention the intramolecular hydrogen bonding, which occurs from the hydroxyl on C3 to the oxygen between C5 and C1, and the hydroxyl on C2 to the hydroxyl on C6. This intra-chain, along with the inter-chain hydrogen bonding creates a stable, highly ordered, crystalline structure.

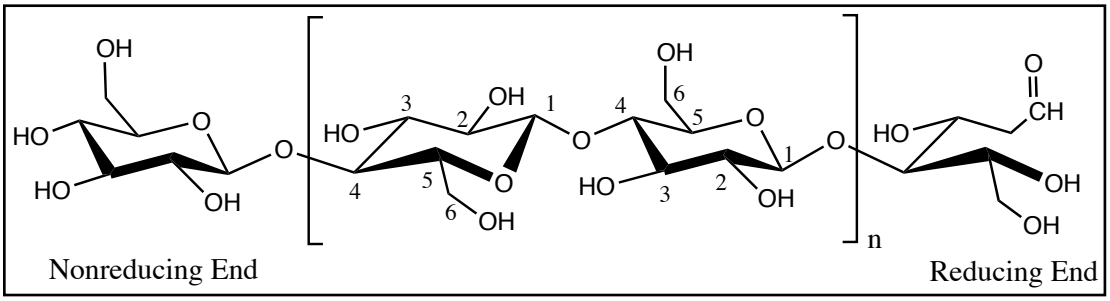

Figure 2.1: Schematic of the molecular structure of a cellulose repeat unit.

2.1.2 Production of BC

BC is a unique natural polymer, which can be created in a static or agitated medium. Unlike other sources of cellulose (plant or wood), BC is much more chemically pure as there is no need for the removal of hemicellulose, pectin, lignin, as well as other

biogenic products, which is often very difficult to remove.[10] BC, synthesized by *Gluconacetobacter xylinus* (reclassified from *Acetobacter xylinum*), is chemically identical to plant cell-wall cellulose (PC) but differs in its macromolecular structure and properties. The structure of a BC fibre has been depicted as long chained molecules aligned parallel in an extended form, where PC have a "fringed micelle" structure which the fibres are inter-tangled within one another. BC has many advantages, as it is possible to alter its culturing conditions to modify the microfibril formation and crystallization.[2]

In 1886, Brown was the first to identify a bacteria, *Gluconacetobacter xylinus* (*G. xylinus*), which synthesized a polymer identical to PC.[11, 12] This discovery was made when he noticed the formation of a thin gelatinous layer on the surface of broth as a result of vinegar fermentation. Later, in 1947 and 1954, Hestrin et al. proved that the bacteria *G. xylinus* synthesized cellulose in the presence of glucose and oxygen.[10, 13, 14] From these findings, further studies have been completed to contribute to the understanding of the production of bacterial cellulose. The gram-negative, aerobic, acetic acid *G. xylinus* can utilize a variety of carbon sources for the production of cellulose, which includes hexoses, glycerol, pyruvate and dicarboxylic acids. BC is only produced as the final product of the metabolism of sugars (glucose & fructose). In general, these organic acids enter the Krebs cycle to undergo conversion to hexoses via gluconeohenesis, similar to glycerol and the intermediates of the pentose phosphate cycle. As shown in figure 2.2, cellulose formation comprises of five enzyme-mediated steps: glucose permease, glucokinase, phosphoglucomutase (PGM), uridine diphospho-glucose (UDPGlc) pyrophosphorylase, and cellulose synthase, each having a specific role in the production process.[4] BC is most commonly produced from glucose and fructose as the starting sugar source. Therefore, the biosynthetic pathway of cellulose involves the glucose phosphorylation to glucose-6-phosphate (Glc-6-P) through a glucokinase catalyst, followed by the isomerization (catalyzed by the enzyme PGM) to glucose-1-phosphate (Glc-α-1-P). This metabolite is converted to UDPGlc by UDPGlc pyrophosphorylase. Finally, the product is converted to cellulose by cellulose synthase.[10]

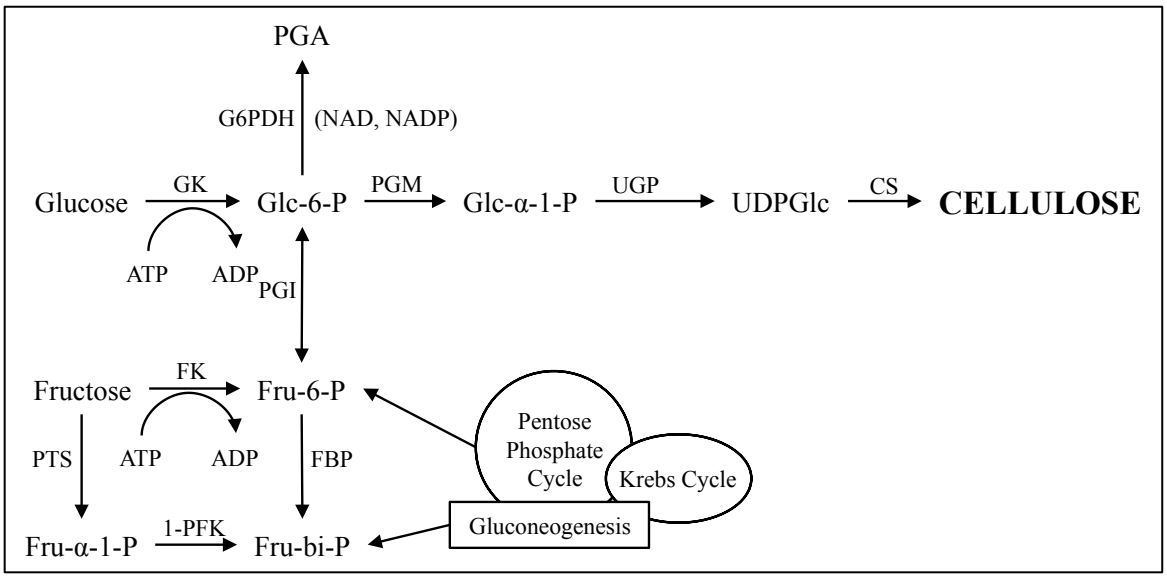

Figure 2.2: Biosynthesis of cellulose from *G. xylinus*. CS (cellulose synthase); FBP (fructose-1-6-biophosphate phosphate); FK (fructokinase); G6PDH (glucose-6-phosphate dehydrogenase); 1-PFK (fructose-1-phosphate kinase); PGI (phosphoglucoisomerase); PMG (phosphoglucomutase); PTS (system of phosphotransferases); UGP (pyrophosphorylase); UDPGlc (uridine diphospho-glucose); Fru-bi-P (fructose-1,6-bi-phosphate); Fru-6-P (fructose-6-P); Glc-6-P (glucose-6-phosphate); PGA (phosphogluconic acid). Adapted from Bielecki et al. (2005).[10]

Bacterial cellulose fibre formation has been extensively studied and the proposed mechanism involves a pellicle formation at the air/liquid interface of the static culture medium. This pellicle is formed by the organization of BC fibrils synthesized and secreted by the bacterium.[3] Since *G. xylinus* are obligate aerobes, this pellicle formation helps maintain their position close to the surface of the culture medium to allow the bacteria to reach the oxygen-rich surface. Many theories of why *G. xylinus* produces a cellulose pellicle have been hypothesized, which include the protection against the lethal effect of ultraviolet light, construct a "cage" like structure to protect themselves from enemies and heavy metal ions, and to create a structure where nutrients can be supplied easily through diffusion. Since the bacteria only generates a cellulose pellicle on the surface of the liquid medium, the productivity of cellulose is strictly dependent on surface area rather than volume of liquid medium.[15]

The production of cellulose by *G. xylinus* begins at the terminal complex (TC, 3 and 4 in Figure 2.3) located between the lipopolysaccharide envelope and cytoplasmic membrane (1 and 2 respectively in Figure 2.3). These TC are aligned linearly along the pores at the surface of the bacterium where 6-8 glucan chains are created. These subfibrils

(1.5 nm in diameter) are crystalized into microfibrils (10-20 nm wide) followed by their final bundling assembly into ribbons, commonly known as BC fibres.[16] A typical BC fibre (highly crystalline and rich in cellulose Iα) consists of ~1000 glucan chains having dimensions of approximately 50 nm in diameter and 1-9 μm in length.[17] At the beginning of static BC synthesis, production yields are relatively low, but increase exponentially with time. As the dissolved oxygen within the flask depletes, only the bacteria on the surface can maintain its activity for the production of BC. It has been shown that these bacteria undergo cell division but reach equilibrium overtime as the pellicle begins to form. The bacteria below the pellicle surface become dormant as a defense mechanism against the depletion of oxygen. These bacteria can be reactivated when inoculated to a new culture.[15]

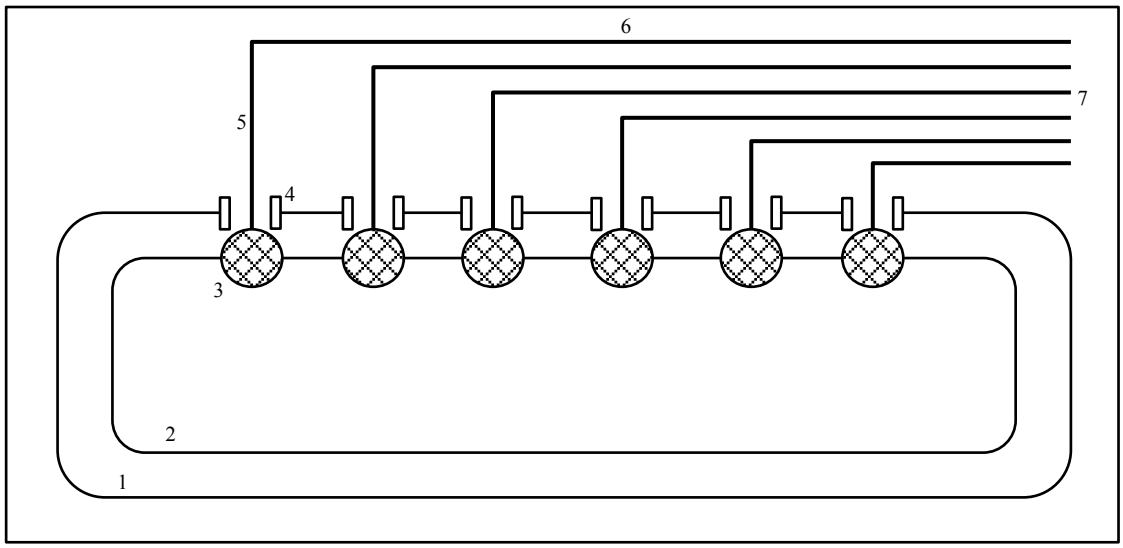

Figure 2.3: BC fibre formation from the *G. xylinus* bacterial membrane. (1)Lipopolysaccharide Envelope; (2)Cyloplasmic Membrane; (3)Cellulose Synthase; (4)Cellulose Export Component; (3+4)Terminal Complex; (5)Glucan Chain Aggregate; (6)Single Microfibril; (7)Ribbon of fibres. Amended from Iguchi et al. (2000) and Klemm et al. (2001).[4, 15]

Bacterial cellulose is most efficiently produced statically (S-BC), however, since *G. xylinus* are obligate aerobes, agitated cultures (A-BC) have also been studied. In a static culture, *G. xylinus* produces parallel β-1-4 glucan chains, which are arranged uniaxially, typical for cellulose I production. However, in agitated cultures, studies have observed cellulose II formation where the β-1-4 glucan chains are arranged randomly. Even though the production of A-BC is quicker, the resulting product has a lower

crystallinity, smaller crystal size and lower yields than S-BC.[10, 15] Figure 2.4 pictorially depicts a S-BC set-up currently being used in our laboratory.

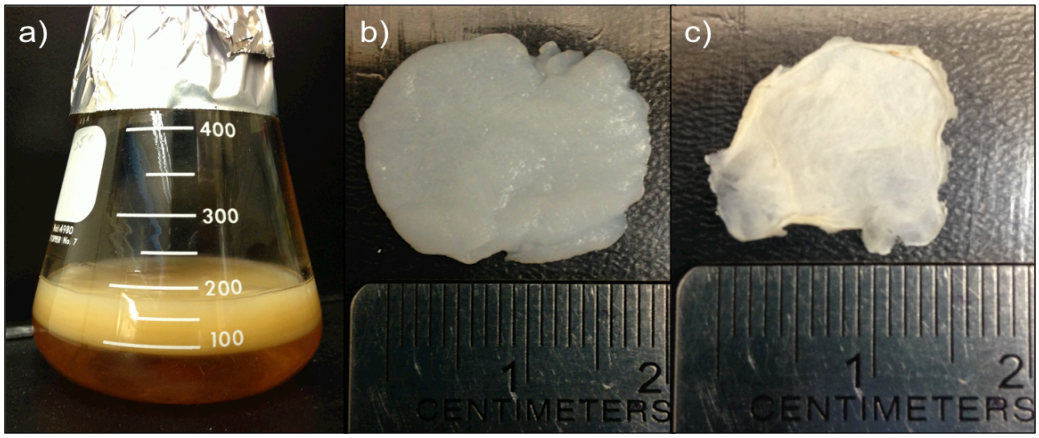

Figure 2.4: Depiction of a) BC pellicle formation in static culture; b) purified BC hydrogel; c) oven-vacuum dried BC film.

2.1.3 Physical and Mechanical Properties of BC

Cellulose is a natural polymer known for its beneficial physical and mechanical properties. Despite its origin, native cellulose has many ordered (crystalline) and disordered (amorphous) regions, which comprise its structure. Its inter- and intra-molecular hydrogen bond network stabilizes the linkage making it fairly stable with high axial stiffness. The high aspect ratio (length/diameter) of the cellulose fibre provides it with the ability to be used as reinforcement materials for composites.[18] The mechanical properties of cellulose are dependent on the source material it originated from. In general, cellulose has been reported to have a greater specific axial elastic modulus than Kevlar and its mechanical properties are within the range of other composite materials.[2] The degree of polymerization (DP) varies between 10,000 for wood cellulose and 15,000 for cotton, before the purification process.[1] Once plant and wood cellulose is purified, typically with sodium hydroxide or sodium sulfide, the resulting "pure" cellulose has an approximate DP of 2,000. As for BC, the DP are generally reported between 2,000 to 6,000 [19] but reaches 16,000 and 20,000 in some cases.[10, 20] Since BC is produced with such high purity, relatively mild and simple purification steps are need. Its DP is largely retained after purification giving it a higher average molecular weight. Due to the complex processing steps used, plant and wood cellulose have crystallinity in the range of 43-65%, which is much lower than that of BC (65-79%).[8] Another prominent feature of

cellulose is the abundance of hydroxyl groups on its surface. Not only are these surface groups ideal for surface modification, it also provides cellulose with high water holding (hydrophilicity) capacity, capable of holding more than 100 times its dry weight in water.[15] This moisture adsorption and swelling is ideal for bacterial barriers for wound dressing in biomedical applications, which will be further discussed in the following section.

2.1.4 Biomedical Applications of BC

The hydrophilicity, structure forming potential, and mechanical properties of BC allow it to be used in the biomedical field. Many studies are currently being conducted to utilize these beneficial qualities as wound healing materials and new skin substitutes for burn victims. As mentioned previously, crystalline cellulose (despite its origin) has a specific modulus, which exceeds common engineering materials such as glass, concrete and steel.[18] However, due to its hydrophilicity, moisture adsorption, and swelling capabilities, BC is optimal for wound healing environments. Currently, commercialized BC products, such as "BioFill" have been used successfully for the treatment of severe burns, skin grafting and chronic skin ulcers.[17, 21] Many of the materials used for nanocomposites are made from synthetic materials, which limit their processability, biocompatibility and biodegradability. BC is an advantageous natural biomaterial as it is highly nano-porous capable of allowing the transfer of antibiotics or other medicines into the wound along with providing the wound with an efficient physical barrier against external infection.[17] Many *in vitro* and *in vivo* studies have been completed to assess the biocompatibility of BC. Krystynowicz et al. successfully implanted pieces of BC into internal pockets within rabbits and noticed fibroblast formation at the interface of the BC and tissue with no inflammatory response.[22] Likewise, Klemm et al. was successful in implanting a hallow BC tube for the replacement of the carotid artery in rats.[4] Lastly, Helenius et al. implanted pieces of BC into internal pockets within rats and observed the formation of new blood vessels within the implanted BC with no evidence of chronic inflammation. It was also noticed that cells were able to navigate through the porous BC structure creating a newly formed tissue only after a 12-week period.[23] These examples verify that BC can be used as an *in vivo* biomaterial for tissue engineering applications.

Due to its moist environment and bacterial barrier forming potential, BC can also be used as a wound-healing device. Solway et al. demonstrated the use of BC as an effective method to heal chronic diabetic foot ulcers by reducing wound size, increasing healing efficiency and creating less discomfort to the patient.[24] Further studies have also shown that bacterial cellulose conforms to the wound surface, maintains a moist environment throughout application, reduces pain, and reduces scar formation much better than previous treatment options.[25]

Bacterial cellulose can be conjugated to other biocompatible polymers, such as polyvinyl alcohol (PVA), to create anisotropic nanocomposites for biomedical applications. Millon et al. developed a PVA-BC nanocomposite for cardiovascular graft replacements. The mechanical properties of the PVA-BC nanocomposite were closely matched to porcine aortic tissue in both circumferential and axial directions. The results were well within physiological range, demonstrating improved resistance to further stretching beyond physiological strains. PVA-BC nanocomposites can replace cardiovascular and connective tissues when the degree of anisotropy is controlled to match the mechanical properties of the soft tissue it might replace.[26]

2.2 Nanocrystalline Cellulose (NCC)

The structure of cellulose is comprised of many crystalline and amorphous regions. NCC is the product of complete or partial removal of the amorphous regions, resulting in nano-sized highly crystalline cellulose fibres (Figure 2.5). The disordered regions throughout the cellulose structure are hydrolyzed, while the crystalline regions are more resistant to hydrolysis, resulting in higher crystalinity.[27] Typical BC fibres have lengths ranging between 1-9 μm, which encompasses all deformities and amorphous regions throughout its structure. However, NCC have dimensions ranging from 50-500 nm in length and 3-5 nm in diameter, and a crystallinity index much greater than that of regular cellulose.[2] The applications of NCC differ from those of natural cellulose. Due to its aspect ratio and relative abundance from the forestry industry, researchers are studying methods in utilizing the crystalline regions of wood and plant cellulose as reinforcement materials. As mentioned in section 2.1.3, natural cellulose already has

mechanical and physical properties in the range of reinforcement materials. By creating NCC from natural cellulose, these beneficial characteristics can be further exploited.

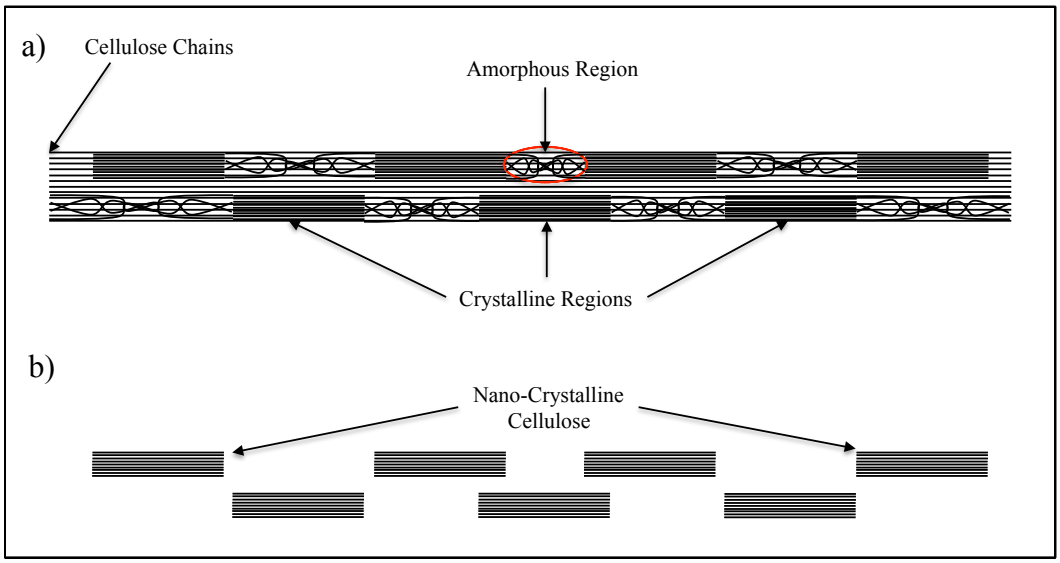

Figure 2.5: Illustration of a) typical cellulose fibre with crystalline and amorphous regions, and b) nano-crystalline cellulose after hydrolysis purification. Adapted from Moon et al. (2011).[2]

It is controversial to call these nano-sized fibres "nano-crystalline cellulose" as the product usually undergoes either chemical functionalization or structural changes. Typical methods used for the production of NCC include harsh acid hydrolysis, enzymatic hydrolysis or oxidation by ammonium persulfate. All methods have been researched and the resulting product seems to differ from the original cellulose fibre. It has been reported that enzymatic hydrolysis of BC produces NCC with chemical and physical properties very similar to that of natural cellulose compared with chemical hydrolysis routes; however, further research still needs to be completed to validate this claim.[28]

2.2.1 Production of NCC

The production of NCC can be completed through harsh acid hydrolysis, ammonium persulfate oxidation or enzymatic hydrolysis, under controlled conditions of temperature, agitation and time. The use of harsh acid treatment was first reported by Ränby in the 1950s, who degraded cellulose fibres by means of sulfuric acid hydrolysis. This gave rise to the discovery of using these nano-fibres as tablet binders in the pharmaceutical industry, as texturizing agents and fat replacers in the food industry, and as an additive in paper and composites.[9] Due to the abundance of wood byproduct from

the forestry industry, researchers are currently researching methods to utilize the high cellulose content within these woodchips for further applications. As mentioned previously, wood and plant cellulose have many impurities, which needs to be dealt with prior to fibre hydrolysis for the production of NCC. The resulting NCC product from wood byproduct is generally used as reinforcement for composites. Therefore, the hydrolysis method used does not have great relevance, as a wide range of surface functionalization and impurities introduced during hydrolysis can be tolerated. However, the production of NCC for biomedical applications must resemble that of the original cellulose fibre without any structural or surface functionalization occurring during hydrolysis. In order for NCC to be used as either drug delivery systems or as a method for wound healing, a pure product with proper surface functionalization must be created.

The nature of acid, and acid-to-cellulose ratios are important aspects, which effect the production of NCC. Common methods for acid hydrolysis include hydrochloric acid (HCl), sulfuric acid (H_2SO_4), and hydrobromic acid (HBr), while phosphoric acid (H_2PO_4) and hydrogen peroxide (H_2O_2) have been used to a lesser extent. Sulfuric acid is the most commonly used acid for cellulose hydrolysis. It has been determined that when using this acid, it reacts with surface hydroxyl groups on cellulose to form sulfate esters. The resulting charged surface would promote dispersion in water and compromise its thermal stability.[9] Roman and Winter have demonstrated the diminishing thermal stability of NCC with sulfuric acid hydrolysis. They also determined that sulfate content increases with increasing acid concentration, acid-to-cellulose ratio and hydrolysis time. They noticed char formation on the surface of the cellulose, which suggests that the abundance of sulfate groups act like flame-retardants and can be used for such applications. This char formation could be due to the intramolecular transglycosylation, along with the decomposition of anhydro sugars and auto-cross-linking of cellulose chains.[29] Further studies have demonstrated the ability of forming NCC with narrow size distribution by means of sulfuric acid hydrolysis. Elazzouzi-Hafraoui et al. subjected three sources of cellulose (cotton, Avicel, tunicate) to sulfuric acid hydrolysis. It was determined that a fraction of tunicin fibres displayed a kinked structural morphology after being subjected to acid attack followed by sonication. Sonication is a relatively common

method used after hydrolysis to generate fibres with narrow size distribution. However, this sonication method usually provokes structural deformities as it generates an abundance of sheer stress on the fibre, which can be clearly displayed by Elazzouzi-Hafraoui's result. It was also determined that cotton and tunicin nano-fibres displayed electrostatic repulsion, which can be attributed to the negative charge from the sulfate groups on the surface of the cellulose.[30] It is also interesting to see that Liu et al. were able to create NCC through sulfuric acid hydrolysis followed by 5 cycles of homogenation with little to no sulfate residues. The thermal stability was also said to remain the same as the original cellulose source. They obtained nanocrystals with diameters ranging between 8 to 10 nm with lengths ranging between 60-120 nm. However, the crystallinity only increased from 58% to 65%, which implies the original cellulose source contained an abundance of impurities and the product still has many amorphous regions. Since the resulting fibre length is in the range of NCC, this suggests the 5 cycles of homogenation caused the decrease in size rather than the removal of the amorphous regions. Therefore, it is uncharacteristic to call these fibres nano-crystalline cellulose.[31]

Hydrochloric acid (HCl) is also a very common method to create NCC. HCl has been shown to increase the thermal stability of the cellulose structure and the chlorine ions are easily removed through multiple washing cycles. In contrast to sulfuric acid, there is no electrostatic force between hydrochloric acid hydrolyzed particles and as a result they tend to agglomerate.[27, 29, 32] Corrêa et al. hydrolyzed curaua fibres by means of sulfuric acid, hydrochloric acid, and a mix of sulfuric/hydrochloric acid. Since curaua cellulose is derived from plants, a pretreatment of sodium hydroxide was necessary for the removal of impurities. Their results demonstrated that HCl hydrolysis resulted in higher crystallinity than the other two methods. Also, the sulfate groups from sulfuric acid hydrolysis created a negative charge, which increased the stability of the product. HCl and H_2SO_4/HCl presented fibres with higher agglomeration, demonstrating a decrease in negative charge. It was also noticed that the H_2SO_4/HCl treated cellulose was slightly more stable that the HCl product, which suggests the presence of sulfate groups on the surface of the nanofibre. It was concluded that sulfuric acid contributes to

more radical hydrolysis conditions, which leads to greater removal of amorphous regions resulting in a lower degree of polymerization.[27] It has also been stated that the H_2SO_4/HCl acid combination occasionally produces spherical NCC instead of rod-like nanocrystals.[32]

Sadeghifar et al. used hydrobromic acid, a relatively common method for hydrolysis, for the production of NCC. Their group demonstrated that the resulting hydrolysis product, with regard to fibre dimensions and additional functional attachment, is related to time as the amorphous regions of the fibre are removed faster at the beginning of hydrolysis. As time increases, the rate of hydrolysis decrease as the acid begins to attack the crystalline regions of the cellulose fibre. This leveling off period is highly discouraged as structural changes begin to occur. The highest yield this group was able to obtain was 70%, which they claim the 30% loss could be attributed to the loss of amorphous groups during hydrolysis. They also noticed that at a high HBr concentration (4M), discolouration occurred. This could be ascribed to dehydration, which is a common occurrence under harsh acid conditions.[33]

Lastly, George et al. produced NCC derived BC fibres through an enzymatic process. The resulting product had thermal stability of nearly two fold higher than NCC produced from the standard sulfuric acid hydrolysis. Likewise, the required activation energy needed for decomposition was much higher. The fibres length was in the range of 100-300 nm while its diameter was between 10-15 nm, which are typical dimensions for NCC. This method showed no chemical or structural change to the product, displaying a more consistent production of “true” NCC fibres.[28] As mentioned previously, it is very important for biomedical applications that a “true” NCC fibre is created. Biocompatibility is the most important aspect when dealing with drug delivery or wound healing devices. Therefore, it is evident that continuing research on the production of NCC is needed to develop a truly pure nano-sized fibre.

2.3 Ionic Functionalization of BC and NCC Derived BC (NCC-BC)

Modifications made to the hydroxyl groups on the cellulose surface have been extensively studied for various applications. As we know, there are three hydroxyl groups per AGU that are available for functionalization. It has been determined that the chemical modification of cellulose has improved the ability to create cellulose derivatives tailored to specific applications. Surface modifications of cellulose have generally been classified into three distinct categories: surface modification as a result of cellulose treatment or extraction (sulfate esters as a result of sulfuric acid NCC production), electrostatic adsorption to the cellulose surface (cetrimonium bromide surfactant adsorption), and covalent attachment of molecules or derivatization of the cellulose surface (utilizing hydroxyl groups for selective modification, i.e. oxidation and amination).[2] Typical modifications made to cellulose include esterification, etherification, oxidation and to a lesser extent, amination. Esterification is the process in which an alcohol and acid react to form an ester and water. Not only are esters introduced to the cellulose surface, it has been noticed that it hydrolyzes the amorphous regions of cellulose creating a one-step isolation reaction of acetylated NCC.[9] This reaction is most commonly used to prepare cellulosic material with hydrophobic properties for the use in composites.[34] The resulting product of esterification has also been noted to be flammable, which limits its potential applications.[35] However, etherification is a reaction in which the alcohol groups on cellulose react with an alkylchloride to form an ether and hydrogen chloride. Sections 2.3.1-2.3.3 will focus on the covalent attachment and review the beneficial properties of oxidation and amination reactions of bacterial cellulose and their potential applications.

2.3.1 Anionic Functionalization

For many years, functionalizing the surface of cellulose for biomedical applications have been of main focus. In 1995, DeNooy et al. demonstrated the selective oxidation through the conversion of the primary alcohol group of polysaccharides to carboxylic acids. This reaction was completed by using 2,2,6,6-tetramethylpiperidine-1-oxyl (a stable and water soluble nitroxyl referred to as TEMPO), and sodium bromide (NaBr) as the catalyst, alongside sodium hypochlorite (NaClO), which acts as the primary

oxidant.[36] Chang and Robyt utilized this TEMPO-mediated oxidation reaction to functionalize the primary alcohol group of natural polysaccharides (such as cellulose) to carboxylic acids, as the primary C6 alcohol is the most reactive of all hydroxyl groups.[37] Extensive chemical and physical characterization has been performed on oxidized cellulose of various origins. It has been determined, through the characterization of cotton derived oxidized cellulose, that the water insoluble fraction was greater than 80% and carboxyl content was 0.7 mmol/g.[38] Due to the hydrophilic properties of the carboxyl groups, the water retention values of oxidized cellulose increased from 60 to 280%, and the introduction of a negative surface charge created a much greater fibre dispersion compared to that of native cellulose.[39] The morphology of the oxidized fibres were also analyzed through carbon-13 nuclear magnetic resonance (^{13}C-NMR) and X-ray diffraction analysis, which demonstrated that the structural integrity of the fibres were maintained after the TEMPO mediated oxidation reaction was performed.[40, 41] Since most of these oxidation reactions have been performed on cellulose sources other than bacterial cellulose, Marko Spaic investigated the oxidation reaction on BC in detail. His results were very similar to the ones listed above however; the carboxylation content was 1.13±0.04 mmol/g. This highly selective carboxyl group is of great benefit for biomedical applications as this creates a pathway for the attachment of therapeutic proteins and drugs to the bacterial cellulose surface.[42]

In order for such a polymer to be used as a drug delivery system, surface functionalization is a necessity. Oxidized cellulose introduces a negative surface charge to the polymer to which cationic proteins, antibiotics and chemotherapeutic agents can be ionically bound to the BC surface. Oxidized cellulose can serve as an immobilizing matrix for proteins while increasing the drug's/protein's half-life by providing sustained release.[43] Also, these hydrophilic polymer networks can swell and hold large amounts of water without dissolving in water. It has also been determined that oxidized cellulose swelling is dependent on the pH condition. This is because the carboxylic acid ionization is pH dependent. [44] As a result, this will affect the swelling properties of the hydrogel through the electrostatic repulsion between cellulose fibres and Donnan equilibrium effects. Therefore, once a drug is attached to the polymer surface, this increase or

decrease in swelling will modulate drug release. Since tumor tissues have a lower pH in the range of 6.5-7.2 (compared to the physiological pH of 7.4), this can trigger a sustained drug release to the tumor site.[44] Currently, anionic polymers are being investigated for oral delivery as the decrease in pH in the stomach will cause a decrease in polymer swelling and increase diffusion of the protein for stomach cancer.[45]

2.3.2 Cationic Functionalization

Chemical modification by means of cationic functionalization is a novel and rapidly growing alternative to the current methods used. Relative to other approaches, cationic functionalization has been investigated to a lesser extent. The focus of this thesis deals with the study of the cationic derivative of BC and NCC derived BC, produced by the conversion of the surface hydroxyl groups of BC and NCC-BC fibres to amines. Dong et al. were the first to utilize the reaction scheme developed by Porath and Fornstedt, which introduced amine groups to the cellulose surface through an epichlorohydrin intermediate (Figure 2.6 a).[46, 47] Others have also tried to introduce cationic groups to the surface of cellulose by attaching chlorocholine chloride-based solvent (ClChCl; $ClCH_2CH_2N(Me)_3Cl$) and epoxypropyltrimethylammonium chloride (EPTMAC) through chemical modification (Figure 2.6 b and c respectively). Cationization by absorption of cationic polyelectrolytes such as polyethylenimine (PEI), polydiallydimethylammonium chloride (PDAD-MAC) and polyallylamine hydrochloride (PAH) have also been reported.[48-52] Cationization by absorption has shown to have disadvantages, as they tend to cause agglomeration. Also, the physical adsorption of cationic polyelectrolytes to cellulose is less sustainable compared to cationic functionalization through chemical functionalization, which creates stable cationically ionized fibres with no structural deformities.

Studies, which currently functionalize cellulose with EPTMAC and chloride-based solvents, show promising advancement in cationic functionalization of cellulose. They demonstrated relatively high degrees of conversion of surface hydroxyl groups to create a polymer with significantly more hydrophilic properties than cellulose. They have also established a potential method to produce materials with a green application from

renewable sources.[49, 53] Hasani et al. converted the surface –OH groups of cellulose with EPTMAC to create aqueous suspensions that are electrostatically stabilized by cationic trimethylammonium chloride groups.[48] Even though these cationic surface functionalization reactions contribute to the goal on creating cationically functionalized cellulose, they do not provide ease for drug conjugation. For drug delivery applications, the cationic functionalized cellulose should allow the attachment (either through ionic or covalent bonding) of therapeutic proteins, vaccines, or chemotherapeutic drugs. The reaction scheme provided by Dong et al. (Figure 2.6a) allows for protein attachment through the primary amine groups. This can either covalently attach the protein to the aminated cellulose surface through a linker, or by ionic attachment. The use of EPTMAC (Figure 2.6b) and chloride-based solvents (Figure 2.6c) allow the potential for ionic bonding only. This thesis will outline the novelty and importance of introducing amine to cellulose through an epichlorohydrin and ammonium hydroxide reaction. This reaction scheme will allow the attachment of a variety of proteins and nucleic acids, along with the ability to attach antibodies for targeted therapeutic delivery applications.

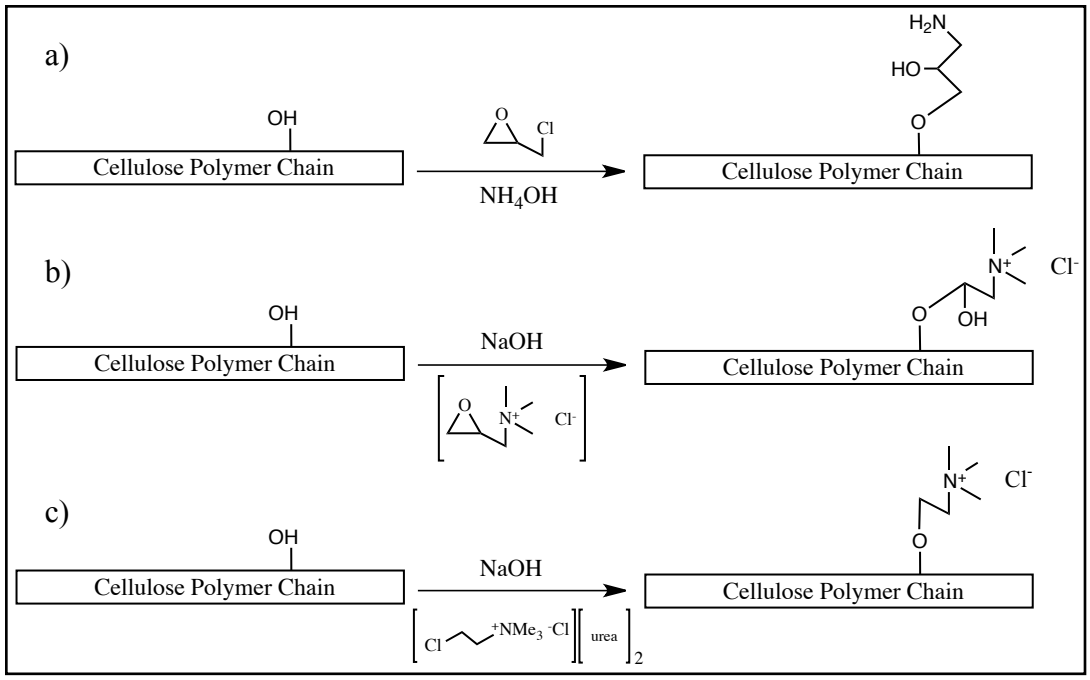

Figure 2.6: Illustration of amine functionalization and cationic ionization of cellulose through chemical modification by a) epichlorohydrin and ammonium hydroxide; b) chlorocholine chloride-based solvent (ClChCl; $ClCH_2CH_2N(Me)_3Cl$); and c) epoxypropyltrimethylammonium chloride (EPTMAC).[46, 48, 53]

2.3.3 Aminated Cellulose for Drug Delivery Applications

The application of natural polymers for drug delivery applications is of much interest to modern researchers. As mentioned previously, natural polymers have several advantages over synthetic polymers, which make natural polymers (such as cellulose) more desirable to be used as targeted drug delivery vehicles. Multiple studies have been completed on cellulose (sources other than bacterial) to demonstrate the ability of attaching florescent dyes, and model drugs to cationically functionalized cellulose.[46, 54] Dong et al. demonstrated the attachment of fluorescein-5'-isothiocyanate (FITC) to the primary amine on softwood pulp derived cellulose, using the reaction scheme shown in Figure 2.6a. This fluorescent attachment allows cellulose to be used for fluorescent techniques, such as spectrofluorometry, fluorescence microscopy, and flow cytometry. Since cellulose has demonstrated the ability to be non-toxic to endothelial cells, and has been FDA approved for internal applications, fluorescent cellulose can be used to demonstrate its interaction with cells and for biodistribution applications *in vivo*.[46] Mahmoud et al. also utilized the reaction scheme developed by Dong et al. to cationically functionalize enzyme treated flax fibres. They utilized the surface amine groups to covalently attach FITC and rhodamine B isothiocyanate (RBITC) to demonstrate cellular uptake and to determine whether this product was cytotoxic through two different cell lines (human embryotic kidney 293 an *Spodoptera frugiperda* cells). They demonstrated, through cell viability assays and cell-based impedance spectroscopy, that no noticeable cytotoxic effect of the RBITC conjugated cellulose occurred. However, they determined that the surface charge of cellulose played an important role in the cellular uptake and cytotoxicity, as negatively charged cellulose conjugated FITC was not observed within cells at physiological pH. By tuning the surface charge of the cellulose product, cellular penetration within the cell is possible. Nonetheless, they concluded that facile surface functionalization along with the demonstration of no cytotoxic effects verified the ability of cellulose to be used for bioimaging and drug delivery applications.[54] Other fluorescence labeling or drug conjugation techniques on cellulose through the use of a thiocarbamate bond[55], esterification reaction (followed by a thiol–ene Michael addition)[55], or Cetyl trimethylammonium bromide (CTAB)[56] have been completed to demonstrate to ability of drug attachment through many pathways.

The reaction scheme developed by Dong et al. will be used throughout this thesis to utilize the primary amines on the surface of either BC or NCC derived BC. Versatility of the amine functionalized BC for conjugation of molecules of interest was assessed using the fluorescent dye FITC and BCG, an indicator that changes color as a function of pH. Subsequently, horseradish peroxidase (HRP), which has been demonstrated for the application of monitoring diabetics for glucose levels when attached to hydrogels, will be used to demonstrate protein conjugation.[57] Due to its large molecular size, the protein HRP can only be conjugated to aminated BC by using bis(sulfosuccinimidyl)suberate (BS3) as the linker to reduce steric congestion on the BC surface. Section 2.4 of this thesis will outline the versatility of the amine functionalized NCC-BC through the use of an avidin-biotin complex.

2.4 Aminated BC and NCC-BC/Avidin-Biotin Complex for Nucleic Acid Delivery

2.4.1 Nanotechnology in Biomedicine

Common methods currently used in combating devastating diseases, like cancer, involve the use of harsh chemotherapeutic drugs, invasive surgeries, and semi-localized laser treatment. Even though the advancement of current technologies is on the rise, many researchers overlook the localized delivery aspect of these treatment types. In addition to killing cancerous cells, harsh chemotherapeutic drugs also target rapidly dividing healthy tissue cells (bone marrow and immune cells).[58] While surgery is a more localized treatment option, it is very invasive and only cancerous cells on the surface of tissues can be removed. It is very rare that a patient can become “cancer free” from this method without other adjuvant treatments. Lastly, radiotherapy is a common method for localized cancer treatment. Even though this method is the most localized, it still has a ~3 mm error range, which can affect the functions of adjacent organs.[59, 60] The approaches in current cancer treatment are limited due to overwhelming side effects it has on healthy tissues. It is evident that there is a need for a localized drug delivery method that is capable of only targeting cancerous cells, without affecting healthy tissues.

Research in targeted therapeutics delivery using sub-micron sized objects is on the rise to overcome some of the issues listed above.[61] Not only are researchers focusing on the targeting aspect of delivery, the delivery method is also of great emphasis. Methods in developing nanoparticles tailored to interact with biological molecules inside the cells, along with on the surface without undesirable interference is of main focus.[62] Due to the size of mammalian cells, typically ~10 μm, targeted delivery vehicles can be created to satisfy intracellular delivery, hence the creation of NCC derived BC (~150 nm in length and ~15 nm in diameter). Therefore, this report focuses on the use of NCC-BC for targeted delivery applications using a novel application of the avidin-biotin complex, to which cancer specific biotinylated therapeutics can be attached. The ability of coupling therapeutics with carriers, such as cellulose, protects the drug during transport maximizing the concentration at the diseased site.

2.4.2 Synthesis of the Avidin-Biotin Complex

The avidin-biotin complex is a well-established technique used for immunohistochemistry, enzyme linked immunosorbent assays, and molecular biology.[63] This complex has also been used as drug carriers[64-66], and systems for linking antibodies, enzymes and other molecules. The avidin-biotin system has been characterized as the strongest non-covalent interaction known to date, having a dissociation constant of $K_D \sim 10^{-15}$ M between protein and ligand.[67] The bond formation between avidin and biotin is very rapid and is unaffected by extreme pH, temperature, organic solvents, and other denaturing agents. Also, this system allows for an unlimited number of primary detection reagents (such as antibodies, nucleic acids and ligands) to be captured, immobilized or detected with a low number of secondary detecting agents. The benefits of this system include the ability of manually biotinylating reagents if they are not available, the biological and physical characteristics of the binder or probe after biotinylation are retained, the ability to modify avidin to meet specific needs, and different biotinylated probes can be bound to a single avidin.[68]

Avidin is a specific glycoprotein with terminal N-acetylglucosamine and mannose residues found in egg whites with an approximate molecular weight and size of 66 kDa

and 5.6 x 5 nm x 4 nm respectively.[69-71] Avidin has a very high affinity for up to four biotin molecules and is stable and functional in the presence of varying pH and temperatures.[72] It can undergo extensive chemical modifications with little to no effect on its function making it ideal for the detection and protein purification of biotinylated molecules at a variety of conditions. Avidin has been used as a clearing agent of circulating biotinylated antibodies and Yeo et al. demonstrated that when administered intraperitoneally, avidin localizes rapidly with high affinity in intraperitoneal tumors.[69, 73] Conversely, biotin is a water-soluble vitamin H synthesized by bacteria that is present in small amounts of living cells and is known to regulate gene expression in mammalian cells. Due to its size (244.3 Da), it can be conjugated to many proteins and other molecules without jeopardizing its biological activity. The biotin binding of proteins can be used as an assay system designed to detect and target biological analytes. The conjugation of biotin to antibodies can be completed through the use of biotinylated reagents. When non-covalently attached to avidin, the complex can be used for a variety of biomedical applications.

Many studies have aimed at improving the avidin-biotin binding properties through modification. In order to allow the regeneration of the respective biointerface, reversible systems with monomeric and whole avidins have been developed.[74-77] Likewise, avidin has been modified through chemical treatment for the improvement in thermal stability, while bifunctional avidins with two different biotin binding pockets and those that bind covalently to biotin have been developed.[74, 78-81] Research on the functionalization of the avidin-biotin complex on cellulose is relatively rare, and Orelma et al. are the most recent group to conjugate avidin to carboxymethylated cellulose or TEMPO-mediated cellulose for the attachment of biotinylated molecules. However, the conjugation of avidin to carbon nanotubes, gold and sol-gel-modified films of polymethylmethacrylate have been previously investigated. Likewise, the strong adsorption of avidin to gold, silica and polypyrole surfaces using quartz crystal microgravimetry has also been reported.[74] Even though Orelma et al. functionalized avidin on cellulose, to date no group has conjugated avidin to bacterial cellulose for the

use of targeted delivery by specifically biotinylating cancer specific therapeutics to avidin-BC.

2.4.3 Avidin-Biotin Complex as Biological Compound Carriers

The goal of targeted therapeutics delivery is to target and treat the cells responsible for disease with the highest drug concentration possible while limiting the side effects and relative drug concentration in the remaining tissue. It is known that only a small dose of therapeutic drug reaches the diseased area due to the non-selectivity of the delivery method. Therefore, it is assumed that the avidin-biotin complex can provide the system with the selectivity it needs to target and treat the diseased area at the site. The avidin-biotin system has generally been used for the delivery of diagnostic agents.[69] However, current research has been devoted to the use of the avidin-biotin complex for targeted therapy. [82]

Currently, targeting of therapeutic agents can either be accomplished through a direct method (attaching a therapeutic agent directly to a targeting ligand)[83] or through pre-targeting treatments (an indirect method where the target site is pre-targeted followed by the accumulation of therapeutics to the targeted site).[82] The direct method only involves a one step procedure, while pre-targeting techniques requires two or more steps but has been shown to enhance results. The avidin-biotin system in targeting has generally been categorized into three distinct classes: pre-targeting in therapy, pre-targeting by expression on the cell surface, and vector targeting. Each class has many benefits, which have demonstrated promising results of the use of avidin-biotin in targeting applications. It has been demonstrated that the high positive charge of avidin increases cellular uptake when conjugated to biotin-coated particles. Avidin has also been shown to accumulate in specific tissues *in vivo*, and undergoes a rapid clearance from the circulation system, which has the added benefit of being used as a clearance agent for any unbound antibodies remaining in blood flow.[82] Current pre-targeting techniques used in therapy include the attachment of a biotinylated antibody directly to the cancer cell surface. From there, a radiolabeled effector molecule (avidin-labeled therapeutic agent) is attached to the biotinylated antibody for targeted delivery (Figure 2.7a). A three-step

procedure can also be implemented (Figure 2.7b), which includes the attachment of a biotinylated antibody to the cancer cell surface. However, in this method, a biotinylated therapeutic agent is bound to the biotinylated antiboby through the use of avidin (Figure 2.7). The drawback of this method includes the use of additional avidin molecules for the clearance of excess biotinylated therapeutic agents and biotinylated antibodies unbound to the cancer cell (creating a four-step or five-step procedure). Many groups have demonstrated the high success of this method. Kalofonos et al. demonstrated the improvement of tumor-to-normal tissue radioactivity in patients with squamous cell carcinoma of the lung.[84] Also, Paganelli et al. targeted ovarian tumors using a two-step procedure involving biotinylated antifolate receptor monoclonal antibody and ^{111}In-labeled streptavidin, which showed no toxic effects to patients and improved the average tumor-to-tissue ratios.[85] Paganelli et al. developed a three-step procedure, which included the use of biotinylated anti-carcinoembryotic antigen (CEA), the injection of unlabeled streptavidin and the use of radiolabeled biotin. Biotinylated anti (CEA) monoclonal antibodies were then injected, unlabeled avidin was added as the clearing agent, followed by a third-step involving ^{111}In-labeled biotin. This method demonstrated no signs of toxicity or adverse effects to the patient and tumor to healthy ratios were improved.[83] Other studies have also been completed to demonstrate the ability of using this pre-targeting system as therapeutic delivery devices.[82, 86]

Other pre-targeting methods use the existing expression of avidin or biotin on the cell surface or by specific vector targeting. For pre-targeting by means of expression of avidin or biotin on the cell surface, biotinylated or avidinylated therapeutics or imaging compounds can be used as an effective "bridge" between the target cell and the effector molecule. Scavidin is a molecule that showed efficient binding and endocytosis of biotinylated ligand *in vitro* and demonstrated its expression *in vivo*.[87] Specific vector targeting can be completed to improve the targeting of gene therapy by stabilizing the vector-adaptor complex under physiological conditions.[82] This method is completed by biotinylating the gene therapy vectors, while bringing the biotinylated targeting molecules together with the use of avidin. Smith et al. demonstrated the use of this system by bridging biotinylating c-Kit receptor ligand to hematopoetic cells through the use of

avidin. This resulted up to a 2400-fold increase in reporter gene expression.[88] The vector targeting system has also been demonstrated for the direct targeting of DNA vectors.[89]

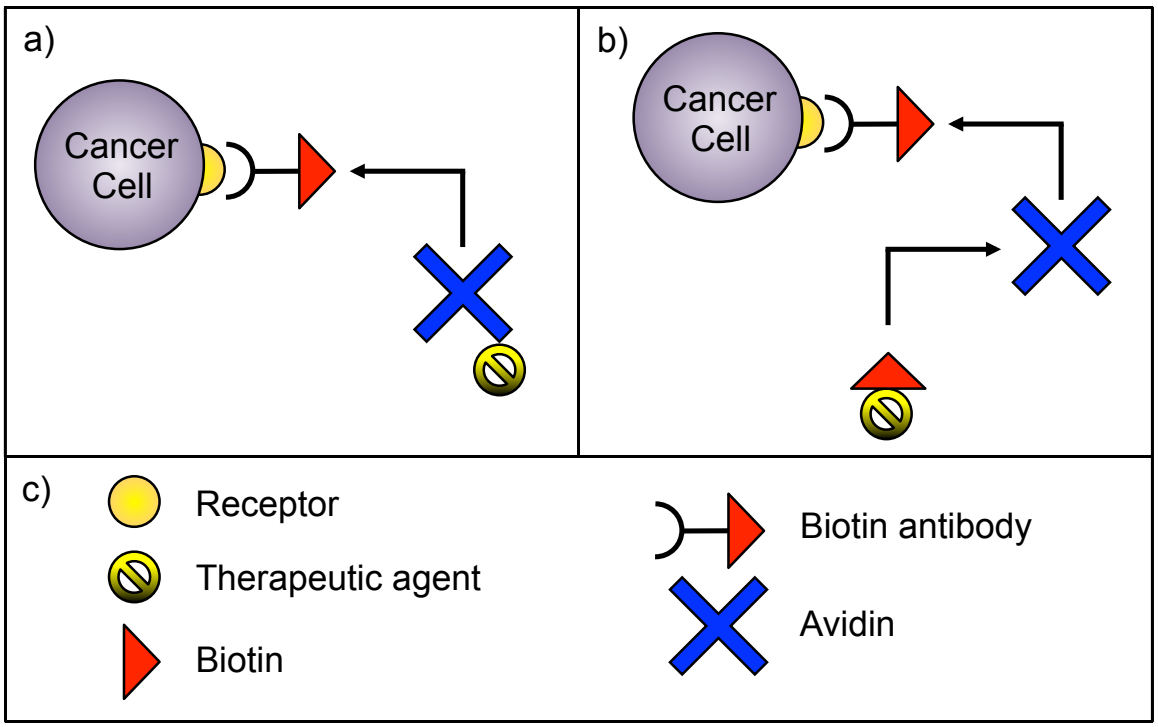

Figure 2.7: Representation of pre-targeting approaches. a) Two-step procedure where an avidin-labeled therapeutic agent is bound to a biotin antibody on a receptor of a cancer cell; b) Three-step procedure where an biotin-labeled therapeutic agent is bound to a biotin antibody on a receptor of a cancer cell through the use of avidin; c) Legend (Adapted from Lesch et al.).[82]

2.4.4 Using the Avidin-Biotin Complex for Targeted Drug Delivery

The avidin-biotin complex has established its use through multiple pathways listed above. However, many of the above procedures include multiple steps and there is still a possibility of side effects occurring if the biotinylated therapeutics does not reach the target cell. The current procedure to avoid this mishap is to inject more avidin in hopes of rapid clearance through the circulatory system. Even though this approach has shown success, it can be further improved by utilizing this avidin-biotin system on a delivery device, which the avidin-biotin complex will be created *ex vivo* followed by the injection to the patient. This method will load the effective amount of therapeutics prior to injection creating no "free floating" therapeutic within the circulatory system. The proposed mechanism will include a biotinylated cancer specific antibody and a biotinylated cancer specific therapeutic complexed to avidin on the same delivery device.

The antibody on the device will specifically target the cancer cell, while the therapeutic element will kill the diseased cell. This process utilizes and refines the procedures described in section 2.4.3.

2.5 Novel Avidin-Biotin Delivery Approach

The proposed avidin-biotin delivery device was conjugated to the BC fibre backbone. The mechanism utilized the surface hydroxyl groups (-OH) of BC for functionalization. However, prior to functionalization, nano-cryalline cellulose must be created to generate fibres with dimensions capable for intracellular delivery (endocytosis). The resulting NCC-BC fibre will be functionalized to create primary amines on the cellulose surface, which will be directly linked to avidin using the available N-terminal amino acid groups. Biotinylated glucose oxidase and biotinylated β-galactosidase will be complexed to the attached avidin for the demonstration of protein conjugation through an avidin-biotin complex. The main function of glucose oxidase is to act as an antibacterial and antifungal agent through the production of hydrogen peroxide. It has been widely used in a variety of applications including food processing, dairy and the lactoperoxidase system, breadmaking, and as an antioxidant for preservatives, to name a few.[90] Conjugation of glucose oxidase through the avidin-biotin complex can be used as a continuous monitoring system of glucose *in vivo*. Likewise, β-galactosidase has many applications, which include the removal of lactose from milk products for lactose intolerant people and the production of galactosylated products. Also, the inability to digest lactose or lactose containing products due to the lack of β-galactosidase activity in the small intestine affects 75% of adults worldwide. The conjugation of β-galactosidase to a delivery device, using the avidin-biotin system, can deliver β-galactosidase to the small intestine for the digestion of lactose. β-galactosidase has the added benefit of being used as biosensors.[91] The application of β-galactosidase in our work is to use this enzyme as validation for intracellular delivery to human endothelial kidney cells using X-gal staining to demonstrate activity after conjugation.[92] Therefore the use of the avidin-biotin complex on NCC derived from bacterial cellulose is of great benefit for the attachment of any biotinylated molecule (Figure 2.8). With the increase surface area and

loading efficiencies of NCC, biotinylated molecules can be conjugated with known quantities and little to no side effects.

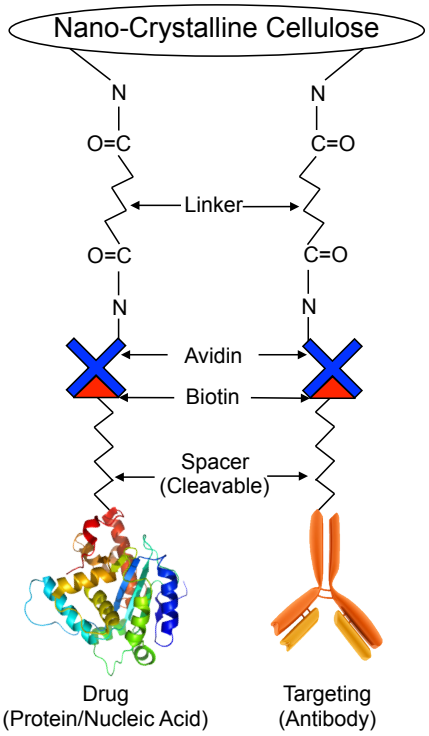

Figure 2.8: Representation of proposed mechanism of a targeted delivery system using the avidin-biotin complex.

CHAPTER 3 – MATERIALS AND METHODS

3.1 Synthesis and Characterization of Amine BC and Amine NCC-BC

3.1.1 Chemicals

All chemicals used were ACS reagent grade and purchased from Sigma-Aldrich (St. Louis, MO, USA), expect Biotin-Glucose Oxidase, which was purchased from Rockland Immunochemicals Inc. (Gilbertsville, PA, USA). Deionized water was used for all experiments.

3.1.2 BC Growth and Harvest

The static medium for the BC culture contained 0.22 M fructose, 26.63 mM ammonium sulphate, 7.34 mM monobasic potassium phosphate, 1.01 mM magnesium sulphate heptahydrate, 14.28 mM tri-sodium citrate, 45.80 mM citric acid and 5 g/L yeast extract. This medium was placed in 500 mL Erlenmeyer flasks each containing 200 mL of media. These flasks were inoculated with *G. xylinus* (BPR 2001) bacteria, which was cultivated in conditions optimized for our lab. They were left in an incubator for three weeks at room temperature, after which time the pellicles were formed and removed from the flasks. They were blended with a Commercial Laboratory Blender (model 51BL30, Torrington, CT, USA) until an "apple sauce" consistency was formed. The BC was purified in 4 L of water four times and collected each time by centrifugation (Sorvall Refrigerated Superspeed Centrifuge; model RC-5B & RC-5C; Asheville, NC, USA) at room temperature at 10,000 RPM for 10 min. *G. xylinus* bacterial cells were removed by washing in 1 % NaOH for 3 h at 80 ^{o}C. Once completed, the dry weight percent (D_w %) of each batch of BC was calculated (Equation 1). A sample of wet BC was weighed and the wet weight (W_w) was recorded. The sample was placed in a vacuum oven (VWR International Economy Vacuum Oven; Model 1400E; Radnor, PA, USA) for 24 hours at 60^{o}C, after which time a dry BC film was formed and the dry weight (D_w) was recorded. The remaining purified wet BC was stored at 4^{o}C for further use. All BC masses are reported as dry weight.

$$D_w(\%) = \frac{D_w}{W_w} \times 100 \quad (1)$$

3.1.3 Production of NCC-BC

NCC-BC was evaluated using a variety of hydrolyzing agents; however, the method involving hydrogen peroxide (H_2O_2) was determined to be optimal for our application. H_2O_2 (11.3% w/v) along with water was measured and placed in a beaker. The reaction mixture was placed on a hot plate with continuous stirring. Once the internal temperature reacted 70^{o}C, BC (77 mg/L) was added to the beaker. The reaction was left for 4 hours with continuous stirring at a rate of 254 RPM using a mechanical stirrer. Once completed, the pH was adjusted to 7 by multiple washing cycles.

3.1.4 BC and NCC-BC Amination

The amination reaction was optimized and performed on both BC and NCC-BC. BC was suspended in a 1 M NaOH solution (396 mL/g reaction volume), at which time the reaction mixture was placed on a hot plate with continuous stirring. Once the internal temperature reached 60^{o}C, an epoxide ring was introduced to the BC surface by a reaction involving epichlorohydrin (18 mmol/g). The reaction was left at 60^{o}C for 2 hours with continuous stirring. Once completed, the pH was adjusted to 12 by washing with deionized water. The epoxide BC was suspended in a 50% (w/v) sodium hydroxide solution (396 mL/g reaction volume). The reaction mixture was placed on a hot plate with continuous stirring. Once the internal temperature reached 60^{o}C, the epoxide ring was opened with 29.4% w/v ammonium hydroxide (15 mL/g) to form primary amines on the BC surface. The reaction was left for 2 hours with continuous stirring. The pH was then adjusted to 7 through multiple washing cycles and stored at 4^{o}C until further use. The same reaction procedure was completed on NCC-BC to create aminated NCC-BC.

3.1.5 Chemical Characterization of Aminated BC, NCC-BC & Aminated NCC-BC

3.1.5.1 Fourier Transform Infrared (FTIR) Spectroscopy

FTIR spectroscopy was used to identify functional groups on our functionalized BC. Samples of control BC, aminated BC, NCC-BC & aminated NCC-BC were prepared by spreading a thin layer of wet cellulose over a glass slide and placed in a vacuum-oven to produce thin dry cellulose films. A BrukerVector 22 FTIR spectrometer (Milton, ON,

Canada), equipped with a Pike Technologies Inc. attenuated total reflectance (ATR) module (Madison, WI, USA) was used to gather the infrared spectra through the diamond crystal attachment. 256 scans were gathered for each sample with wavenumbers in the range of 4000 to 600 cm^{-1}, and a resolution of 4 cm^{-1}.

3.1.5.2 Acid/Base Titration

An endpoint titration was used to quantify the amount of amine functionalization introduced to the cellulose sample. For aminated BC and aminated NCC-BC, 0.03 g of cellulose was suspended in 10 mL of 0.1 M NaOH solution. The mixture was titrated against 0.01 M HCl until a level off pH was reached. Likewise, for NCC-BC, 0.03 g of cellulose was suspended in 10 mL of 0.01 M HCl solution. The mixture was titrated against 0.1 M NaOH until a level off pH was reached. The difference in the number of moles of acid between aminated BC/NCC-BC and the control BC/NCC-BC was considered to be the number of moles of amine introduced to the aminated BC or NCC-BC surface. Similarly, the difference in the number of moles of base between NCC-BC and the control BC was considered to be the number of moles of carboxylic acid functional groups introduced to the NCC-BC. Equations 2 & 3 were used for all acid/base quantifications. The pH half way to the equivalence point on the titration curve was used to calculate pKa. 50% of acid or base groups are deprotonated or protonated at the half-equivalence point. Therefore, the pH at this point is equal to the pKa using the Henderson-Hasselbalch equation.

$$Amine\ Content\ \left(\frac{mmol}{g\ Aminated\ Cellulose}\right) = \frac{\left(\frac{Aminated\ Cellulose - Control\ BC\ (volume\ of\ 0.01\ M\ HCl\ to\ Neutralize)}{1000}\right)}{Mass\ of\ Aminated\ Cellulose} \quad (2)$$

$$Carboxyl\ Content\ \left(\frac{mmol}{g\ NCC}\right) = \frac{\left(\frac{NCC - Control\ BC\ (volume\ of\ 0.1M\ NaOH\ to\ Neutralize)}{1000}\right)}{Mass\ of\ NCC} \quad (3)$$

3.1.6 Physical Characterization of Aminated BC, NCC-BC & Aminated NCC-BC

3.1.6.1 Transmission Electron Microscopy (TEM)

TEM was used to capture high-resolution images of the functionalized BC fibres. 3 mg of BC was suspended in 10 mL of deionized water and sonicated for three minutes

at 30 W using a Misonix XL-2000 sonication probe (Newtown, CT, USA) to create uniform fibre dispersion. One drop of each suspension was placed on a Formvar carbon-coated 100 mesh copper grid (Electron Microscopy Specialists, Hatfield, PA, USA) for 25 minutes. A filter paper was then used to remove any un-evaporated solution remaining on the grid, at which time 2% uranyl acetate was used to negatively stain the sample for two minutes. The excess stain was removed by gently applying a filter paper to the grid's surface. Each sample was imaged using a Philips TEM (model CM-10, New York City, NY, USA) at an accelerating voltage of 80 kV, and the images were captured using a Hamamatsu digital camera. BC fibre analysis and measurement was done through the use of ImageJ (1.43U Java 1.6.0_10 32 bit, Wayne Rasband, National Institute of health, Bethesda, MD, USA). Statistical analysis was preformed with SigmaStat v.3.5 for Windows (Systat Software, San Jose, CA, USA). Mean lengths and diameters were compared using a one-way ANOVA with a Tukey's Post Hoc Test, and a P value of $\leq$ 0.01 was considered significant.

3.1.6.2 X-Ray Diffraction (XRD) Analysis

XRD measures the crystalline or partial crystalline portion of a solid by computing the inter-atomic spacing of the respective atomic units. All samples were vacuum oven dried and placed on Beta Diamond Products 27 x 46 mm Frosted Petrographic Slides (Yorba Linda, CA). The XRD patterns were recorded using the Rigaku-Rotaflex Diffractometer (RU-200BH, The Woodlands Texas, USA) with a Co-k_α radiation (λ =1.79 Å) at 30 kV and 44 mA. All spectra were scanned with a 2θ diffraction angle ranging from 0.0^o to 90.0^o with a 0.2^o step size. The diffraction patterns were fitted using the Pearson VII function (equation 4), where ω is the full width at half maximum (FWHM), x_c is the center of the peak, and m is the shape factor (set to 1). The resulting peaks were used to determine the spacing between similar planes (d-spacing).[93]

$$f(x) = \left[1 + \frac{4\left(2^{\frac{1}{m}} - 1\right)}{\omega^2}(x - x_c)\right]^{-m} \quad (4)$$

The average crystalline size was calculated using Scherrer's equation (equation 5), where ω is the FWHM, θ is the Bragg's angle, and k is the shape factor (set to 1).[93]

$$P = \frac{k\lambda}{\omega cos\theta} \quad (5)$$

The Herman and Weidinger method was used to determine the crystal spacing (equation 6) in the amorphous region. This was estimated from the position of the maximum of the amorphous halo.[94]

$$R = \frac{5\lambda}{8sin\theta} \quad (6)$$

The Herman and Weidinger method was also used to evaluate the degree of crystallinity (equation 7), where A_c and A_a are the respective areas of the crystalline and amorphous regions within the sample.[95]

$$X_c = \frac{A_c}{A_c + A_a} \quad (7)$$

3.1.6.3 Zeta (ζ) - Potential

ζ-potential was used to measure the electrostatic potential generated as a result of BC surface functionalization. 3 mg of BC was suspended in 10 mL of deionized water and sonicated for three minutes at 30 W using a Misonix XL-2000 sonication probe (Newtown, CT, USA) to create a uniform dispersion. The ζ-potential of BC was measured with Zetasizer 3000HSa (model DS5301, Malvern Instrument, UK) and the ζ-potential plot was analyzed using the Zetasizer software PCS V.1.4 (Malvern Instruments, UK).

3.1.6.4 Water Retention Value (WRV)

WRVs were calculated at various pH conditions to measure the swelling behavior of aminated BC and aminated NCC-BC as a function of pH. Samples of aminated BC and aminated NCC-BC were suspended in pH specific solutions (pH 4, 7, 10 and 13) and the product was centrifuged at room temperature for 10 min. This method was repeated three times to ensure the correct pH was obtained, after which time the wet weight (W_w) of the

sample was recorded. The W_w of a pH 7 BC and NCC-BC sample was measured as the control. All samples were dried using the vacuum oven for 24 hours. The dry weight (D_w) of all samples were measured and recorded and the WRV were calculated using equation 8.

$$WRV\ (\%) = \frac{W_w - D_w}{D_w} \times 100 \quad (8)$$

3.2 Fluorescence and Protein Conjugation

3.2.1 Fluorescence and Protein Selection

In order to demonstrate successful conjugation of the aminated BC product, a fluorescent tag, a pH indicator and a model protein were attached to the aminated BC surface. The fluorescent tag fluorescein-5'-isothiocyanate (FITC) was selected because the conjugated FITC-BC product will exhibit a strong fluorescent emission at ~521 nm, denoting successful attachment. The pH indicator bromocresol green (BCG) was used to demonstrate a stable conjugated product over a broad range of pH to avoid premature release. The colour of the conjugated BCG-BC will differ with varying pH (yellow at pH < 3, blue at pH > 7) indicating attachment under harsh pH environments. Lastly, horseradish peroxidase (HRP) was used to demonstrate protein conjugation, as HRP hydrogels have been used for the application of monitoring diabetics for glucose levels. Assays were used to demonstrate the activity of the conjugated HRP-BC product, which verified the idea of attaching other therapeutic proteins to the aminated BC surface for therapeutic delivery.

3.2.2 Aminated BC/FITC Conjugation

FITC was conjugated to aminated BC through the isothiocynate group on the FITC molecule. Aminated BC was suspended in a 50 mmol sodium borate buffer (150 mL/g cellulose), containing 5 mM ethylene glycol tetraacetic acid, 0.15 M sodium chloride, and 0.3 M sucrose, at room temperature with constant stirring. Once the aminated BC was well dispersed, FITC (0.32 mmol FITC/g cellulose) was added to the reaction mixture. The mixture was stirred overnight in the dark at room temperature, at which time the product was centrifuged multiple times to remove any aggregates.

3.2.3 Aminated BC/BCG Conjugation

BCG was conjugated to the aminated BC surface through a two-step reaction. Before BCG attachment, the sulfate group on free BCG was converted to sulfonyl chloride to make it more reactive. This was completed by adding 4.65 g BCG, along with 0.673 g triethylamine and 1.23 g cyanuraic chloride to 90 mL of acetone for three hours at reflux temperature.[96] The resulting product was left to cool until room temperature was reached. Once completed, 5 g of activated BCG and 0.3 g of aminated BC was added to 500 mL of acetone for two hours at room temperature. The product was centrifuged multiple times to remove any aggregates.

3.2.4 Aminated BC/HRP and Aminated NCC-BC/HRP Conjugation

In order to outline the importance of amine groups on cellulose, HRP was attached to aminated BC and NCC-BC through two different reaction mechanisms. The first approach involves a direct linkage between the amines of aminated BCC or NCC-BC, directly to the amines on the surface of the HRP protein. The second approach (BS3 linkage) involves the attachment of HRP through a bis(sulfosuccinimidyl) suberate (BS3) linker, linking the amine groups attached to cellulose directly to the amines on the surface of HRP. This BS3 linker, links amine groups to other amine groups with high efficiency, along with creating distance between polymer and protein to limit cluster formation to optimize maximum protein attachment. For the direct linkage, purified aminated BC or NCC-BC was added to a sodium phosphate buffer (2.47 mg/mL reaction volume), containing 45.75 mL 0.2 M-Na_2HPO_4, 4.25 mL 0.2 M-NaH_2PO_4; diluted to 100 mL with distilled water. The mixture was continually stirred until well mixed at which time HRP (15 mg/mL reaction volume) was added to the mixture and left stirring for four hours at room temperature. The product was centrifuged in 1 M Trizma buffer for 20 min at 15000 rpm followed by three washing cycles of distilled water/centrifugation and three cycles of 0.1 M sodium citrate buffer/centrifugation. Likewise, for the BS3 linkage, purified aminated BC or NCC-BC was added to a sodium phosphate buffer (2.47 mg/mL reaction volume), containing 45.75 mL 0.2 M-Na_2HPO_4, 4.25 mL 0.2 M-NaH_2PO_4; diluted to 100 mL with distilled water. The mixture was continually stirred until well mixed at which

time BS3 (2.94 mg/mL reaction volume) was added. HRP (15 mg/mL reaction volume) was added to the mixture and left stirring for four hours at room temperature. The product was centrifuged in 1 M Trizma buffer for 20 min at 15000 rpm followed by the same six washing cycles mentioned above.

3.2.5 Aminated NCC-BC/HRP Optimization

In order to examine the full potential of BS3, varying amounts of linker was conjugated with double the amount of HRP protein. Purified aminated NCC-BC was added to a sodium phosphate buffer (2.47 mg/mL reaction volume), containing 45.75 mL 0.2 M-Na_2HPO_4, 4.25 mL 0.2 M-NaH_2PO_4; diluted to 100 mL with distilled water. The mixture was continually stirred until well mixed at which time varying amounts of BS3 (2.94 mg/mL, 29.4 mg/mL, and 44.1 mg/mL reaction volume) was added. HRP (30 mg/mL reaction volume) was added to the mixture and left stirring for four hours at room temperature. The product was centrifuged in 1 M Trizma buffer for 20 min at 15000 rpm. The resulting product was washed with three cycles of distilled water/centrifugation followed by three cycles of 0.1 M sodium citrate buffer/centrifugation.

3.2.6 Aminated BC Conjugation Characterization

3.2.6.1 UV-Vis Spectroscopy

UV-Vis spectroscopy was used to gather an absorbance spectrum and quantify the loading of BCG-BC. 3 mg of conjugated aminated BC was suspended in 10 mL of deionized water and sonicated for three minutes to create uniform fibre dispersion. The dispersed solution was placed in Plastibrand UV-Vis Cuvettes (Ocean Optics, Henderson, NV, USA) and the UV-Vis spectroscopy was preformed using a Beckman DU-520 UV-Vis Spectrophotometer (Beckman Coulter, Mississauga, ON, Canada). The absorbance readings within the visible wavelength region (400-700 nm) were compared for all samples (Control BC and BCG-BC).

3.2.6.2 Fluorescence Spectroscopy

Fluorescence spectroscopy was used to gather an emission spectrum and quantify the loading of FITC-BC. This form of spectroscopy will allow the identification of the

fluorescent compound FITC based on its excitation and emission wavelength. 3 mg of conjugated aminated BC was suspended in 10 mL of deionized water and sonicated for three minutes to create uniform fibre dispersion. The dispersed solution was placed in Greiner Bio-One 96 well transparent flat bottom plates (Germany) and the fluorescence spectrum was obtained using a Tecan Infinite Spectrophotometer (model M2000, Switzerland). The emission readings within wavelength of 500-600 nm and the excitation wavelength was 494 nm. The emission spectrum was analyzed with i-control™ Microplate Reader Software (Tecan Group Ltd., Switzerland).

3.2.6.3 HRP Activity Assay

The following HRP activity assay was used to quantify the loading of protein to the aminated cellulose surface. This activity assay involves the reaction of benzidine with HRP, which will create a colour change (white to blue). The assay consists of 0.1 M sodium citrate buffer (pH 5.8), 10 mM ascorbic acid, 0.2 M peroxide, 5% w/v benzidine and HRP-BC sample with a ratio of 1:1:1:0.04:1. The solutions were added to a 15 mL glass test tube in the order listed above with the HRP-BC sample added last. As soon as the HRP-BC sample was added, a timer was started until all the contents within the test tube turned blue, at which time the timer was stopped and time was recorded. The difference in the time taken for the sample to turn blue will correspond to the amount of conjugated HRP to the aminated cellulose surface.

3.3 Aminated NCC-BC/Avidin-Biotin Complexation For Therapeutic Protein Delivery

The avidin-biotin complex is the strongest non-covalent bond known to date. This complex will allow up to four times the amount of protein loading as a single avidin can bind up to four biotin molecules. Numerous therapeutic proteins can be biotinylated for the specific attachment to avidin through the avidin-biotin complex. Avidin-HRP was chosen to compare the projected increase in attachment yield against the use of BS3 linker alone. Avidin-biotin glucose oxidase was used as a model therapeutic protein to demonstrate the importance of the role the avidin-biotin complex plays in protein conjugation. Finally, avidin-biotin β-galactosidase was chosen for the *in-vitro* delivery to

human endothelial kidney (HEK) 293 cells. When HEK cells are inoculated with β-galactosidase, the cell will fluoresce blue denoting successful delivery without toxic contamination.

3.3.1 Aminated NCC-BC/Avidin-HRP Complex

Purified aminated NCC-BC was added to a sodium phosphate buffer (2.47 mg/mL reaction volume), containing 45.75 mL 0.2 M-Na_2HPO_4, 4.25 mL 0.2 M-NaH_2PO_4; diluted to 100 mL with distilled water. The mixture was continually stirred until well mixed at which time BS3 (2.94 mg/mL reaction volume) was added. Avidin-HRP (15 mg/mL reaction volume) was added to the mixture and left stirring for four hours at room temperature. The product was centrifuged in 1 M Trizma buffer for 20 min at 15000 rpm followed by the same six washing cycles mentioned above in section 3.2.4.

3.3.2 Aminated NCC-BC/Avidin Conjugation

Purified aminated NCC-BC was added to a sodium phosphate buffer (2.47 mg/mL reaction volume), containing 45.75 mL 0.2 M-Na_2HPO_4, 4.25 mL 0.2 M-NaH_2PO_4; diluted to 100 mL with distilled water. The mixture was continually stirred until well mixed at which time BS3 (2.94 mg/mL reaction volume) was added. Avidin (15 mg/mL reaction volume) was added to the mixture and left stirring for four hours at room temperature. The product was centrifuged in 1 M Trizma buffer for 20 min at 15000 rpm followed by the same six washing cycles mentioned above in section 3.2.4.

3.3.3 Aminated NCC-BC/Avidin-Biotin Glucose Oxidase Complex

Purified avidin-aminated NCC-BC was placed in a pH 7.8 phosphate buffered saline solution (0.3 mg/mL) and left stirring until contents were evenly mixed. 1 mg of biotin-glucose oxidase was added to the reaction mixture and left overnight at room temperature with constant stirring. The resulting product was washed several times with deionized water to remove any aggregates.

3.3.4 Aminated NCC-BC/Avidin-Biotin β-Galactosidase Complex

Purified avidin-aminated NCC-BC was placed in a pH 7.8 phosphate buffered saline solution (0.3 mg/mL) and left stirring until contents were evenly mixed. 5 mg of biotin-β-galactosidase was added to the reaction mixture and left overnight at room temperature with constant stirring. The resulting product was washed several times with deionized water to remove any aggregates.

3.3.5 Amine NCC-BC/Avidin-Biotin Complex Characterization

3.3.5.1 HRP Activity Assay

The same HRP activity assay procedure used in section 3.2.6.3 was used for the quantification of aminated NCC-BC/avidin-HRP complex formation.

3.3.5.2 UV-Vis Spectroscopy

UV-Vis spectroscopy was used to gather an absorbance vs. time plot to quantify the loading of both amine NCC-BC/avidin-biotin glucose oxidase and amine NCC-BC/avidin-biotin β-galactosidase.

For aminated NCC-BC/avidin-biotin glucose oxidase, the activity assay was amended from Bergmeyer et al. (1974).[97] 2.5 mL of a pH 7 phosphate buffered saline solution was prepared with o-Dianisidine (26.4 mg/L), along with 0.5 mL of glucose (100 mg/mL), 0.01 mL HRP (2 mg/mL) and 1 mL test solution (1.5 mg of aminated NCC-BC/avidin-biotin glucose oxidase per mL deionized water) was added to a Plastibrand UV-Vis Cuvette. The absorbace vs. time plot was constructed (every 10 seconds for four minutes) at a wavelength of 436nm. The resulting plot was analyzed against a calibration curve created prior to analysis.

For aminated NCC-BC/avidin-biotin β-galactosidase, the activity assay was amended from Miller (1972).[98] 1 mL of Z-buffer (excluding β-mercaptoethanol), along with 0.5 mL o-nitrophenyl-ß-D- galactoside (4 mg/mL in 0.1 M phosphate buffer, pH 7.8), and 0.5 mL of test solution (3 mg aminated NCC-BC/avidin-biotin β-galactosidase

per mL deionized water) was added to a Plastibrand UV-Vis Cuvette. The absorbace vs. time plot was constructed (every 10 seconds for three minutes) at a wavelength of 420nm. The resulting plot was analyzed against a calibration curve created prior to analysis.

3.4 Summary of Reaction Schemes

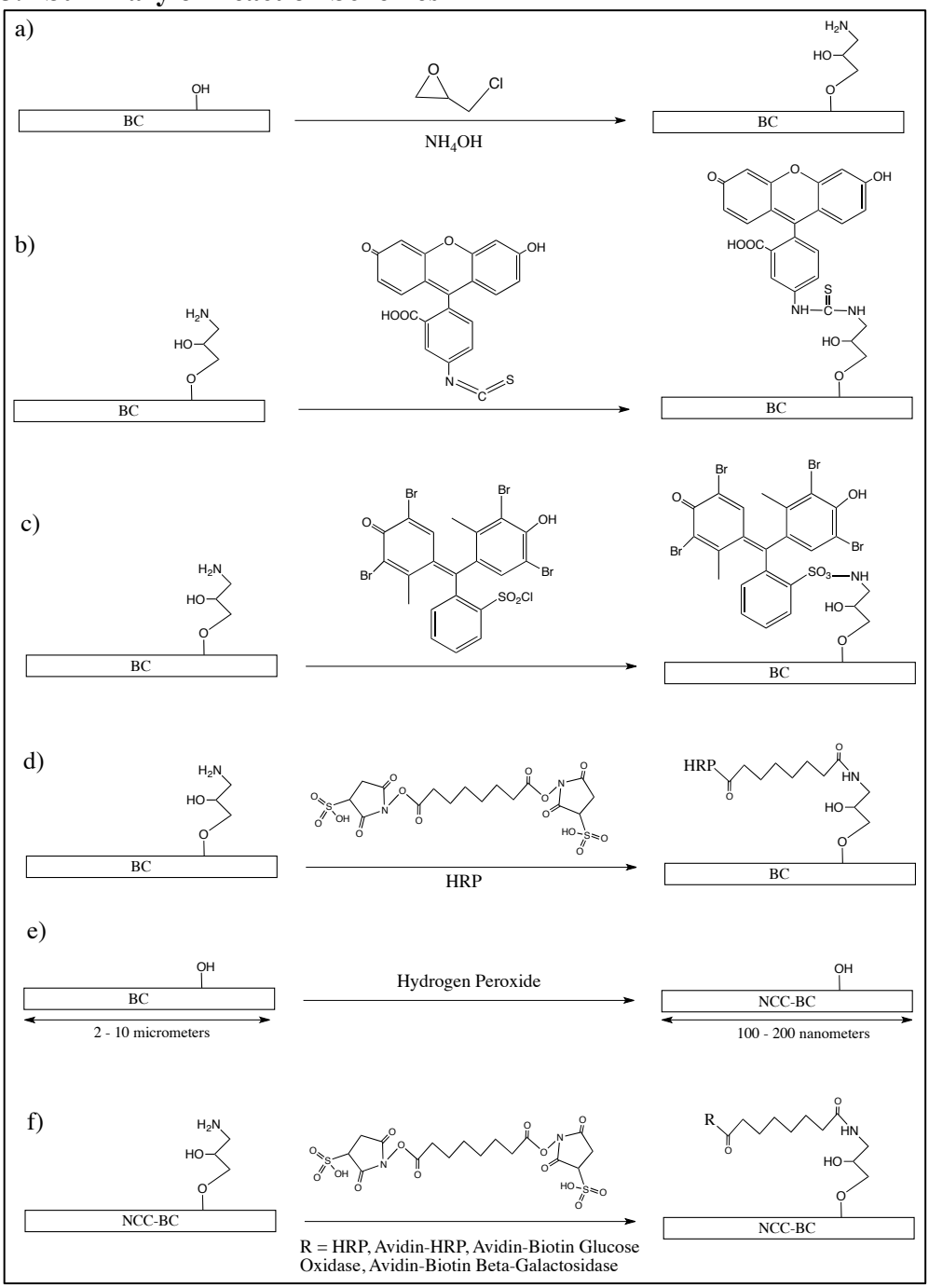

Figure 3.1: Summary of completed reactions. a) amination of BC; b) FITC conjugated aminated BC; c) BCG conjugated BC; d) HRP conjugated aminated BC; e) Hydrogen peroxide hydrolysis of BC; f) HRP, avidin-HRP, avidin-biotin glucose oxidase, and avidin-biotin β-galactosidase conjugated amine NCC-BC.

CHAPTER 4 – RESULTS AND DISCUSSION

Bacterial cellulose was produced by the *G. xylinus* bacteria in the form of fibres with dimensions ranging from 2-10 μm in length and 20-30 nm in diameter (Figure 4.1 a). Functionalization through a two-step reaction, involving epichlorohydrin and ammonium hydroxide, introduced primary amine groups to BC (Figure 4.1 b). Aminated BC was functionalized with the fluorescent tag fluorescein-5'-isothiocyanate (FITC) and a pH indicator, bromocresol green (BCG). Subsequently, horseradish peroxidase (HRP) was used to demonstrate protein conjugation (Figure 4.1 c). Through the successful demonstration of protein conjugation, a nano-sized fibre capable of cellular delivery of therapeutics must be created for intracellular delivery. Hydrogen peroxide was used as the hydrolyzing agent to create NCC-BC with narrow size distribution with approximate dimensions of 150 nm in length and 15 nm in diameter (Figure 4.1 d). The NCC-BC fibre was functionalized to introduce primary amine groups (Figure 4.1 e), to which HRP, avidin-HRP and avidin was directly linked using the available N-terminal amino acid groups. Biotinylated glucose oxidase and biotinylated β-galactosidase was complexed to the attached avidin for the demonstration of protein conjugation through an avidin-biotin complex (Figure 4.1 f).

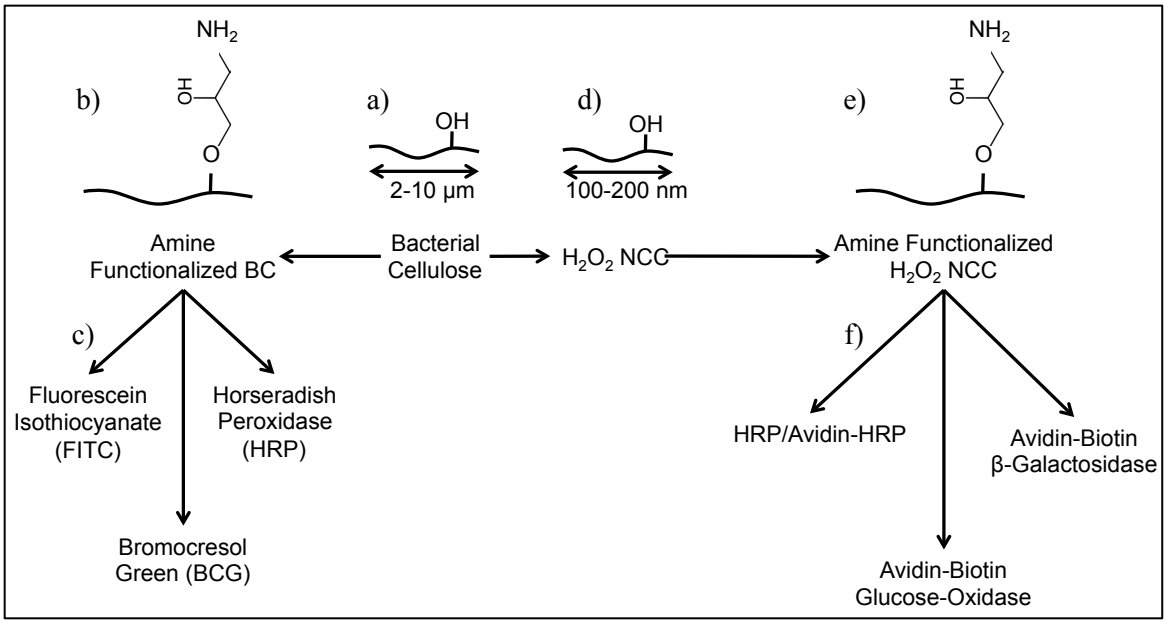

Figure 4.1: Outline of completed work. a) BC production; b) Amination of BC; c) Fluorescence and protein conjugation of aminated BC; d) Hydrolysis of BC; e) Amination of NCC-BC; f) protein conjugation and avidin-biotin complexation of aminated NCC-BC.

4.1 Physiochemical Characterization of Aminated BC

4.1.1 Chemical Structure Determination

In order to proceed with the conjugation of either a fluorescent tag or a model protein, it is necessary to confirm the presence of primary amine on the bacterial cellulose surface. Several techniques have been used to characterize the aminated BC product. Fourier transform infrared (FTIR) spectroscopy was used to demonstrate the addition of primary amine groups to BC (Figure 4.2).

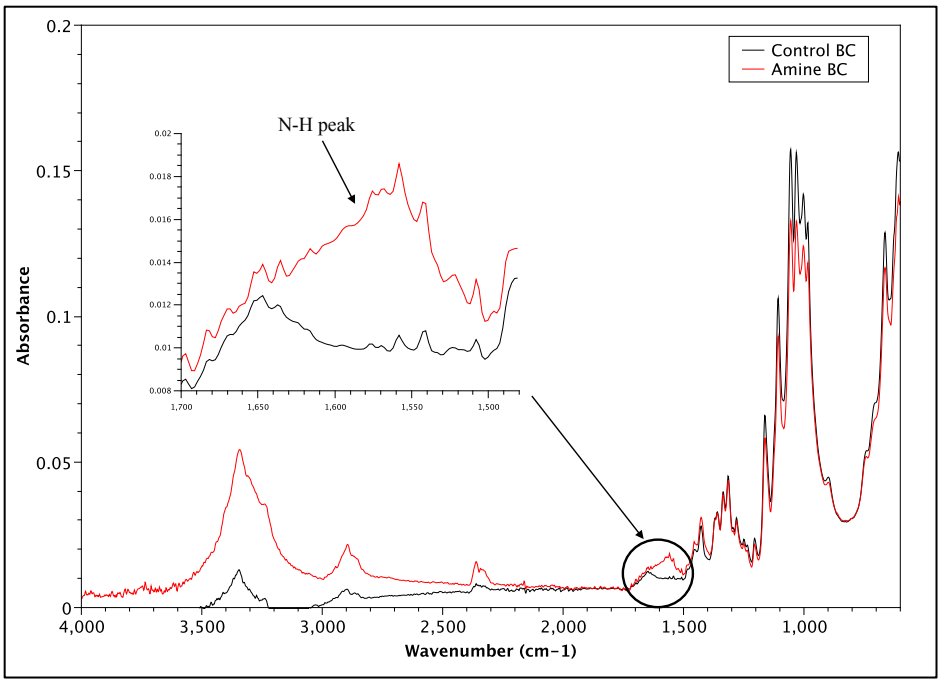

Figure 4.2: FTIR spectra of BC and aminated BC.

A typical infrared spectrum of a primary amine consists of absorbance peaks between 3500 and 3200 cm^{-1} and 1640 to 1500 cm^{-1}. The peak formation between 3500 and 3200 cm^{-1} is often masked by the O-H absorption of the OH group. However, the other characteristic peak at 1640 to 1500 cm^{-1} can be used for further characterization. The structure of BC consists of many surface hydroxyl groups, which sometimes makes it very difficult to distinguish additional groups chemically functionalized to its backbone. Nonetheless, the control BC FTIR spectrum shown in figure 4.2 is consistent with the literature.[99] The presence of C-O-C stretching vibrations is outlined by the sharp band at 1080 cm^{-1}, whereas the carbonyl groups at the reducing end of each BC fibre is

displayed by the absorption around 1490 cm^{-1}. As mentioned previously, the broad band ranging from 3500 to 3200 cm^{-1}, peaking at approximately 3400 cm^{-1}, is the characteristic peak for the presence of hydroxyl groups. Finally, the band at 2800 cm^{-1} is characteristic for the aliphatic C-H stretching vibration. Although the primary amine peak at 3500 - 3200 cm^{-1} is masked by OH absorption, the other distinctive peak ranging from 1640 to 1500 cm^{-1} is easily distinguishable from the control BC as shown in figure 4.2. The presence of this peak confirms that a primary amine was successfully conjugated to the BC surface. However, using FTIR spectroscopy does not determine to which carbon the primary amine is functionalized. It has been speculated that amine functionalization to the BC surface occurs either through the C6 or C2 carbon. Since the epichlorohydrin intermediate procedure is considered to be an etherification reaction, etherification reactions generally show slight preference for the hydroxyl groups on the C6 and C2 carbons verses C3 carbons (C2 > C6 > C3); although, it can access any hydroxyl group on the cellulose surface.[100]

4.1.2 Quantification of Amine on Bacterial Cellulose

The quantification of the amount of amine in aminated BC is essential for the application of therapeutics delivery. Greater concentrations of amine on the BC surface equate to greater loading of therapeutics. The quantification of amine was obtained through the use of acid-base pH titration (Figure 4.3). Through acid-base titration, quantification of amine groups, along with the pKa of the aminated BC can be obtained. The shift of the titration curve, either left or right, to the control can give valuable information with regard to the functionalization of the product. When titrating an acid to a base, a shift to the right of the control titration curve demonstrates additional basic functional groups, as a greater amount of acid is required to neutralize the product (Figure 4.3). Using equation 2 in chapter 3, the amine content was calculated to be 1.75 ± 0.18 mmol/g of BC, which equates to 28.3% of hydroxide groups being aminated, or approximately 1 per 3.5 anhydroglucose repeating units.

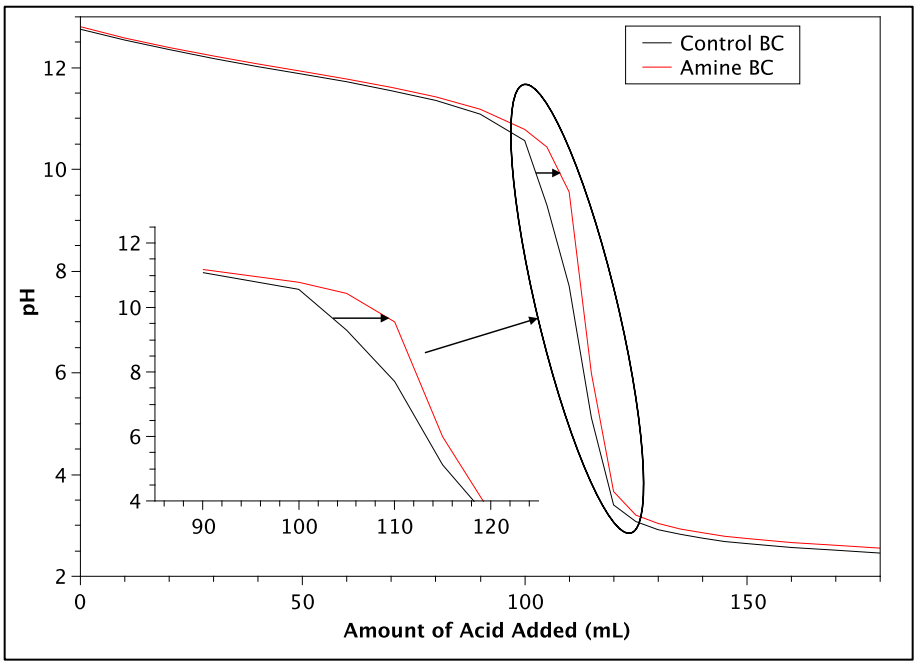

Figure 4.3: Acid-base titration curve comparing aminated BC and control BC.

When comparing this result to the selective carboxylation reaction reported by Spaic, the functionalization of amine is greater as the carboxyl content reported is 1.13 ± 0.02 mmol/g of BC.[42] This increase in functional attachment can be attributed to the etherification reaction, as epichlorohydrin can access the two more sterically hindered secondary alcohols at C2 and/or C3, where the TEMPO-mediated oxidation reaction is selective to C6. However, in both cases, the functionalization is relatively low compared to the available hydroxyl groups capable for functionalization. This can be due to the accessibility of the hydroxyl groups buried within the crystalline region of the cellulose I structure. The hydrogen bonding within the crystalline portion of the structure decreases the accessibility of the hydroxyl groups, therefore limiting their availability. Nonetheless, amination of the bacterial cellulose fibre has the added potential benefit of being capable of functionalizing to all hydroxyl groups without the limitation to only the primary hydroxyl group on carbon six. The increase in functionalization of amine compared to carboxylation further supports the hypothesis of epichlorohydrin reacting with any available hydroxyl group.

The apparent pKa was calculated, using the Henderson-Hasselbalch equation, to be 11.0 ± 0.1.[101] This high apparent pKa demonstrates that the amine groups will be

protonated at physiological pH, making it ideal for gene therapy. The amines can form an ionic complex with negatively charged proteins, RNA and DNA.[102] This pKa is relatively high compared to the values reported in the literature, as chitosan containing a primary amine had a pKa of 6.5[102] and a tertiary polyelectrolyte amine derivative had a pKa of 9.5.[103]

4.1.3 Crystallinity of Aminated BC

X-ray diffraction (XRD) patterns of BC and aminated BC are shown in figure 4.4, which analyzes the crystallinity, crystal size and inter-crystal spacing of the product. It has been reported in the literature that the structure of cellulose I has three characteristic peaks located at $2\theta=17^{o}$, $2\theta=19^{o}$ and $2\theta=26^{o}$, which is consistent with the XRD pattern provided in figure 4.4.[104] When comparing the XRD pattern for aminated BC product to the control BC, no apparent peak shifting, or new peak formation was observed verifying that the introduction of amine groups to the bacterial cellulose surface occurred on the crystal surfaces and amorphous regions, and did not affect the crystal structure of native BC.

As mentioned in Section 2.1.1, two forms of cellulose I exist (Iα and Iβ) and it is very difficult to differentiate between the phases by observing a standard XRD pattern since the planes are crystallographically equivalent. However, it has been determined that all cellulose I structures contain some amounts of both Iα and Iβ but differ in their ratio. Bacterial cellulose is a cellulose I structure with an Iα dominance, but does contain trace amounts of Iβ. Since the planes are crystallographically equivalent, it is evident that there is difficulty in differentiating between the two-cellulose structures. Nonetheless, the diffraction peaks located at 17^{o}, 19^{o}, and 26^{o}, are identical in both cases but differ in the plane characterization. As shown in figure 4.4, the diffraction peak located at 17^{o} corresponds to the (1 0 0) plane of cellulose Iα, and the (1 $\bar{1}$ 0) plane of 1_{β}, whereas the diffraction peak at 19^{o} corresponds to the (0 1 0) plane of I_{α} and the (1 1 0) plane of I_{β}.[104] The diffraction peak located at 26° corresponds to the (1 1 0) plane of cellulose I_{α} and the (2 0 0) plane of I_{β}. The d-spacing of the three diffraction peaks for cellulose I had

previously been characterized to have values of 0.614 nm, 0.532 nm and 0.394 nm [104], which is consistent with the results reported in Table 1.

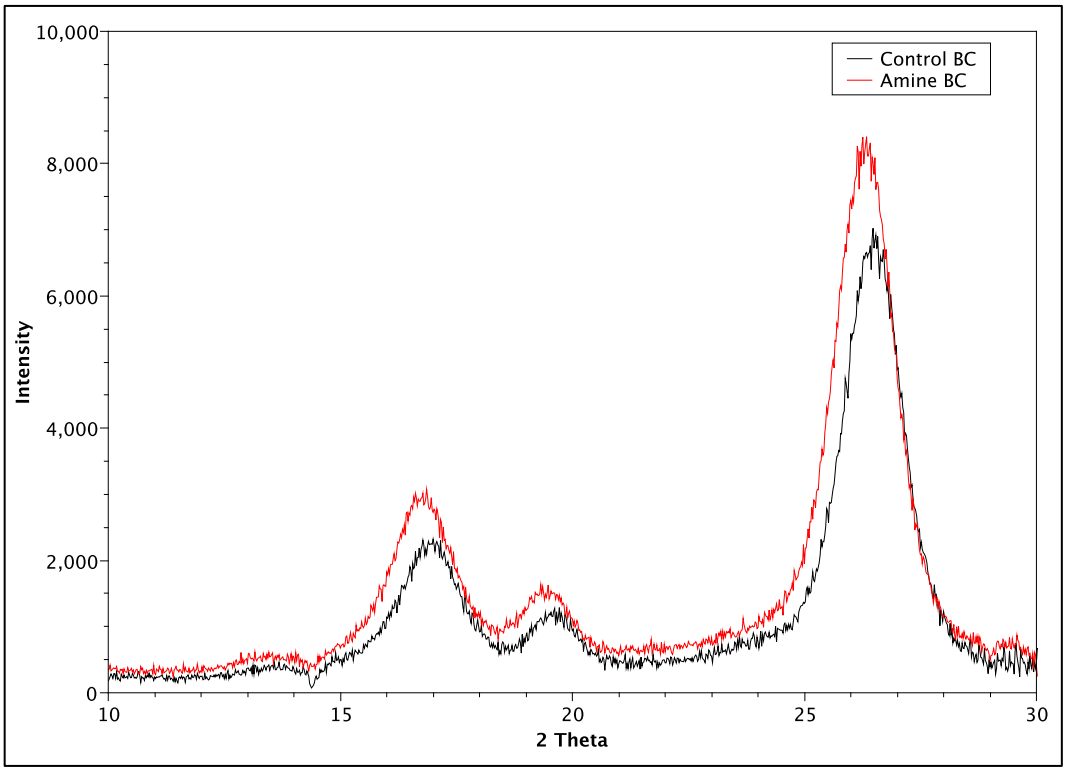

Figure 4.4: XRD patterns of aminated BC and control BC.

Table 1: Summary of crystallinity parameters obtained from the XRD patterns for BC and aminated BC. Values are shown ± one standard error, and significantly different values ($P \leq 0.05$) between control BC and aminated BC for the same parameter are marked with a * (n=3).

	Crystallinity (%)	Location (2θ)	d-spacing (nm)	Crystal size (nm)	Inter-crystal distance (nm)
Control BC	69 ± 1	17°	0.61 ± 0.01	5.13 ± 0.02	6.4 ± 0.1
Aminated BC	73 ± 1*		0.61 ± 0.01	4.67 ± 0.02*	6.0 ± 0.1*
Control BC		19°	0.53 ± 0.01	5.6 ± 0.1	6.9 ± 0.2
Aminated BC			0.53 ± 0.01	5.1 ± 0.1*	6.2 ± 0.1*
Control BC		26°	0.39 ± 0.01	7.17 ± 0.04	8.7 ± 0.1
Aminated BC			0.39 ± 0.01	7.00 ± 0.07	8.3 ± 0.2*

It is also important to note the difference in crystallinity between the control BC and the aminated BC. The crystallinity increase of approximately four percent can be attributed to a loss in water-soluble fractions from the degradation of aminated BC to celluronic acids in the amorphous regions. It is assumed that the amination reaction also targets the amorphous region of the cellulose structure due to its vulnerability to chemical

attack. The d-spacing (spacing between similar crystal planes) does not change following amination since the reaction is taking place on the surface of the crystalline regions. However, there was a decrease in inter-crystal distance observed, which can be attributed to the degradation to soluble products and the loss of the amorphous regions caused by the amination reaction. Finally, the decrease in crystal size can be ascribed to the reaction occurring on the crystal surface, which results in a change of the hydrogen bonding with water.

4.1.4 Surface Charge of Aminated BC Fibres

In order to determine surface charge on bacterial cellulose, ζ-potential measurements were performed on sonicated 0.3 mg/mL suspensions at pH 7. Figure 4.5 displays the results obtained for both control BC and aminated BC, which had values of -12.2 ± 0.7 and -3.0 ± 0.3 mV respectively. In the literature, typical ζ-potential values for cellulose are in the range of -5 to -50 mV at pH 7, which is strongly dependent on the origin of cellulose used.[105, 106] Sources of plant cellulose, such as cotton, have demonstrated low negative ζ-potential values ranging between -10 to -20 mV.[107] It has also been reported that the magnitude of the negative ζ-potential can vary with water content of the fibres, salt concentration and formation of a double layer. Many studies have determined that polymers with large absolute values of ζ-potential have a more colloidally stable structure compared to those whose values are close to 0 mV. It was also determined that the ζ-potential can also fluctuate with pH as acidic conditions cause a decrease in ζ-potential for cellulose.[105] Variations in ζ-potential can also be due to differences in the type and quantity of electrolyte ions absorbed to the BC surface. The low ζ-potential of BC can be attributed to the hydrogen-bonded ions originally present in the bacterial culture media, which were not completely removed, even though vigorous washing did take place. The purity and conductivity of water during the purification process is an important factor as conductivity increases with increasing concentration of ions. Variations have also been noticed within the same cellulose origin. The ζ-potential value of BC reported in this thesis (-12.2 ± 0.7 mV) is much higher than the ones reported previously in our work (-40 and -47 mV). This increase in ζ-potential is due to a new culture production of *G. xylinus*. The previous values were reported from a previous

batch of BC whose ζ-potential was slightly lower. Since native cellulose does not contain any functional groups, other than the surface hydroxyls, it is estimated that negative ions are adsorbed onto the fibre surface through hydrogen bonding.

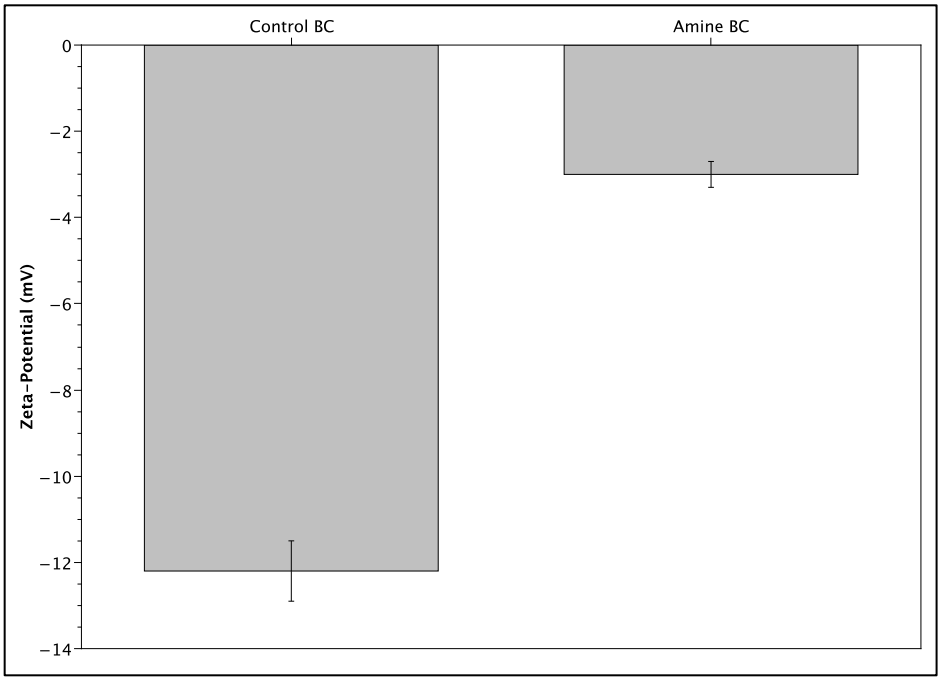

Figure 4.5: ζ-potential measurement at pH 7 of control BC and aminated BC.

Surface functionalization of the bacterial cellulose fibre can also lead to a change in surface charge. Mahmoud et al. (2010) used the same amination reaction reported in this thesis to conjugate FITC and RBITC to the surface of NCC derived flax cellulose fibres. They reported that NCC derived flax cellulose fibres has a ζ-potential of -31.3 mV at pH 7, due to sulfate ester groups that are deprotonated under these conditions. However, when binding RBITC to the aminated NCC product, a positive ζ-potential value of 8.7 mV at pH 7 was noted. Also, it was noticed that when binding FITC to the aminated NCC surface, the ζ-potential decreased to -46.4 mV. It was concluded that the functional groups on both RBITC (amine) and FITC (carboxylic acids) play a critical role in the surface charge. More importantly, it was noticed that the ζ-potential of RBITC becomes more positive at lower pH (amine becomes protonated and charged), where the ζ-potential of FITC becomes more negative at higher pH (carboxylic acid becomes deprotonated and charged).[54]

As demonstrated by Mahmoud et al., surface functionalization plays an important role on the effect of surface charge. This is further exemplified through the increase in ζ-potential through the amination reaction. Figure 4.5 displays the increase in ζ-potential from -12.2 ± 0.7 for the control BC to -3.0 ± 0.3 mV for aminated BC, which validates the surface functionalization of cellulose. These results have also been obtained on the previous batch of BC, which resulted in a ζ-potential of -42 ± 7 mV for control BC, and a -4 ± 6 mV ζ-potential for the aminated product. This increase in surface charge can also be seen in figure 4.6, as an increase in surface charge can cause slight agglomeration and poor dispersion of the fibres since there is a slight decrease in electrostatic repulsion of the amininated BC fibres. However, this decrease in electrostatic repulsion is so slight that no noticeable agglomeration was noted throughout this study. Nonetheless, this increase in ζ-potential demonstrates that the amine groups will be protonated at physiological pH, further validating its application for gene therapy, as an ionic complex can be formed with negatively charged proteins, RNA and DNA.

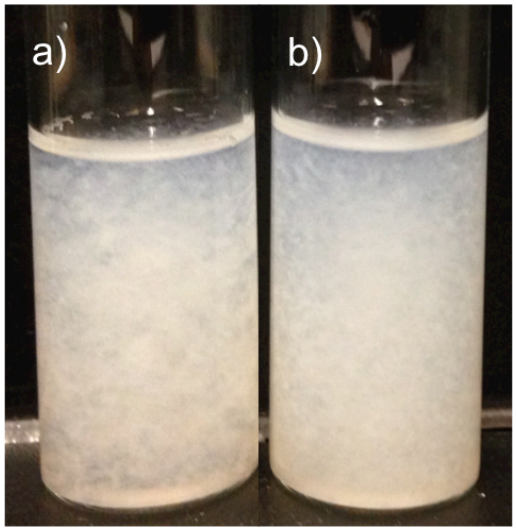

Figure 4.6: Photograph of a) control BC and b) aminated BC immediately after sonication.

4.1.5 Effect of Surface Charge of Aminated BC Fibres

In order to demonstrate the effect of the surface charge, water retention values (WRV) of functionalized aminated BC hydrogels were calculated under varying pH conditions, to demonstrate its swelling behavior as a function of pH. Aminated BC was tested from pH 4 (fully protonated and charged) to pH 13 (fully deprotonated and uncharged). Figure 4.7 displays the results of the swelling behavior of aminated BC, and

can be seen that the WRVs decrease as pH increases past the pKa and becomes neutral. These results are not pronounced to the degree reported for carboxylated cellulose[42], which might be due to the ζ-potential value of aminated BC, as the interaction with the polar solvent water is much weaker for aminated BC than oxidized BC. Decreasing the pH of aminated BC from pH 13 increases its surface charge. This in turn pushes the polymer to a near-zero ζ-potential at pH 7, which could be a strong driving force for increased water absorption.

The WRV of plant cellulose (PC) have reported values between 50 to 150%, which is significantly lower than the values reported in this thesis for BC (3,160 ± 70 %) at pH 7.[38, 39] Since the reported studies have been completed on cellulose sources other than bacterial (hardwood kraft pulp and cotton linters), the diameters of those fibres are between 25-50 μm, which is approximately 1,000 times larger than that of BC. The volume specific surface area of a cylindrical fibre is inversely proportional to its diameter, which can be attributed to the approximate 100-fold increase in WRV from PC to BC at a pH of 7.

The WRV of aminated BC has shown to be pH sensitive (Figure 4.7). It was demonstrated that aminated BC has an increasing swelling trend with decreasing pH, as the amine group becomes protonated and surface charge increases. However, the changes were not found to be statistically significant. This might be due to the ζ-potential of aminated BC nearing zero, which could lead to agglomeration of fibres and weaker interaction with the solvent. This will cause a reduction in electrostatic repulsion and hydrogen bonding to water, and cause slight agglomeration of the fibres, which attributes to the lack of stronger pH dependence and lower WRVs. Nonetheless, aminated BC demonstrated a maximum WRV increase of 280% at pH 7, which is much higher than that found in the literature for other sources of cellulose.[108]

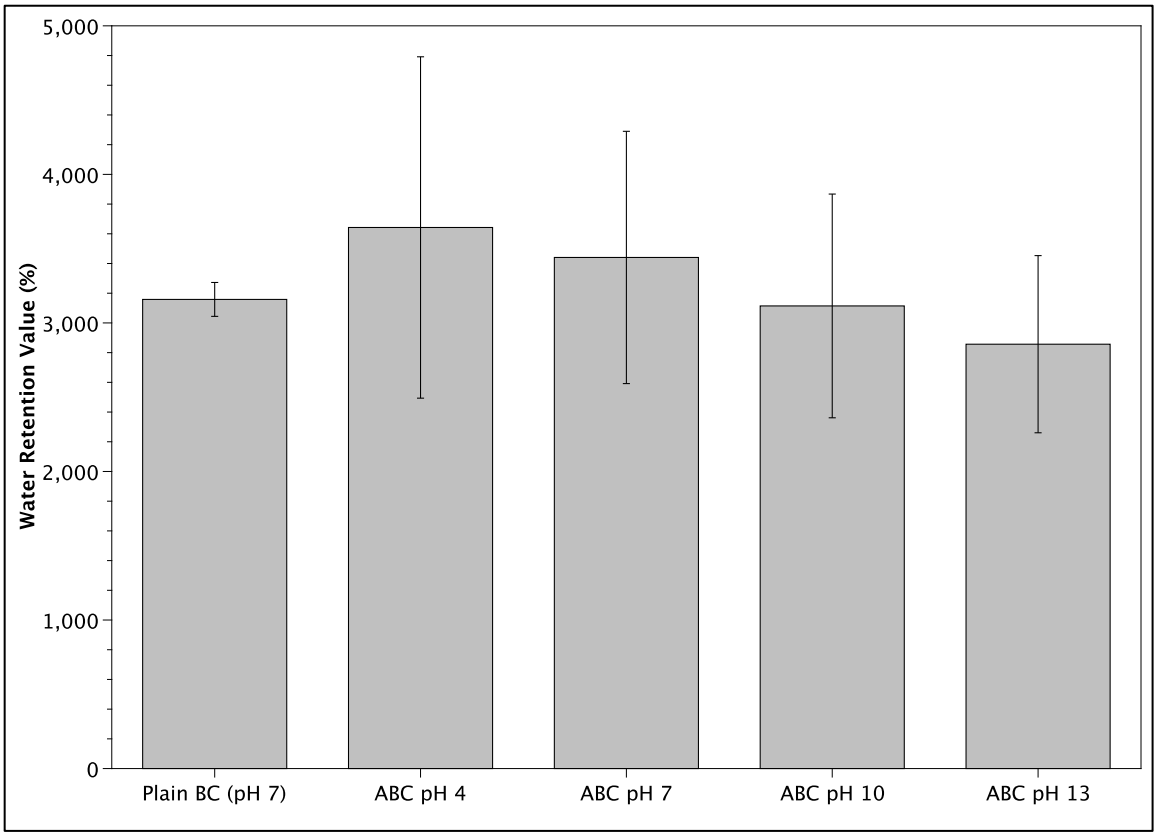

Figure 4.7: Water Retention Values of control BC (pH 7) and aminated BC (pH 4 - 13).

4.1.6 Morphology of Aminated BC Fibres

The morphology of the aminated fibres were analyzed by transmission electron microscopy (TEM) by depositing sonicated 0.3 mg/mL suspension of BC fibres on a carbon-coated TEM grids, followed by negatively staining the sample with uranyl acetate to develop a contrast. Figure 4.8 pictorially demonstrates the morphological differences between native BC and aminated BC. It can be seen though Figure 4.8b, that aminated BC displays a frayed appearance, with individual fibrils diverging from the ordered bundles that make the fibres in native BC. The speculation of this occurrence is due to the introduction of new cationic functional groups to the fibril surface, which disorders the hydrogen-bonding network between the fibrils, causing an unbundling of fibres.

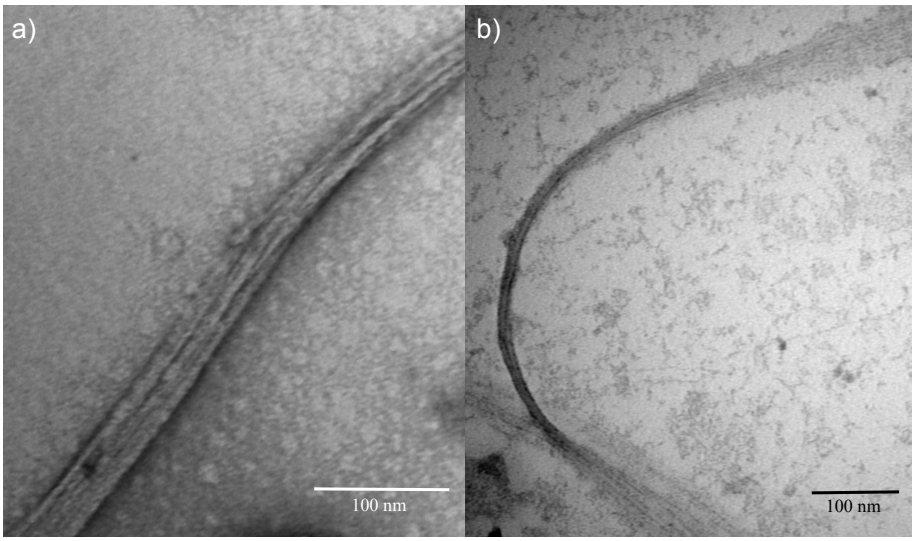

Figure 4.8: TEM images of a) control BC; and b) aminated BC with a frayed appearance.

To further analyze this phenomenon, the diameters of native BC were compared to those of aminated BC (Figure 4.9). It is clearly shown that the aminated BC fibres have significantly decreased in diameter from 24.3 ± 14.3 to 13.6 ± 7.1 nm with the introduction of functional groups. Even though there was high functionalization of amine to the BC surface, the average diameter of the aminated BC fibres did not decrease by a statistically significant amount following the amination reaction. As mentioned previously, the addition of functional groups also causes a partial loss to the amorphous regions, which also adds to the decrease in the fibre diameter. However, it cannot be said that all fibres were separated into fibrils as many retained their bundled form, as the amination reaction is mild enough to not completely cleave all amorphous regions. No previous study on the frayed appearance of aminated BC fibre is known, however Saito et al. quantified the diameters of TEMPO oxidized cellulose to be 3-5 nm.[109] The diameters of the smallest element in the cellulose structure are fibrils consisting of glucan chains, which have diameters ranging between 3 to 5 nm. Therefore, in order to achieve this diameter, pre-treatment of the cellulose must be done either through blending, mercerization or other methods. As mentioned chapter 2, these pre-treatment methods often compromise the crystal structure of cellulose.

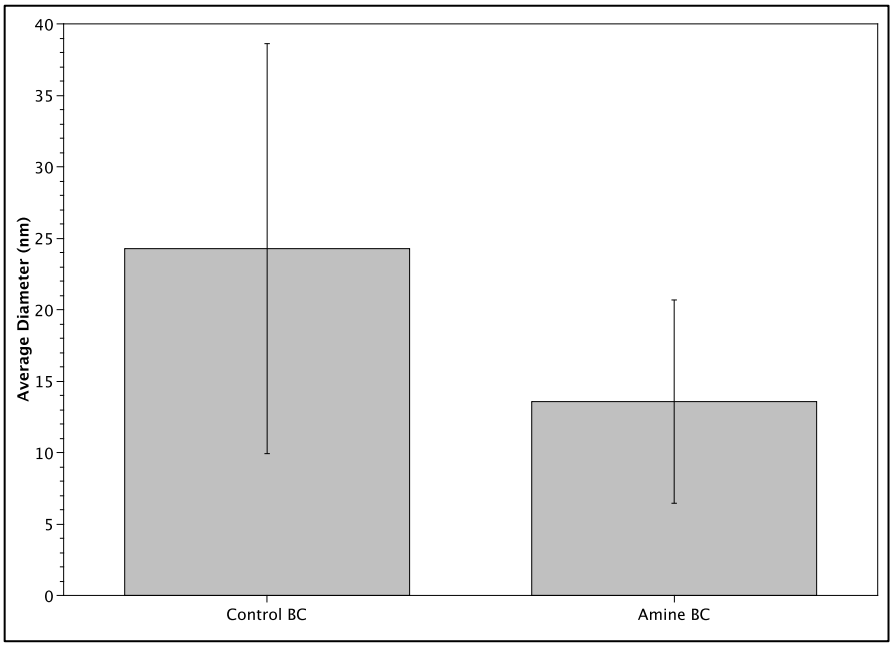

Figure 4.9: Average diameter comparison of 324 control BC and aminated BC fibres from TEM images.

4.2 Fluorescence and Protein Conjugation to Aminated BC

4.2.1 Aminated BC/FITC Conjugation

Versatility of the aminated BC product for the conjugation of molecules of interest was displayed through the attachment of the fluorescent dye FITC. FITC was covalently bound to aminated BC and florescence spectroscopy was used to quantify its loading. Figure 4.10a and 4.10b pictorially display the unlabeled and FITC labeled BC suspensions under ultraviolet light, and under normal lighting conditions respectively. The unlabeled BC suspension was colourless, opaque, and did not fluoresce under ultraviolet light, while the FITC labeled suspension appeared opaque, slightly yellow in natural light and fluoresced under ultraviolet conditions. This colour change denotes the successful attachment of FITC to the aminated BC surface. To further quantify the loading, fluorescence spectroscopy was done on the resulting product. Figure 4.10c displays the emission spectrum of the unlabeled and FITC labeled aminated BC suspensions. Unlabeled aminated BC showed no emission while the FITC labeled aminated BC suspension showed an emission peak at 521 nm, which is accurate to the emission peak of FITC. By using the emission intensities of free FITC and FITC labeled aminated BC, the labeling content was calculated to be 0.42 ± 0.03 FITC moieties per 100

anhydroglucose units (AGU). This loading is comparable to the one reported by Dong et al. on cellulose nanocrystals derived from softwood pulp.[46]

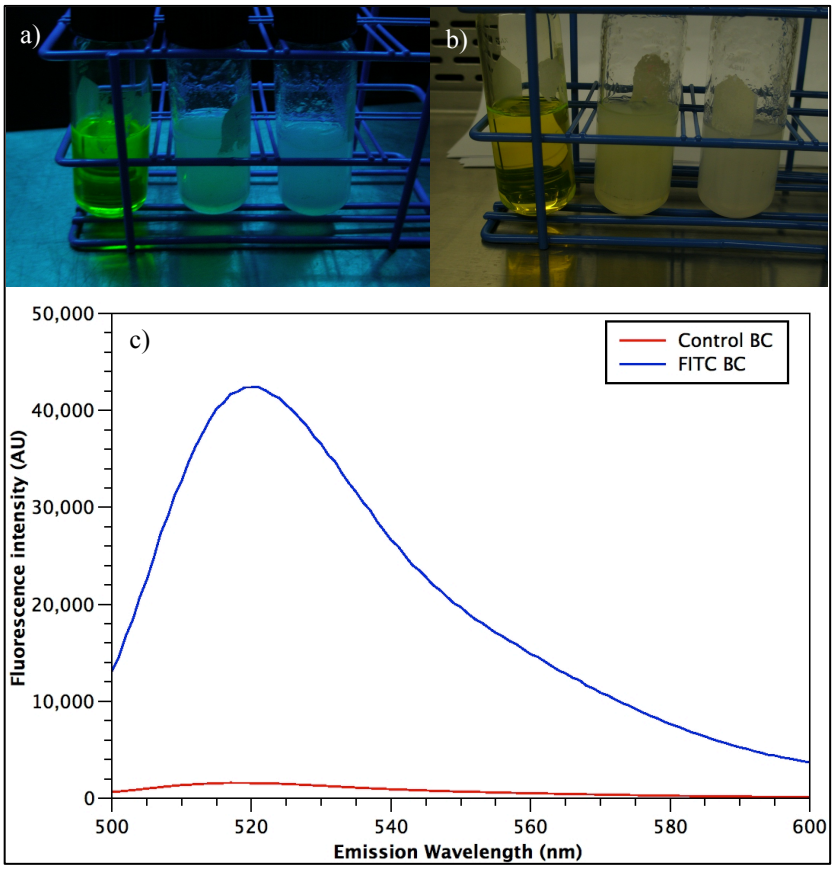

Figure 4.10: Images comparing; a) free FITC (left), FITC conjugated BC (center), and aminated BC (right) under ultraviolet lighting; b) free FITC (left), FITC conjugated BC (center), and aminated BC (right) under natural lighting; c) Fluorescence spectrum comparing FITC conjugated BC to control aminated BC.

It was also noticed that the conjugation of FITC to aminated BC displays a slight dispersion of fibres. Mahmoud et al. demonstrated the same FITC conjugated cellulose product on enzyme treated flax fibres using the same reaction scheme developed by Dong et al. as utilized in this thesis.[54] They measured the ζ-potential to be -46.4 mV after FITC was conjugated to the aminated cellulose compared to -31.3 mV of pristine cellulose nanocrystals at pH 7. They also analyzed the ζ-potential after increasing the pH to 8, which decreased the ζ-potential of FITC conjugated cellulose even further to -48.7 mV. It is important to note that the reference ζ-potential of pristine cellulose does not consider the increase in ζ-potential attributed to the amination reaction. Therefore, the decrease in ζ-potential from aminated-cellulose to FITC-cellulose would have had a

greater impact. The acidic functional group on FITC has a noteworthy influence on the total surface charge of the entire system. This is further displayed in the cellular uptake studies preformed by the same group. They noticed that FITC-cellulose aggregates only around the cells and could not permeate the cell surface. This occurrence was due to the repulsive forces between the anionic hydroxyl-terminated FITC-cellulose and the anionic cellular membrane.[54] This also explains the fibre dispersion noticed in our study. The interaction of the FITC conjugated aminated BC fibres are similar to oxidized BC fibres as both systems contain an acidic functional group, which increases its electrostatic repulsion to introduce a dispersion effect. In the case of cellular delivery of acidic systems, altering the medium pH will adjust the surface charge of the nanopartics, creating an effective charge distribution for fluorescent probe delivery.

4.2.2 Aminated BC/BCG Conjugation

It is useful to attach fluorescent labels to the aminated BC surface as it can be used to study the interaction of aminated BC fibres with cells to demonstrate the biodistribution and biocompatibility of aminated BC when put *in vivo*. However, it is important to consider the effect of pH when attaching either fluorescent labels or therapeutic proteins. Bromocresol green (BCG), mainly used as a pH indicator and as a tracking dye for DNA agarose gel electrophoresis, was used to show the attachment of a florescent label to the aminated BC surface under varying pH conditions. Not only will this demonstrate a colour change to the product, by denoting a successful attachment, it will also be used to validate the attachment under harsh pH conditions. For certain delivery methods (oral), delivery systems must withstand and remain conjugated to the therapeutic molecule under the harsh pH environments of the stomach.

BCG was covalently bound to the aminated BC and UV/VIS spectroscopy was used to quantify its loading. Figures 4.11a displays the BCG labeled aminated BC suspensions under varying pH conditions. The phenol groups of BCG ionize at pH 2 to give the monoanionic form (yellow), which further deprotonates at pH 6 to give the dianionic form (blue). This pH dependent colour change is expected to occur with the BCG labeled BC suspension, as the phenol group will be subjected to the pH difference.

The BCG labeled BC suspension varied in colour from yellow (pH < 3) to green (pH > 7), which suggests that the BCG was not fully deprotonated. This could be due to the concentration difference of BCG between the calibration and labeled suspension. As mentioned previously, only 28.3% of the available anhydroglucose residues are being aminated, which will limit the amount of BCG to be attached to the aminated BC fibre. Due to the limitation of BCG attachment, the colour will not be as potent as the calibration BCG suspension. By displaying the colour change, it denotes the successful attachment of BCG to the aminated BC surface under difference pH conditions.

To further quantify the loading, UV/VIS was completed on the resulting product. Figure 4.11b displays the absorbance spectrum of the unlabeled suspension at neutral pH and BCG labeled aminated BC suspensions at varying pH conditions (< 3 and > 7). Unlabeled aminated BC showed no absorbance while BCG labeled aminated BC at pH > 7 showed an absorbance peak at 610 nm, which illustrates the yellow-green colour. The labeling content was calculated to be 2.6 ± 0.2 BCG moieties per 100 AGU, which is 5 times the amount of loading compared to FITC conjugated aminated BC. The increase in loading can be attributed to the modified reactive site on BCG making it more readily available for functionalization.

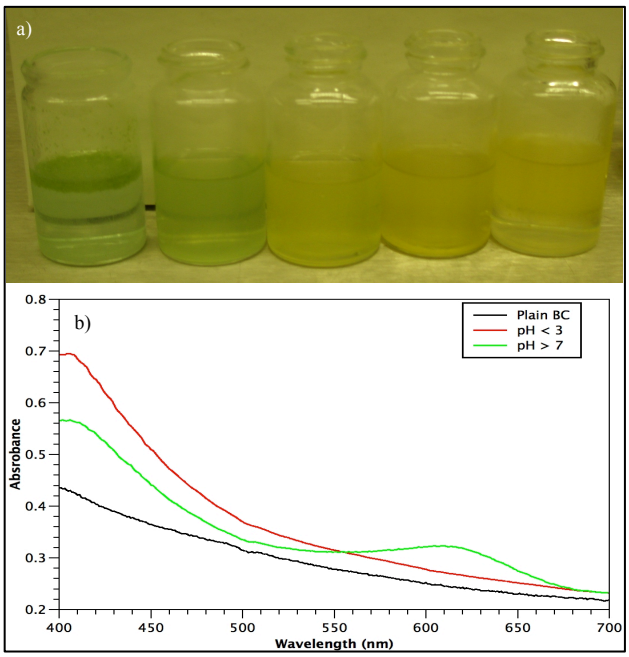

Figure 4.11: a) Image of 22 mg/L BCG BC suspension in varying pH conditions from pH 1 (right) to 12 (left); b) UV/VIS spectrum of BCG (pH < 3, pH > 7) and control BC at neutral pH

4.2.3 Aminated BC/HRP Conjugation

To demonstrate the ability of delivering therapeutic proteins and antibodies, the protein horseradish peroxidase (HRP) was used. HRP was covalently attached to the aminated BC surface through two different reaction mechanisms. The first approach involves the direct linkage of aminated BC to the surface amines on HRP. The second method involves the use of a bis(sulfosuccinimidyl) suberate (BS3) linker, linking the surface amines on aminated BC to the amines on HRP, increasing attachment yields. Table 2 displays the quantified values for both methods. The results were calculated either through an HRP activity assay or through the absorbance of the loading solution, where both quantification methods display the same results and outline the importance the BS3 linker. For the direct method, 0.01 ± 0.01 HRP moieties per 100 AGU was calculated, where for BS3 linker, 0.17 ± 0.01 HRP moieties per 100 AGU BC was determined.

Table 2: Quantification of HRP loading on aminated BC.

	Control Amine-BC	Amine-BC + BS3 Linker
mg HRP/g BC	0.02 ± 0.01	0.43 ± .03*
HRP/100 AGU	0.01 ± 0.01	0.17 ± 0.01*

(*)indicates significant statistical difference ($P<0.05$)

For the attachment of a protein molecule with a molecular weight like HRP (~ 40 kDa) to the aminated BC surface, the use of a linker would reduce the steric congestion at the attachment sites. The linker will act as the spacer arm to link HRP to the aminated BC surface to maximize loading. From table 2, it is evident that the attachment yield of the direct linkage between the available amines on BC to HRP is low, which can be attributed to steric congestion around the BC fibre. However, by aminating the surface of BC, an amine-to-amine linker can be used to attach available amines of therapeutic proteins to the BC surface to maximize loading efficiency.

When analyzing the attachment yield of the BS3 linker method, the relative loading is quite low compared to the results previous obtained from FITC and BCG conjugation. This low loading efficiency can be attributed to the linker choice (BS3). Since BS3 is an amine-to-amine linker, it is hypothesized that BS3 can also link the surface amines on BC to other surface amines on adjacent aminated BC fibres. Likewise,

the same occurrence can arise on HRP as BS3 can link the available amine residues on HRP to other amines on adjacent HRP moieties, which decrease the loading efficiency drastically. This phenomenon will be further analyzed in section 4.4, where the same reaction will be applied on nano-crystalline derived BC. Nonetheless, the significant increase in conjugation using the BS3 linker compared to the direct method illustrates the importance of the use of BS3 to reduce steric hindrance at the reactive sites on the aminated BC surface.

4.3 Physiochemical Characterization of Aminated NCC-BC

4.3.1 Chemical Structure Determination

FTIR was used on native BC, hydrogen peroxide hydrolyzed BC and aminated NCC-BC to identify the chemical functional groups introduced during both the hydrolysis and amination reactions (Figure 4.12). Since hydrogen peroxide is a strong hydrolyzing and oxidizing agent, we expect BC fibres with nano-sized dimensions (length and diameter), chemical oxidation (introduction of a carboxyl groups), and improved crystallinity (hydrolysis of amorphous regions). Through the amination reaction, the introduction of primary amines to the NCC-BC surface should be evident. In order to proceed with the conjugation of an avidin-biotin complex, verification of a primary amine on the aminated NCC-BC surface must be demonstrated and quantified.

When comparing the FTIR spectra of NCC-BC to control BC, the characteristic peaks for cellulose are present (C-O-C stretching vibrations at 1080 cm^{-1}, carbonyl groups at the reducing end of each BC fibre are displayed around 1490 cm^{-1}, characteristic peak for hydroxyl groups ranging from 3500 to 3200 cm^{-1}, peaking at approximately 3400 cm^{-1}, C-H stretching vibration characteristic for the aliphatic at 2800 cm^{-1}). However, when analyzing the peak differences, there is an additional peak present at ~1610 cm^{-1} for the NCC-BC spectra, which represents the signature peak of $O=C-O^-$ (carboxylate ion) stretching vibration band. Likewise, there is an additional peak at 1720 cm^{-1} for NCC-BC, which represents the characteristic band for the O=C-OH (protonated carboxylic acid) group. Since, the intensity is higher at 1610 cm^{-1}, it is concluded that the carboxyl groups were predominantly in the deprotonated form at neutral pH, but there is some trace of

protonated carboxylic acid groups present on the NCC-BC fibre. It is established that hydrogen peroxide is not only a dominant hydrolyzing agent; it can also be used as a strong oxidizing agent. When comparing this FTIR spectrum to the spectra of the highly selective oxidized BC reaction, the identical characteristic peak for a carboxylic acid at 1610 cm^{-1} is present. However, the protonated carboxylic acid group at 1720 cm^{-1} was not displayed for oxidized BC.[42] It was also noticed that the carboxylic acid groups on the oxidized BC surface was also primarily in its deprotonated form at neutral pH, which is consistent with our result. It has been extensively noted that the highly selective TEMPO-mediated oxidation reaction on BC and other sources of cellulose, occurs predominantly on the C6 primary alcohol of the BC fibre. Therefore, the literature can support the conclusion that the oxidation occurring through the hydrogen peroxide hydrolysis reaction is taking place on the primary alcohol groups, as the C6 hydroxyl is the most reactive.[42]

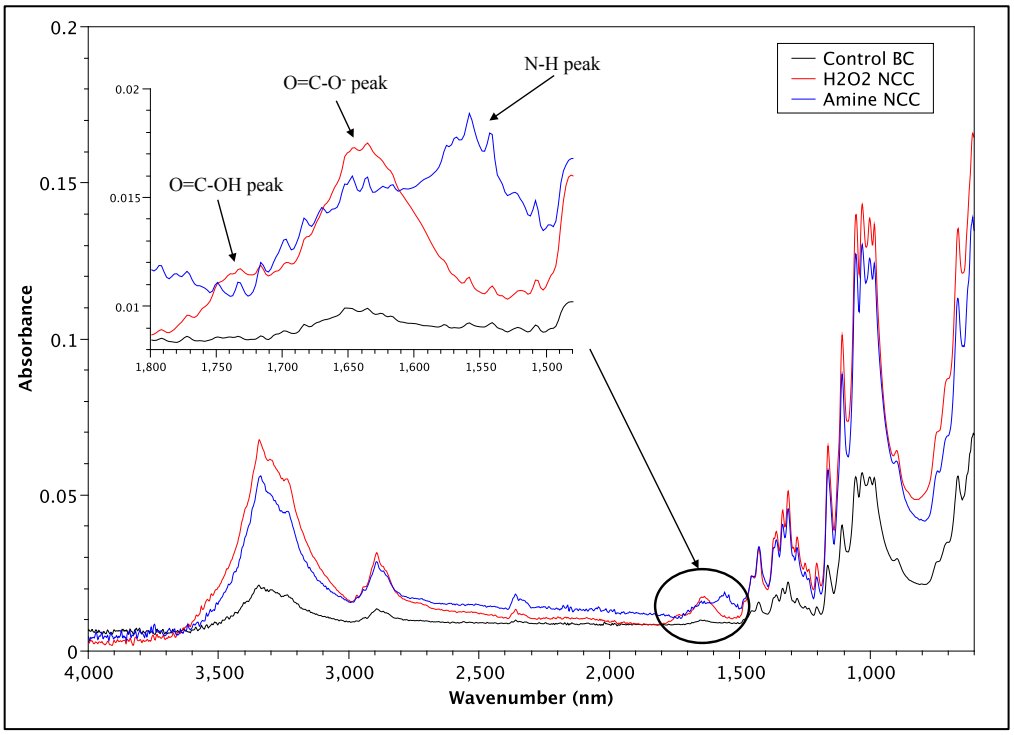

Figure 4.12: FTIR spectra of control BC, NCC-BC and aminated NCC-BC.

For the functionalization of NCC-BC with amines, a characteristic peak between 3500 and 3200 cm^{-1} and a peak ranging from 1640 to 1500 cm^{-1} should be present. As demonstrated in section 4.1.1, the characteristic N-H peak between 3500 and 3200 cm^{-1} was obscured by the intense O-H absorption of hydrogen-bonded water. The same

phenomenon is displayed here as the N-H peak was masked by the O-H absorption of alcohol, which shares the same frequency range. However, aminated NCC-BC exhibits many of the characteristic peaks displayed in native cellulose, which sometimes makes it very difficult to distinguish additional functional groups chemically functionalized to the backbone of BC. Nonetheless, the characteristic peak of a N-H (ranging from 1640 to 1500 cm^{-1}) is distinguishable from both the control BC and hydrogen peroxide hydrolyzed BC (Figure 4.12). Based on this peak, it can be said that a primary amine was successfully conjugated to the NCC-BC surface. The increase in intensity from 1720 to 1640 cm^{-1} is attributed to the carboxylic acid functional groups present on the surface of the aminated NCC-BC. Since hydrogen peroxide oxidized the NCC-BC product, carboxylic acid residues will evidently be present on amine functionalized NCC-BC. However, it is important to note that it is speculated that the amine functionalization to the NCC-BC surface occurs through the C2 carbon, and the oxidation of hydrogen peroxide will occur on the C6 carbon. Therefore, there should be no conflict of functionalization of amine to the NCC-BC fibre after hydrogen peroxide hydrolysis.

4.3.2 Quantification of Carboxylic Acid and Amine on Bacterial Cellulose Derived Nano-Crystalline Cellulose

As indicated by the FTIR results, the conversion of BC into NCC-BC using the hydrogen peroxide reaction results in the introduction of carboxylic acid groups on the surface of NCC-BC. This reaction is considered to be similar to the selective TEMPO-mediated oxidation reaction used to introduce carboxyl groups to the cellulose surface.[42] Quantification of the carboxyl content introduced to NCC-BC was determined through the use of acid-base pH titration (Figure 4.13a). Since carboxyl groups are an acidic addition to the NCC-BC surface, the acidic solution containing NCC-BC is titrate with base. The additional base need to neutralize the NCC-BC product compared to the control BC will determine the amount of carboxylic acid groups introduced to the NCC-BC surface. Through the use of equation 3 (Chapter 3), the carboxyl content was calculated to be 0.97 ± 0.18 mmol/g of NCC-BC, which equates to 15.8% of OH groups being oxidized, or approximately 1 per 6.3 anhydroglucose repeating units.

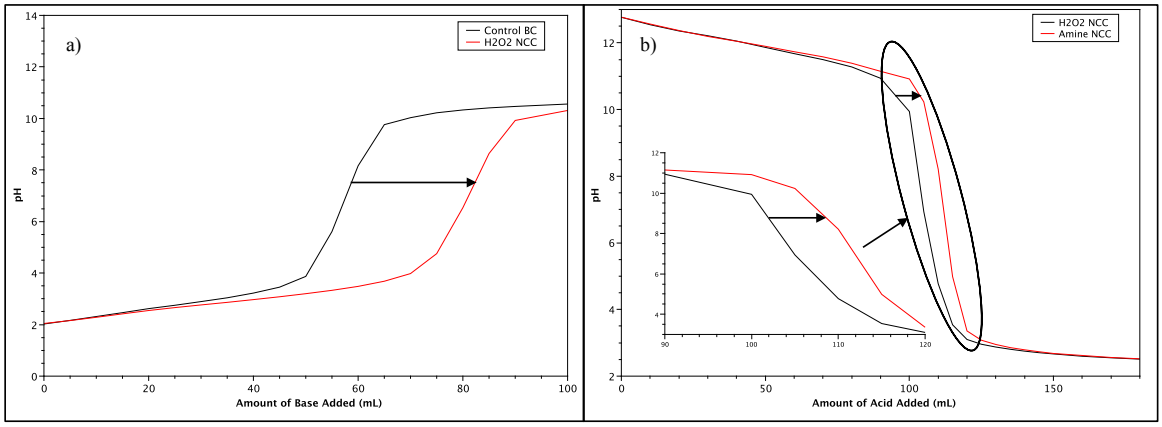

Figure 4.13: Acid-base titration curve of comparing a) NCC-BC to control BC; and b) aminated NCC-BC to unfunctionalized NCC-BC.

When comparing this result to the selective TEMPO-mediated reaction on native BC fibres, there is no statistical difference reported (1.13 ± 0.02 mmol/g of BC).[42] The carboxylic acid introduction through hydrolysis was not expected to reach the amount of carboxyl's introduced to cellulose through TEMPO-mediated oxidation. The oxidation associated with hydrogen peroxide is a byproduct of the hydrolysis method, and lower carboxyl content would have been more beneficial as the goal is to achieve an aminated NCC-BC product identical to native BC with smaller dimensions. Even though the introduction of carboxyl groups to NCC-BC was not expected, they provide the fibre with the necessary dispersion properties needed to prevent the agglomeration associated with the introduction of primary amines to the NCC-BC surface (further discussed in section 4.2.4). The calculated apparent pKa of NCC-BC was determined to be 2.96 ± 0.05, which is slightly lower than that reported by Spaic for TEMPO-mediated carboxylation (pKa of 3.90).[42] The low pKa demonstrates that the carboxyl groups on NCC-BC are entirely deprotonated at pH 7.

Primany amines were introduced to the NCC-BC surface after the hydrolysis of BC was completed (Figure 4.1e). It is now known that the NCC-BC product has a carboxyl content of 0.97 ± 0.18 mmol/g of NCC-BC. However, as discussed previously, this carboxyl formation is assumed to occur on the primary alcohol attached to C6, where the amination of cellulose is primarily occurring on the secondary alcohol on C2. Therefore, the amine content on NCC-BC should not be significantly affected by the

hydrogen peroxide hydrolysis of BC fibres. Quantification of the amine content introduced to the NCC-BC surface was determined through the use pH titration (Figure 4.13b). A basic solution containing the aminated NCC-BC product was titrated with acid. The additional acid needed to neutralize the aminated NCC-BC product compared to unfunctionalized NCC-BC will determine the amount of amine groups introduced to the NCC-BC fibre. The amine content was calculated to be 2.4 ± 0.9 mmol/g of NCC-BC using equation 2 (Chapter 3), which equates to 38.8% of hydroxide groups being aminated, or approximately 1 per 2.6 anhydroglucose repeating units. This quantification of amine is much higher than that reported in section 4.1.2 for aminated BC; however, due to the large standard error, there is no statistical difference between aminated BC and aminated NCC-BC, which demonstrates the consistency of the amine reaction. As mentioned previously, the high functional attachment can be attributed the etherification reaction, as epichlorohydrin can access the two more sterically hindered secondary alcohols at carbons two and three, and any unreacted primary alcohol groups that were not functionalized with carboxylic acids. The apparent pKa was determined to be 11.79 ± 0.02, which is slightly higher than the value reported in section 4.1.2. Again, this high pKa demonstrates that the amine groups on aminated NCC-BC will be protonated at physiological pH, demonstrating its use for gene therapy. Even though there is an average increase in amine content, the functionalization relative to the available hydroxyl groups capable for functionalization is low. One main function of hydrogen peroxide hydrolysis is to remove the amorphous regions of bacterial cellulose to provide a highly crystalline product. The hydrogen bonding within the crystalline portion of NCC-BC decreases the accessibility of the hydroxyl groups, therefore limiting their reactivity within the crystalline region of the cellulose I structure. Therefore, it is much more difficult to access these hydroxyls to obtain complete functionalization. Nonetheless, due to the non-selectivity of the amine reaction among the OH groups, a higher functionalization is expected and demonstrated compared to the highly selective carboxylation reaction.

4.3.3 Crystallinity of NCC-BC

XRD was used to determine the crystallinity, crystal size and spacing of BC and NCC-BC fibres. As mentioned previously, the structure of cellulose I has three

characteristic peaks located at $2\theta=17^{o}$, $2\theta=19^{o}$ and $2\theta=26^{o}$, which is consistent with the XRD pattern of the newly formed NCC-BC fibres provided in Figure 4.14.[104] The NCC-BC fibres demonstrated no apparent peak shifting, or new peaks verifying that the hydrolysis method used to remove the amorphous regions within the cellulose fibre did not affect the crystal structure of native BC. BC has a cellulose I structure with a Iα dominance, but does contain trace amounts of Iβ. As shown in Figure 4.14, the diffraction peak located at 17^{o} corresponds to the (1 0 0) plane of cellulose Iα, and the (1 $\bar{1}$ 0) plane of 1_{β}, whereas the diffraction peak at 19^{o} corresponds to the (0 1 0) plane I_{α} and the (1 1 0) plane of I_{β}.[104] The diffraction peak located at 26° corresponds to the (1 1 0) plane of cellulose I_{α} and the (2 0 0) plane of I_{β}. The d-spacing of the three diffraction peaks for cellulose I had previously been characterize to have values of 0.614 nm, 0.532 nm and 0.394 nm [104], which is consistent with the ones reported in Table 3.

The difference in crystallinity between BC and NCC-BC is of great significance. The crystallinity of NCC-BC has increased from 70 to 88%, which is directly related to the loss of water-soluble fractions from the degradation of BC to celluronic acids in the amorphous regions. Hydrogen peroxide is a hydrolyzing agent that targets the amorphous regions of the cellulose fibre. By removing the amorphous regions, the relative crystallinity of the resulting NCC-BC is greatly increased and the dimensions of the fibre would be significantly reduced. The d-spacing does not change following hydrolysis since the hydrolysis is taking place on the surface of the crystalline regions and only attacking the amorphous regions. If the reaction was left for a longer time period, nearly all the amorphous regions would be removed and the hydrogen peroxide would begin to attack the crystalline regions of the cellulose fibre. Since the d-spacing remained unchanged, degradation of the crystalline region did not occur. A decrease in inter-crystal distance observed, which can be attributed to the degradation to soluble products and the loss of the amorphous regions caused by hydrolysis, which is expected. However, the increase in crystal size is somewhat surprising. This increase in crystal size could be from the degradation of smaller crystals and the agglomeration of crystal domains as amorphous regions are digested.

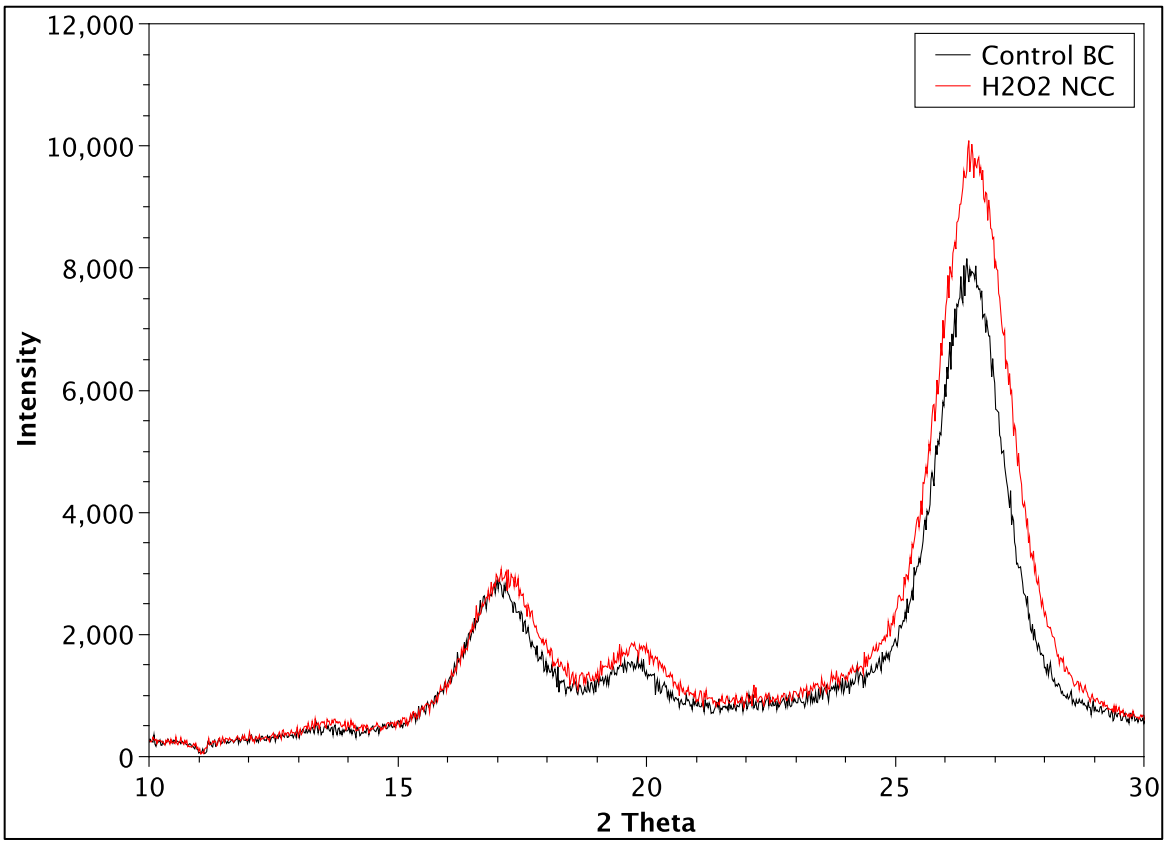

Figure 4.14: XRD patterns of control BC and NCC-BC.

Table 3: Summary of crystallinity parameters obtained from XRD for control BC and NCC-BC. Values are shown ± one standard error, and significantly different values ($P \leq 0.05$) between control BC and NCC-BC for the same parameter are marked with a * (n=3).

	Crystallinity (%)	Location (2θ)	d-spacing (nm)	Crystal size (nm)	Inter-crystal distance (nm)
Control BC	70 ± 1	17°	0.60 ± 0.01	5.10 ± 0.02	0.772 ± 0.001
H2O2 NCC	88 ± 1*		0.60 ± 0.01	5.20 ± 0.03*	0.750 ± 0.001*
Control BC		19°	0.52 ± 0.01	5.6 ± 0.1	0.688 ± 0.001
H2O2 NCC			0.52 ± 0.01	5.7 ± 0.1	.652 ± 0.001*
Control BC		26°	0.39 ± 0.01	7.07 ± 0.04	0.495 ± 0.002
H2O2 NCC			0.39 ± 0.01	7.34 ± 0.06*	0.477 ± 0.001*

4.3.4 Surface Charge of NCC-BC and Aminated NCC-BC Fibres

ζ-potential was used to measure the surface charge of all samples (control BC, NCC-BC, and aminated NCC-BC) to determine the effect of carboxylic acid groups on surface charge distribution. Likewise, the introduction of amine to NCC-BC will also show a positive shift in ζ-potential, demonstrating successful functionalization. All samples were sonicated (0.3 mg/mL suspensions) at pH 7 and the results are displayed in

Figure 4.15. The control BC had a measured ζ-potential value of -12.2 ± 0.7 mV compared to -63.2 ± 4.8 mV from NCC-BC. This significant decrease in ζ-potential is attributed to the carboxylic acid residues on the NCC-BC surface as a result of hydrogen peroxide hydrolysis. The ζ-potential of BC is well within the range of the typical ζ-potential values of cellulose (-5 to -50 mV), however, the significant decrease in ζ-potential of NCC-BC is characteristic of the negative charge brought on by the introduction of anionic carboxylate groups to the surface of cellulose. Again, the negative ζ-potential of the control BC is attributed to the hydroxyl groups on the surface of cellulose. The hydrolysis reaction is very characteristic of a typical TEMPO-mediated oxidation reaction, which has been extensively studied. Several groups have analyzed the ζ-potential of TEMPO-mediated oxidized cellulose and determined that even though the carboxyl content varied from cellulose source, the oxidized cellulose all had similar ζ-potential values around -75 mV, which is similar to the value reported in this thesis for NCC-BC.[110] The introduction of the negative surface charge will present a characteristic fibre dispersion property, which is easily visualized in Figure 4.16b. Saito et al. determined that carboxyl content influences the dispersion behavior, which is characteristic of the result found here.[39] Along with the nano-sized dimensions of the NCC-BC fibre, the electrostatic repulsion of the negative surface charge will further distribute the fibre within the aqueous solution creating a clear appearance. Also, once NCC-BC is created from BC, the differences in the physical properties of the hydrogel can be visually seen as greater water retention values are introduced by the negative surface charge (further discussed in Section 4.3.5).

By introducing amine groups to the NCC-BC surface, a positive shift in ζ-potential is expected as amine carries a positive surface charge. Figure 4.15 displays the positive ζ-potential shift from -63.2 ± 4.8 to -21.7 ± 5.0 mV through the introduction of amine to the NCC-BC surface. Also, this increase in ζ-potential demonstrates that the amine groups are protonated at pH 7. Due to the high functional attachment of amine (2.4 ± 0.9 mmol/g), ζ-potential of aminated NCC-BC almost reached that of the control BC. A slight negative ζ-potential is still present in aminated NCC-BC, which is attributed to the abundance of carboxyl groups on the surface of cellulose. Through the introduction of

amine, agglomeration of fibres is expected, as there is a slight decrease in electrostatic repulsion; however, due to the dimensions of the NCC-BC fibre and the carboxyl functionalization, agglomeration was not observed (Figure 4.16c). The nano-size dimensions of aminated NCC-BC do not allow entanglement of the fibres, which reduces the agglomeration noticed in figure 4.16a. Also, the carboxyl groups benefits the aminated NCC-BC by providing further fibre dispersion, a beneficial property when attaching therapeutic proteins to the fibre surface.

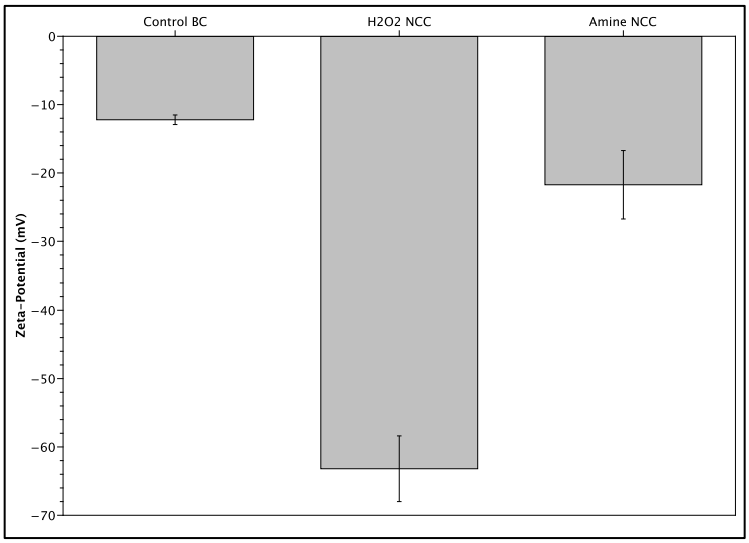

Figure 4.15: ζ-potential measurement of control BC, NCC-BC and aminated NCC-BC.

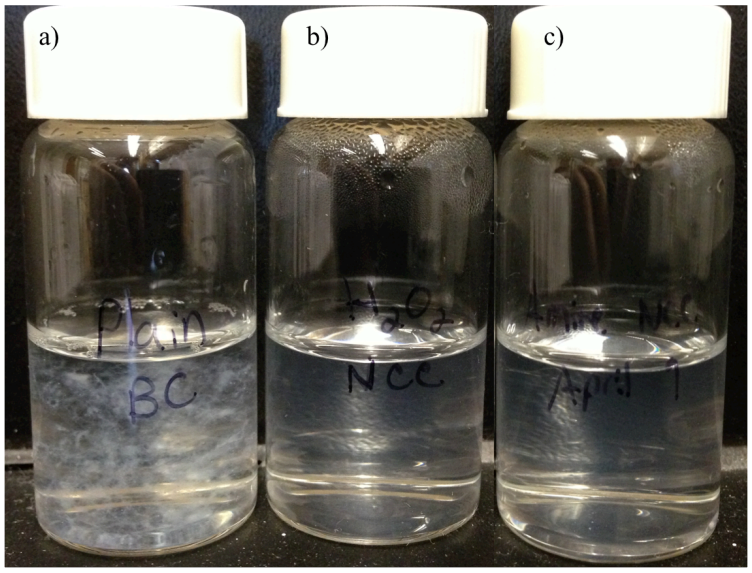

Figure 4.16: Photograph of 0.3 mg/mL sonicated a) control BC; b) NCC-BC; and c) aminated NCC-BC.

4.3.5 Effect of Surface Charge of NCC-BC and Aminated NCC-BC Fibres

Water retention values (WRV) for all samples (control BC, NCC-BC and aminated NCC-BC) were collected and analyzed (Figure 4.17). The NCC-BC WRV increased from 2477 ± 112% (control BC) to 3385 ± 239% at pH 7, which is characteristic of the negative surface charge introduced by the carboxyl groups to the NCC-BC surface. This increase in WRV can be attributed to the highly negative ζ-potential, which creates a strong interaction with the polar solvent water. In the literature, it has been demonstrated that the introduction of a carboxyl groups to the cellulose surface will increase the WRV of cellulose.[39] The introduction of carboxyl groups (0.75 mmol/g) reported by Saito et al. was associated with an increase of the WRV by 450%, which is a lower value than the value reported here (908%). The carboxyl content of 0.75 mmol/g is also lower than that of our NCC-BC product (0.97 ± 0.18 mmol/g), which can account for the lower increase of WRV percentage. Nonetheless, the 908% increase in WRV of BC upon hydrolysis at pH 7 is consistent with that reported for hardwood pulp.[39]

The swelling behavior as a result of the positive surface charge introduced by the amination of NCC-BC was evaluated at varying pH (4-13). At a pH of 4, the aminated product should be fully protonated and charged (swelling), whereas at a pH of 13, aminated NCC-BC should be fully deprotonated and uncharged (contracting). In figure 4.17, aminated NCC-BC follows this behavior from pH 7 to pH 13, contracting as pH increases. This behavior is also represented by the high R^2 value of 0.990, which demonstrates an increasing swelling trend with decreasing pH as the amine group becomes protonated and surface charge increases. This behavior is characteristic of a cationic hydrogel, and to the results displayed in section 4.1.5. However, the data point at pH 4 is not characteristic of a cationic polymer and can be attributed to the presence of carboxyl groups through the hydrolysis of BC. Since the hydrolysis reaction oxidized the NCC-BC fibre, the carboxyl groups at a low pH are protonated, resulting in a lower expansion between cellulose fibres due to the lack of electrostatic repulsion. This leads to a decrease in surface area for the hydroxyl and carboxyl groups to interact with water,

resulting in a statistically significant decrease in swelling at pH 4 from 3547 ± 403% (aminated BC at pH 7) to 2383 ± 378% (Figure 4.17).

Unlike section 4.15, the swelling behavior as a function of pH was found to be statistically significant. This might be due to the ζ-potential of aminated NCC-BC below zero, which could lead to an increase in dispersion of fibres and stronger interaction with the solvent. Also, the hydrolysis of BC creates a fibre with nano-sized dimensions contributing to good fibre dispersion properties. Likewise, the amine groups at a high pH are deprotonated, resulting in a lower expansion between cellulose fibres due to the lack of electrostatic repulsion. This leads to a decrease in surface area for the hydroxyl and carboxyl groups to interact with water, resulting in a statistically difference decrease in swelling at pH 13 from 3547 ± 403% (aminated BC at pH 7) to 1628 ± 207% (Figure 4.17).

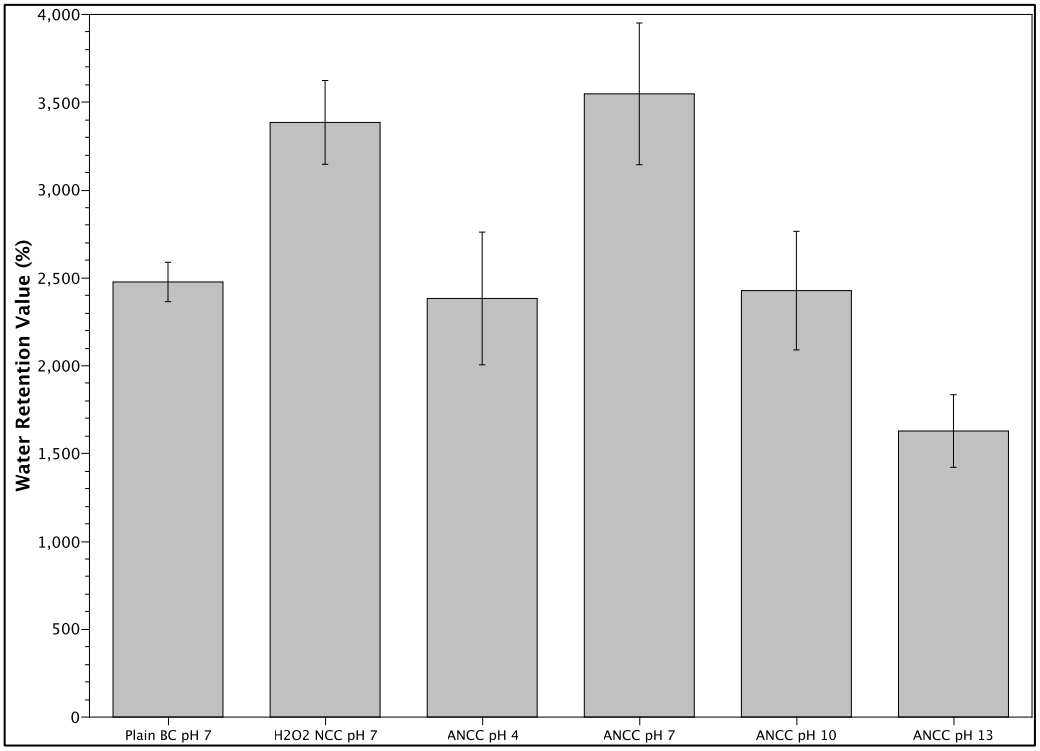

Figure 4.17: Water Retention Values of control BC (pH 7), NCC-BC (pH 7) and aminated NCC-BC (pH 4 - 13).

The introduction of carboxyl groups to the aminated NCC-BC surface plays an important role in the swelling behavior of aminated NCC-BC. At a lower pH, the aminated NCC-BC fibre will contract, releasing most of its water due to the interaction of

surface carboxyls with the water, causing a protonated and neutral surface. Likewise, at higher pH, the interaction of amine groups with the water causes a fully deprotonated and uncharged surface leading to the contraction of the hydrogel. Therefore, the functional groups associated with the aminated NCC-BC hydrogel have a significant impact on the swelling behavior.

4.3.6 Morphology of NCC-BC and Aminated NCC-BC Fibres

The purpose of hydrolyzing the BC fibre is to create a fibre with nano-sized dimension capable to intracellular delivery of therapeutics. By removing the amorphous regions through hydrogen peroxide hydrolysis, highly crystalline, nano-sized fibres can be created. The morphology of NCC-BC was examined with high-resolution transmission electron microscopy (TEM) (Figure 4.18).

Sonicated 0.3 mg/mL suspensions of native BC and NCC-BC fibres were placed on carbon-coated TEM grids, followed by negatively staining the sample with uranyl acetate to develop a contrast. Figure 4.18a and b demonstrates the morphological differences between native BC and NCC-BC respectively. It can be seen though the fibre dimensions that NCC-BC (Figure 4.18b) produces fibres with uniform nano-sized dimensions with a slight branched appearance compared to native BC (Figure 4.18a). This decrease in length from native BC to NCC-BC is attributed to the removal of the amorphous regions within the cellulose fibre. As mentioned in section 2.2, BC fibres are comprised of many ordered (crystalline) and disordered (amorphous) regions, which can generally be removed through harsh acid treatments. The use of hydrogen peroxide removes the amorphous regions with high efficiency. The carboxylic acid groups introduced to the NCC-BC surface has been demonstrated to be useful for drug delivery.[42] The removal of the amorphous regions results in decreased fibre dimensions providing the NCC-BC fibre with increased surface area capable of a greater loading capacity. Since hydrogen peroxide is an oxidizing agent, it has been reported that oxidation of cellulose fibres splits the fibres into fibrils due to the attack on the amorphous regions. In figure 4.18b, no splitting of fibres was noticed. This is because nearly all amorphous regions were removed during the hydrolysis of BC, creating fibrils

that are not attached to a bundled fibre. As a result of the hydrolysis, the average fibre length and diameter of NCC-BC was calculated to be 176.7 ± 121.0 and 14.8 ± 8.3 nm respectively, which decreased by a statistically significant amount compared to BC (length of 2941.0 ± 1165.8 nm and diameter of 24.3 ± 14.3 nm). This is an approximate 10-fold decrease in length, and 10 nm decrease in diameter from native BC fibres, which are amenable to cellular uptake (Figure 4.19, 4.20).

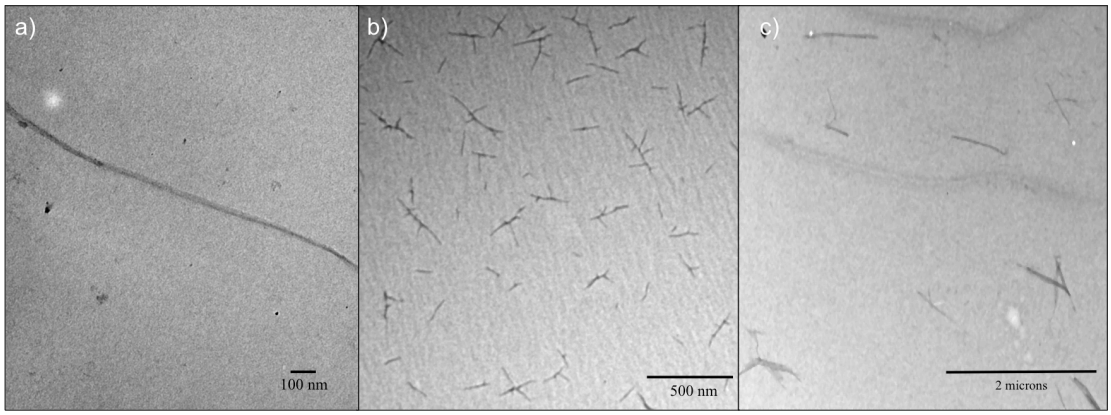

Figure 4.18: TEM images of a) control BC; b) NCC-BC; and c) aminated NCC-BC.

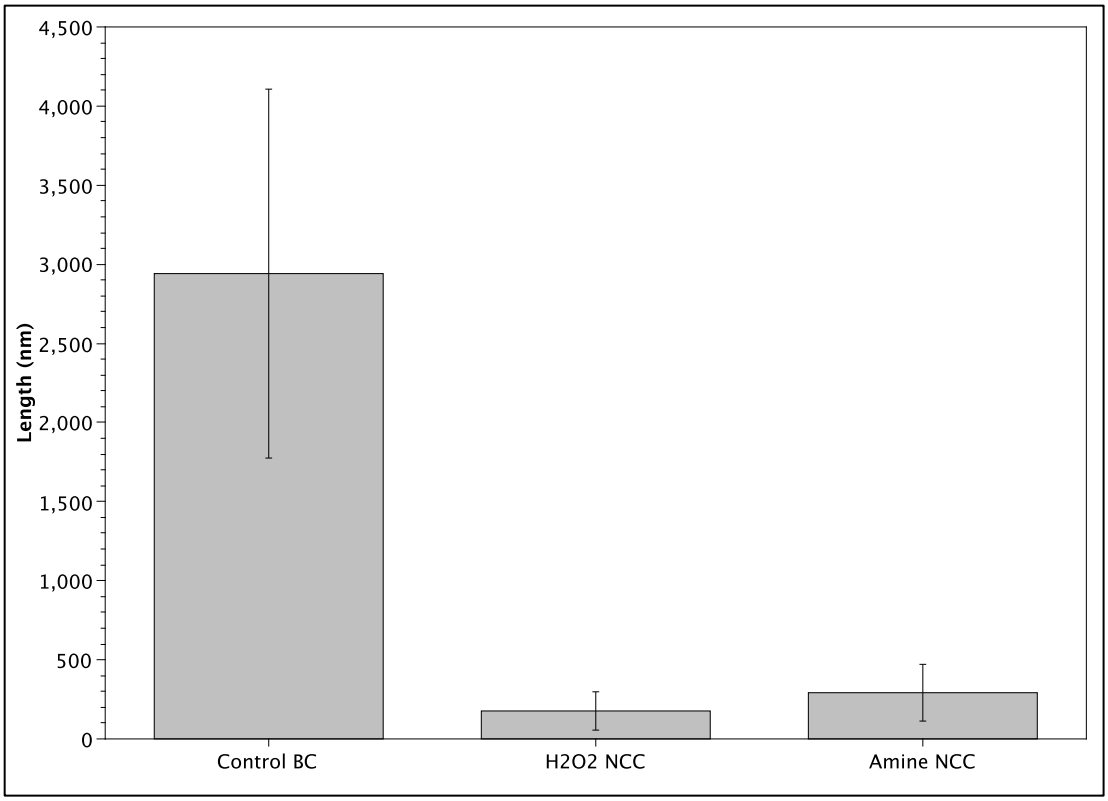

Figure 4.19: Length distribution of 150 control BC, NCC-BC and aminated NCC-BC fibres from TEM images.

Figure 4.18c displays the TEM of the aminated NCC-BC product. It is easily seen that the resulting fibres are in nano-sized dimensions, with no morphological differences compared to the NCC-BC fibres. The length of the aminated NCC-BC fibres were calculated to be 292.1 ± 179.3 nm and resulted in no statistical difference compared to the fibre length of NCC-BC (176.7 ± 121.0 nm). The diameters of native BC, and NCC-BC were compared to those of aminated NCC-BC (Figure 4.20). It was found that there was no statistical difference in the diameter between NCC-BC (14.8 ± 8.3 nm) and aminated NCC-BC (23.5 ± 8.2 nm); although there is a difference in the mean diameter.

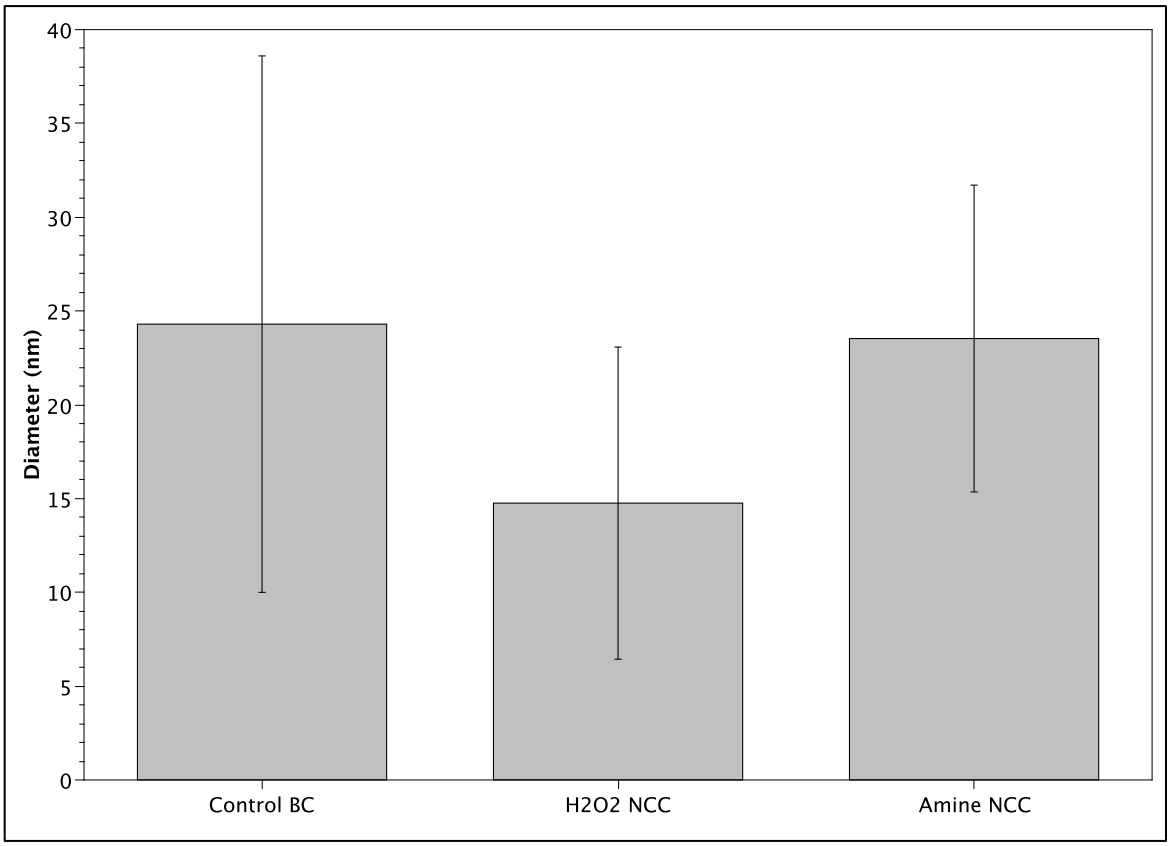

Figure 4.20: Diameter distribution of 150 control BC, NCC-BC and aminated NCC-BC fibres from TEM images.

4.4 Protein Conjugation to Aminated NCC-BC

4.4.1 Aminated NCC-BC/HRP Conjugation

The attachment of a protein to the aminated NCC-BC surface will demonstrate the use of this system for the application of therapeutics delivery. Currently, targeted delivery is of main focus among researchers. Despite successful development of numerous

vaccines and therapeutics for a variety of diseases, a target delivery vehicle that is capable of delivering accurate and localized drug dosages has yet to be developed. The succeeding work will demonstrate the ability of nano-crystalline cellulose to be used as a natural biocompatible, targeted drug delivery vehicle, to which cancer specific drugs and therapeutics can be attached to its surface for localized delivery.

Horseradish peroxidase (HRP) is a protein that has been demonstrated for the use of monitoring glucose levels in diabetics when attached to hydrogels. Therefore, by validating successful attachment of this protein to the aminated NCC-BC surface, HRP conjugated aminated NCC-BC can be used for this application. Please note HRP was only used to demonstrate protein conjugation in this thesis. Successful attachment of HRP to an aminated BC surface was demonstrated in section 4.2.3. As mentioned previously, in order to achieve intracellular delivery of therapeutics, a delivery device with dimensions smaller than that of mammalian cells needs to be created. It has been validated that aminated NCC-BC follows this criteria and by conjugating HRP to the aminated NCC-BC surface, successful demonstration a therapeutic delivery system can be expected.

The importance of a linker to maximize loading of HRP to the aminated BC surface was demonstrated in section 4.2.3. For the attachment of HRP to the aminated NCC-BC surface, the same BS3 linker will be used. Likewise, a variety of BS3 linker ratios along with varying protein concentrations will be tested to optimize the HRP-aminated NCC-BC loading (Figure 4.21 & Table 4). A very interesting phenomenon was recognized through this investigation, which is of great importance for the use of BS3 for amine-to-amine attachment. Firstly, it can be seen that the control amine NCC-BC (HRP conjugated to aminated NCC-BC without the use of a BS3 linker) obtained a greater surface functionalization of HRP to the aminated NCC-BC surface (0.277 ± 0.005 mg enzyme/g NCC) than that reported in section 4.2.3 for the control amine BC (0.02 ± 0.01 mg enzyme/g BC). This approximate 10-fold increase can be ascribed to the ionic complex formation occurring between the anionic functional groups of the carboxylic acid and the amine residues of the HRP protein on the aminated NCC-BC surface. Also, an increase in surface area can explain the increase in protein attachment yield. Since aminated BC had no anionic functionalization, the loading of HRP to the aminated BC

surface was significantly lower, which is expected. This loading is still very low compared to the maximum loading potential. Another consideration for the low yield can be attributed to steric hindrance of the relatively large protein at the conjugation site.

When the BS3 linker was used, an increase in HRP conjugation to the aminated NCC-BC surface was observed (Table 4). The use of a BS3 linker increased the HRP loading on the aminated NCC-BC surface to 0.409 ± 0.007 mg enzyme/g NCC-BC, which is a statistically significant increase of HRP loading compared to the control. This loading is almost identical to the loading demonstrated by the HRP-BS3 conjugated aminated BC (Table 2). This finding is significant as this tell us that BS3 plays an important role for the attachment of proteins to the BC surface, which validates the hypothesis proposed in section 4.2.3. It seems as though the loading of HRP achieved with the current reaction conditions is relatively consistent despite the BC fibre size. It is also important to notice that there was no increase in HRP loading to the aminated NCC-BC surface, which was expected due to the introduction of carboxyl groups from the hydrolysis reaction forming ionic complexes. The relatively same HRP loading from aminated NCC-BC to aminated BC tells us that the BS3 dominated the loading capability and that a spacer arm provides the decongestion needed for protein attachment.

Further investigation on maximizing the loading of HRP to aminated NCC-BC was completed by varying the amount of BS3 and HRP concentrations attached to the aminated NCC-BC surface. From figure 4.21, it can be seen that by doubling the HRP concentration, its loading can be increased significantly by varying the BS3 concentration up to 10 fold. Further increase in BS3 will lead to a decrease in HRP loading.

This finding was of great importance, as this outlines the significance and pitfalls of using an amine-to-amine linker such as BS3. An amine-to-amine linker has been determined to link the surface amines on aminated NCC-BC to other surface amines on adjacent aminated NCC-BC fibres. Likewise, the same occurrence can arise on HRP as BS3 can link the available amine residues on HRP to other amines on adjacent HRP moieties, which decrease the loading efficiency drastically. Nonetheless, the significant increase in conjugation using the BS3 linker compared to the control method illustrates

the importance of the use of BS3 to reduce steric hindrance at the reactive sites on the bacterial cellulose surface.

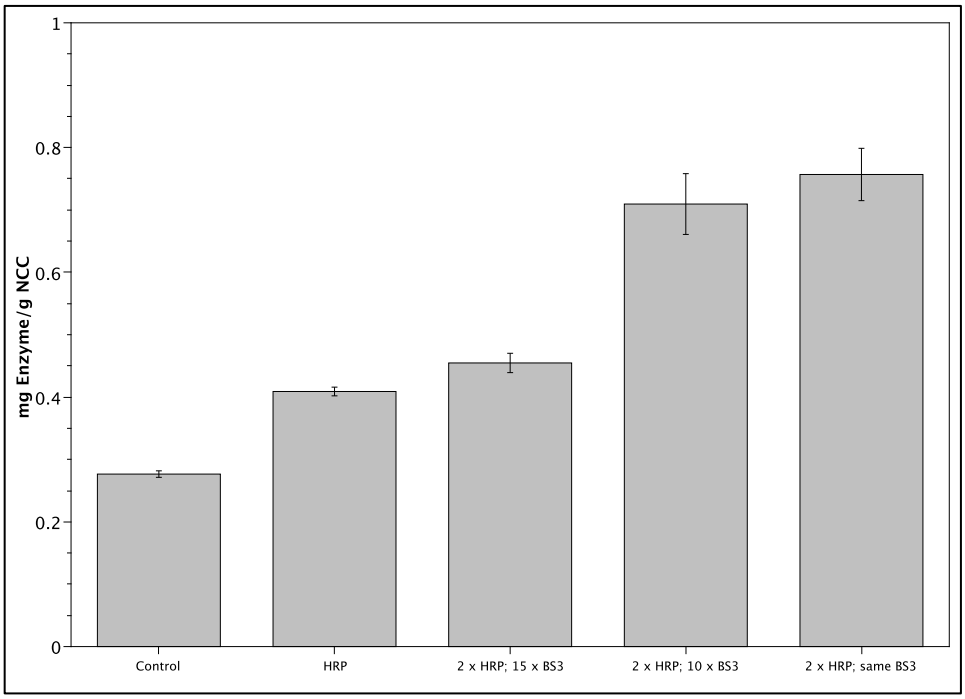

Figure 4.21: Quantification of HRP on the aminated NCC-BC surface through the use of different cross-linking and protein ratios.

Table 4: Quantification of HRP loading on aminated NCC-BC.

Type	Average mg of Enzyme/g of NCC-BC
Control Amine NCC-BC	0.277 ± 0.005
HRP-BS3 Amine NCC-BC	0.409 ± 0.007[a]
2 x HRP; 15 x BS3 Amine NCC-BC	0.455 ± 0.016[b]
2 x HRP; 10 x BS3 Amine NCC-BC	0.709 ± 0.049[c]
2 x HRP; BS3 Amine NCC-BC	0.757 ± 0.042[c]

([a, b, c])indicates significant statistical difference compared to the Control Amine NCC-BC ($P<0.05$)

4.4.2 Aminated NCC-BC/HRP Conjugation Using Avidin

Avidin, as mentioned previously, is a specific glycoprotein with terminal N-acetylglucosamine and mannose residues found in egg whites with an approximate molecular weight of 66 kDa.[69-71] Avidin has a very high affinity for up to four biotin molecules and is stable and functional over a broad range of pH and temperatures.[72] It can undergo extensive chemical modifications with little to no effect on its function making it ideal for the detection and protein purification of biotinylated molecules at a

variety of conditions. Therefore, an avidin molecule will be used to demonstrate its potential for biomedical applications.

HRP conjugated avidin (avidin-HRP) will be used to demonstrate the increase in loading achievable. The avidin-HRP conjugate is mainly used as a second step for detection of biotinylated antibodies through staining. The avidin molecules are decorated with an abundance of HRP moieties creating an increase loading of HRP attachment to the aminated NCC-BC surface. Like HRP conjugated aminated NCC-BC, BS3 will be used as the linker/spacer-arm to reduce steric hindrance at the reactive sites. The BS3 linker will link the surface amine of aminated NCC-BC to the available surface amines on the avidin molecule. The HRP protein is already conjugated to the avidin surface; therefore, by conjugating avidin to the aminated NCC-BC surface, HRP should be attached with greater yields. Through this investigation, avidin-HRP was conjugated to the aminated NCC-BC surface with a significant greater loading yield than previously investigated in section 4.4.1 (Figure 4.22 & Table 5). An increase of approximately 8 mg of enzyme/g of NCC was calculated between the conventional HRP-BS3 conjugation (0.409 ± 0.007 mg enzyme/g NCC) and the avidin-HRP-BS3 conjugation (8.50 ± 1.07 mg enzyme/g NCC) to aminated NCC-BC. This substantially statistically significant difference between the two approaches demonstrates the importance of the use of an avidin molecule for the attachment of therapeutic molecules to the cellulose surface. It is also important to note that since BS3 is once again used, the high surface conjugation of HRP can be ascribed to the unselective amine attachment. Also, the avidin concentration used for this reaction was identical to the protein concentration used for the HRP-BS3 conjugation to aminated NCC-BC before optimization. It was also noted that there is a possibility that there are several HRP moieties per avidin molecule. Since it was concluded in section 4.4.1 that the protein concentration was the limiting factor for protein conjugation, an increase in HRP corresponds to an increase in protein functionalization to aminated NCC-BC.

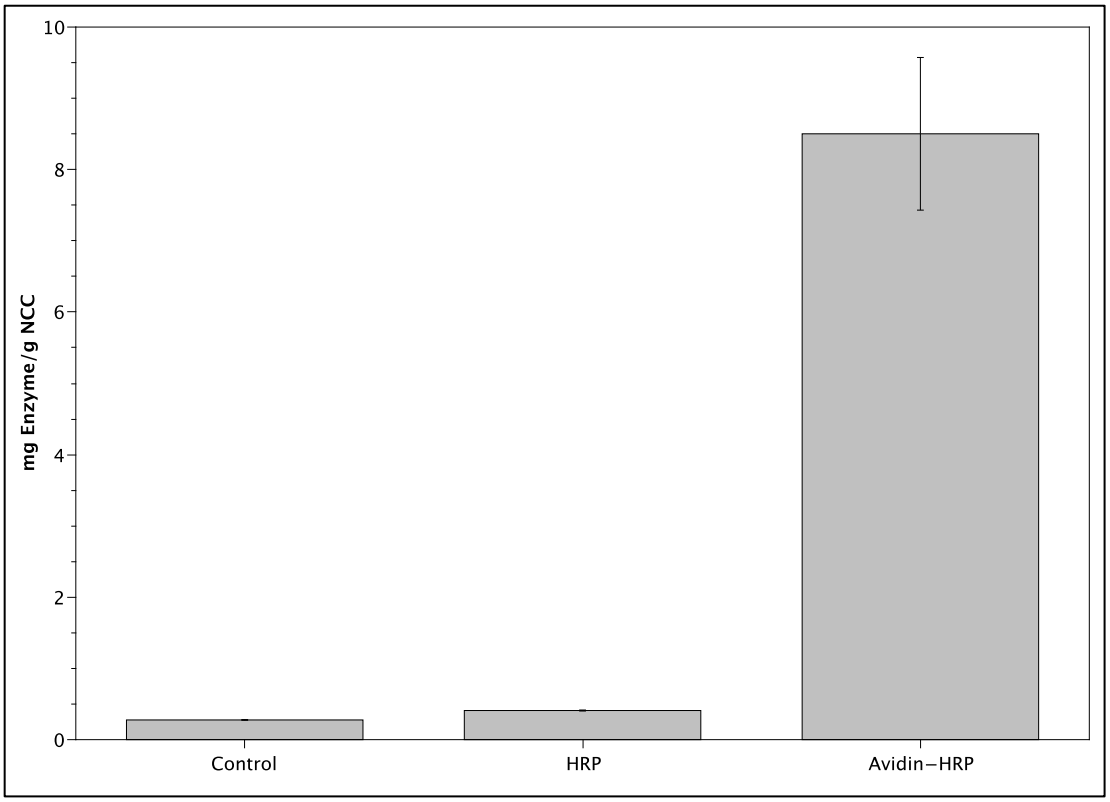

Figure 4.22: Comparing the quantification of HRP on the aminated NCC-BC through the use of avidin.

Table 5: Comparing the quantification of HRP on the aminated NCC-BC through the use of avidin.

Type	Average mg of Enzyme/g of NCC-BC
Control Amine NCC-BC	0.277 ± 0.005
HRP-BS3 Amine NCC-BC	0.409 ± 0.007[a]
Avidin-HRP-BS3 Amine NCC-BC	8.50 ± 1.07[b]

([a, b]) indicates significant statistical difference compared to the Control Amine NCC-BC ($P<0.05$)

Currently, many groups are using a protein conjugated avidin complex for the delivery of proteins to cells. They achieve this by biotinylating a cell specific antibody, which will attach to the receptor of that cell. Once completed, the avidin-protein is injected and the avidin will bind directly to the biotinylated cell for localized delivery. However, the downfall of this system is that additional biotin needs to be injected to remove any unconjugated free-floating avidin not attached to the cell surface. This can cause many complications within the body, which is not beneficial to the patient. By developing an avidin-biotin complex on a biocompatible fibre, therapeutic proteins and antibodies can be conjugated to the same system for localized targeted delivery of therapeutics. This will be further investigated in section 4.5.

4.5 Avidin-Biotin Complexation to Aminated NCC-BC

In order to develop a truly localized targeted delivery system, antibodies and therapeutics must be attached to the same delivery system. This can be achieved through the use of an avidin-biotin complex. The avidin-biotin system has been characterized as the strongest non-covalent interaction known to date, having a dissociation constant of $K_D \sim 10^{-15}$ M between protein and ligand.[67] The bond formation between avidin and biotin is very rapid and is unaffected by extreme pH, temperature, organic solvents, and other denaturing agents. Also, this system allows for an unlimited number of primary detection reagents (such as antibodies, nucleic acids and ligands) to be captured, immobilized or detected. The benefits of this system include the ability of manually biotinylating reagents if they are not available, the biological and physical characteristics of the binder or probe after biotinylation are retained, the ability to modify avidin to meet specific needs, and different biotinylated probes can be bound to a single avidin.[68]

In order to demonstrate the application of an avidin-biotin complex conjugated to the aminated NCC-BC fibre, avidin was attached to the aminated NCC-BC surface through the use of a BS3 linker, followed by the attachment of two different biotinylated molecules (glucose oxidase and β-galactosidase). These molecules have been chosen for their use as detection agents. Conjugated avidin-biotin glucose oxidase can be used as a continuous monitoring system of glucose *in vivo*, where β-galactosidase can be delivered to the small intestine for the digestion of lactose or as a biosensor. For this thesis, glucose oxidase is used to demonstrate protein conjugation, while β-galactosidase will be used to validate intracellular delivery into human endothelial kidney cells using X-gal staining to demonstrate activity after conjugation.

The avidin-biotin system is of great benefit for use as a component of a therapeutic delivery vehicle. The goal of our system is to decorate the surface of aminated NCC-BC with avidin, followed by conjugating a portion of the available avidin moieties with biotinylated cancer specific antibodies, while the remaining avidin moieties will be biotinylated with a cancer specific therapeutic agent. By incorporating both a targeting element (antibody) and a therapeutic element (protein) to the aminated NCC-BC surface,

the system can specifically target and attach to the cancer cell, while providing the cancerous cell with the drug needed at the attachment site. This pre-attachment of drug loading will reduce side effects and relative drug concentration in the surrounding tissue. Also, it is known that only a small dose of the therapeutic drug reaches the diseased area; therefore, by specifically targeting the cancerous area, concentrated localized delivery is possible. The avidin-biotin system provides the delivery system with the selectivity it needs to target and treat the diseased area at the site.

Figure 4.23 and table 6 display the results obtained following the avidin-biotin conjugation to the aminated NCC-BC product. Due to the difference in molecular weight between HRP, glucose oxidase and β-galactosidase, the following results are displayed by micromole of enzyme per gram of NCC-BC. For both, glucose oxidase and β-galactosidase, it was noticed that the use of an avidin-biotin complex further functionalizes the surface of aminated NCC-BC with the intended protein. Avidin-biotin β-galactosidase (0.0243 ± <0.0001 micromol enzyme/g NCC-BC) surpasses the protein loading obtained through HRP-BS3 conjugated NCC-BC (0.0093 ± 0.0002 micromol enzyme/g NCC-BC). This statistically significant difference can be attributed to the fact that avidin has up to four binding sites for biotinylated molecules (β-galactosidase). This binding efficiency of avidin-biotin is highly selective which increases its protein attachment. Also, since avidin is conjugated to the aminated NCC-BC surface with a spacer arm, this reduces the steric hindrance for protein conjugation. Likewise, the biotinylation of β-galactosidase to biotin is completed through a spacer arm, which further decongests the surface of the cellulose fibre. The result of avidin-biotin β-galactosidase is what was expected for this reaction as the avidin-biotin complex is expected to have a greater protein loading.

When comparing the result of avidin-biotin β-galactosidase to avidin-biotin glucose oxidase, a statistically significant decrease in protein attachment is noticed. The avidin-biotin glucose oxidase conjugation on the aminated NCC-BC surface (0.0059 ± 0.0011 micromol enzyme/g NCC-BC) is significantly lower than its avidin-biotin counterpart β-galactosidase (0.0243 ± <0.0001 micromol enzyme/g NCC-BC). Many hypotheses can be used to justify this phenomenon (electrostatic repulsion of glucose

oxidase, blocking of binding sites, affinity of attachment to cellulose, different accessibility to avidin from biotin, and amount of available biotin binding sites). It is very difficult to make a definitive conclusion on the cause of the significant decrease of glucose oxidase conjugation. However it can be estimated that since the biotinylation of glucose oxidase to biotin is not amine specific, multiple biotins can be attached to the same glucose oxidase molecule. This will cause the surface biotin moieties of the same glucose oxidase molecule to bind to multiple avidin moieties at once, reducing he effective loading of glucose oxidase. This phenomenon can also be attributed to the fact that the loading efficiency of the avidin-biotin complex (for both glucose oxidase and β-galactosidase) did not reach the loading potential achieved from the avidin-HRP-BS3 aminated NCC-BC system. This indicates that optimization and selective biotinylation of proteins needs to be understood to maximize loading efficiencies.

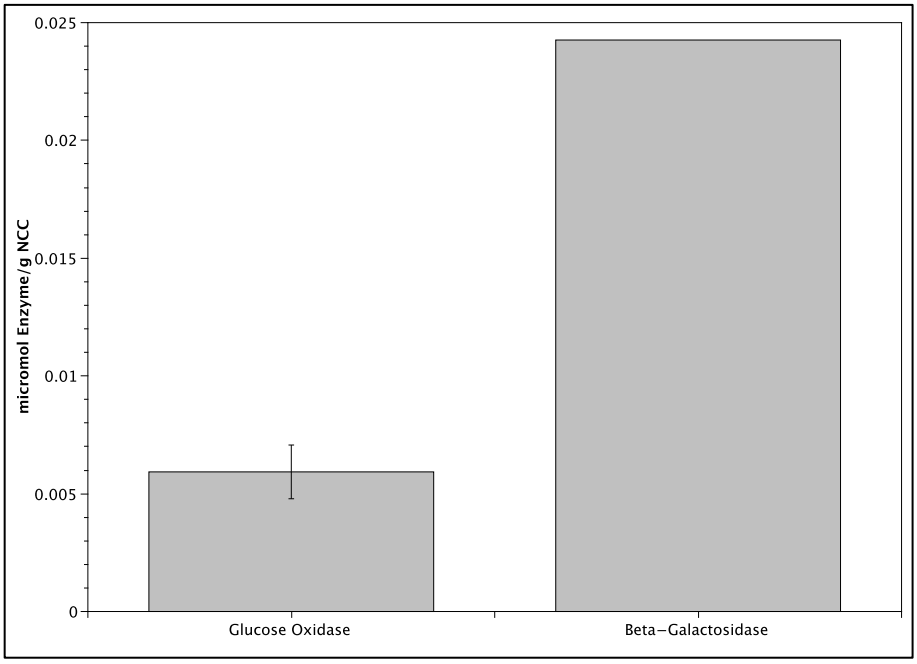

Figure 4.23: Comparing the quantification of glucose oxidase and β-galactosidase on the aminated NCC-BC through the use of an avidin-biotin conjugate.

Table 6: Comparing the quantification of glucose oxidase and β-galactosidase on the aminated NCC-BC through the use of an avidin-biotin conjugate.

Type	Average micromol of Enzyme/g of NCC-BC
HRP-BS3 Amine NCC-BC	0.0093 ± 0.0002
Avidin-HRP-BS3 Amine NCC-BC	0.1932 ± 0.0243[a]
Avidin-Biotin Glucose Oxidase NCC-BC	0.0059 ± 0.0011[b]
Avidin-Biotin β-Galactosidase NCC-BC	0.0243 ± <0.0001[c]

([a, b, c]) indicates significant statistical difference compared to the HRP-BS3 Amine NCC-BC ($P<0.05$)

Further experimentation is needed to better understand the discrepancy between the attachment yields of the two systems. Nonetheless, successful attachment of both glucose oxidase and β-galactosidase to the aminated NCC-BC surface, through an avidin-biotin complex, has been demonstrated and quantified. Since avidin-biotin β-galactosidase was conjugated to aminated NCC-BC with high attachment yields, cellular delivery into human endothelial kindney cells looks promising. The applications of using this avidin-biotin complex on a biocompatible fibre are endless. As mentioned previously, any biotinylated antibody and therapeutic protein can be conjugated to this avidin-NCC-BC system, making it useful for a full range of therapeutic applications.

CHAPTER 5 – CONCLUSIONS

5.1 Summary

Cationic functionalization of cellulose has not been studied to the extent of anionic functionalized cellulose. It is however a rapidly growing alternative to current methods used for surface modification. To date, amine functionalization of bacterial cellulose has not been systematically investigated, adding to the novelty of this thesis. Currently, researches are developing innovative methods of attaching therapeutic drugs to biocompatible polymers for targeted drug delivery applications. Oxidation of cellulose has been extensively studied for this application, where the addition of a carboxyl group can form ionic complexes with therapeutic elements. This thesis provides an alternative to this method, where the bacterial cellulose was functionalized with amine to covalently attach therapeutic elements through a spacer arm to reduce steric hindrance at the reactive sites to maximize drug loading. Also, an avidin-biotin complex was used to conjugate proteins to the aminated NCC-BC surface with high selectivity and binding affinity, to which a targeting element (antibody) and therapeutic element (drug) can be attached to the same surface for a "truly" localized delivery system.

The amination of BC was completed through a two-step reaction involving epichlorohidrin and ammonium hydroxide. The structure of aminated BC was characterized with FTIR spectroscopy, where the characteristic peak for a primary amine was demonstrated. Likewise, pH titration was used to quantify the amount of amine introduced to the bacterial cellulose surface to be 1.75 ± 0.18 mmol/g of BC (corresponding to 28.3% of available hydroxyl groups). In order to demonstrate the functionality of aminated BC, FITC, BCG and HRP were conjugated to its surface. Loadings of 0.42 ± 0.03 FITC and 2.6 ± 0.2 BCG moieties/100 anhydroglucose units were achieved, demonstrating the ability of attaching fluorescent dyes to the aminated product. Likewise, HRP was conjugated to demonstrate protein conjugation. Due to its large molecular size, HRP can best be conjugated to aminated BC by using bis(sulfosuccinimidyl)suberate (BS3) as a linker to reduce steric congestion on the BC surface. HRP loading of 0.17 ± 0.01 moieties/100 anhydroglucose units was achieved demonstrating the ability to conjugate proteins.

The hydrolysis of bacterial cellulose was completed through a hydrogen peroxide treatment to create a fibre with increased crystallinity and nano-sized dimensions capable for intracellular delivery. Subsequently, amination of the hydrolyzed product was completed to introduce amine groups to the NCC-BC surface. The structure of NCC-BC and aminated NCC-BC was characterized with FTIR spectroscopy. It was found that a characteristic carboxyl peak at approximately 1610 cm^{-1} was demonstrated, indicating the introduction of carboxyl groups to the NCC-BC surface after hydrolysis. Likewise, a characteristic primary amine peak ranging from 1640 to 1500 cm^{-1} was demonstrated, indicating the introduction of primary amines to the aminated NCC-BC surface. Acid-base pH titration was again used to quantify the amount of carboxyl and amine groups introduced to the NCC-BC and aminated NCC-BC surface to be 0.97 ± 0.18 mmol/g of NCC-BC (corresponding to 15.8% of available primary hydroxyl groups) and 2.4 ± 0.9 mmol/g of NCC-BC (corresponding to 38.8% of available hydroxyl groups) respectively. The crystallinity of NCC-BC was studied with XRD spectroscopy, and it was determined that the hydrolysis of BC increased the degree of crytallinity from 70% to 88%, signifying the significant removal of amorphous regions within the cellulose fibre. TEM was used to demonstrate the morphological differences between native BC and NCC-BC. The length and diameter of NCC-BC was found to be 176.7 ± 121.0 nm and 14.8 ± 8.3 nm respectively, which is a significant decrease in dimension validating its potential to be used for intracellular delivery.

The final goal of this thesis is to once again demonstrate the functionality of aminated NCC-BC for the application of therapeutics delivery. HRP was used to demonstrate protein attachment to the aminated NCC-BC surface and validate the importance of the use of a spacer-arm. The optimization of this protein was also tested. Loading increased from 0.409 ± 0.007 mg enzyme/g NCC-BC to 0.757 ± 0.042 mg enzyme/g NCC-BC by doubling the amount of protein introduced to the aminated NCC-BC surface. Avidin-HRP was used to demonstrate the ability of maximizing protein loading through avidin. The loading of HRP through avidin increased from 0.409 ± 0.007 mg enzyme/g NCC-BC to 8.50 ± 01.07 mg enzyme/g NCC-BC signifying the importance of avidin. Finally, an avidin-biotin complex was attached to the aminated NCC-BC

surface for the attachment of two proteins (glucose oxidase and β-galactosidase). Avidin-biotin β-galactosidase showed a protein conjugation of 0.0243 ± <0.0001 micromol enzyme/g NCC-BC, where avidin-biotin glucose oxidase did not show as high of a conjugation as the protein loading was only 0.0059 ± 0.0011 micromol enzyme/g NCC-BC. Nonetheless, successful attachment of both glucose oxidase and β-galactosidase to the aminated NCC-BC surface, through an avidin-biotin complex, was demonstrated and quantified.

Since avidin-biotin β-galactosidase was conjugated to aminated NCC-BC, cellular delivery into human endothelial kindney cells looks promising. The applications of using this avidin-biotin complex on a biocompatible fibre are endless. As mentioned previously, any biotinylated antibody and therapeutic protein can be conjugated to this avidin-NCC-BC system, making it useful for a full range of therapeutic applications. The avidin-biotin system is of great benefit for the use as a component of a therapeutic delivery vehicle. By incorporating both a targeting element (antibody) and a therapeutic element (protein) to the aminated NCC-BC surface, the system can specifically target and attach to the cancer cell, while providing the cancerous cell with the drug needed at the site. This pre-attachment of drug loading will reduce side effects and relative drug concentration in the remaining tissue. Also, it is known that only a small dose of the therapeutic drug reaches the diseased area; therefore, by specifically targeting the cancerous area, concentrated localized delivery is possible. The avidin-biotin system provides the delivery system with the selectivity it needs to target and treat the diseased area at the site.

5.2 Future Work

Now that a protein and an avidin-biotin conjugation have been validated on the surface of aminated BC and aminated NCC-BC respectively, further investigation can be completed on this delivery system. However, further optimization of protein loading should be addressed to maximize loading efficiencies on the BC fibre. The success of utilizing a BS3 linker to reduce the steric hindrance around the reactive sites has been displayed; however, modification can improve this system further. It has been outlined throughout the thesis that the potential for cross-linking proteins to proteins and aminated

cellulose to aminated cellulose is inevitable when using an amine-to-amine cross-linking agent. In order to reduce this occurrence, a staudinger reaction is proposed. This is a two-step reaction, which the first step conjugates the aminated cellulose with phosphine, while the second step conjugates the protein with an azide linker. Once both reactive sites come in close proximity to one another, they form a strong selective covalent bond attaching the protein to the cellulose surface. This will eliminate the potential for inter-protein and inter-cellulose cross-linking to occur.

Further testing on the determination of the significant low yield associated with the avidin-biotin glucose oxidase needs to be addressed. Likewise, the binding of various biotinylated chemotherapeutic drugs through the avidin-biotin system should be tested and quantified to demonstrate the full potential of this system. Due to the significantly high yield obtained through the avidin-biton β-galactosidase conjugated amine NCC-BC, cellular delivery into human endothelial kindney should be completed using X-gal staining to demonstrate biocompatibility and protein activity *in vitro*.

CHAPTER 6 – REFERENCES AND CURRICULUM VITAE

6.1 References

1. Azizi Samir, M.A., F. Alloin, and A. Dufresne, *Review of recent research into cellulosic whiskers, their properties and their application in nanocomposite field.* Biomacromolecules, 2005. **6**(2): p. 612-26.

2. Moon, R.J., et al., *Cellulose nanomaterials review: structure, properties and nanocomposites.* Chem Soc Rev, 2011. **40**(7): p. 3941-94.

3. Cannon, R.E. and S.M. Anderson, *Biogenesis of bacterial cellulose.* Crit Rev Microbiol, 1991. **17**(6): p. 435-47.

4. Klemm, D., et al., *Bacterial synthesized cellulose - artificial blood vessels for microsurgery.* Progress in Polymer Science, 2001. **26**(9): p. 1561-1603.

5. Ishikawa, A., T. Okano, and J. Sugiyama, *Fine structure and tensile properties of ramie fibres in the crystalline form of cellulose I, II, IIII and IVI.* Polymer, 1997. **38**(2): p. 463-468.

6. Nishiyama, Y., et al., *Crystal structure and hydrogen bonding system in cellulose I(alpha) from synchrotron X-ray and neutron fiber diffraction.* J Am Chem Soc, 2003. **125**(47): p. 14300-6.

7. O'Sullivan, A., *Cellulose: the structure slowly unravels.* Cellulose, 1997. **4**(3): p. 173-207.

8. Klemm, D., et al., *Cellulose: fascinating biopolymer and sustainable raw material.* Angew Chem Int Ed Engl, 2005. **44**(22): p. 3358-93.

9. Habibi, Y., L.A. Lucia, and O.J. Rojas, *Cellulose nanocrystals: chemistry, self-assembly, and applications.* Chem Rev, 2010. **110**(6): p. 3479-500.

10. Bielecki, S., et al., *Bacterial Cellulose*, in *Biopolymers Online*2005, Wiley-VCH Verlag GmbH & Co. KGaA.

11. Brown, A.J., *XIX.-The chemical action of pure cultivations of bacterium aceti.* Journal of the Chemical Society, Transactions, 1886. **49**(0): p. 172-187.

12. Brown, A.J., *XLIII.-On an acetic ferment which forms cellulose.* Journal of the Chemical Society, Transactions, 1886. **49**(0): p. 432-439.

13. Hestrin, S., M. Aschner, and J. Mager, *Synthesis of cellulose by resting cells of Acetobacter xylinum.* Nature, 1947. **159**(4028): p. 64.

14. Hestrin, S. and M. Schramm, *Synthesis of cellulose by Acetobacter xylinum. II. Preparation of freeze-dried cells capable of polymerizing glucose to cellulose.* Biochem J, 1954. **58**(2): p. 345-52.

15. Iguchi, M., S. Yamanaka, and A. Budhiono, *Bacterial cellulose - masterpiece of nature's arts.* Journal of Materials Science, 2000. **35**(2): p. 261-270.

16. Ohad, I. and D. Danon, *On the Dimensions of Cellulose Microfibrils.* J Cell Biol, 1964. **22**: p. 302-5.

17. Czaja, W., et al., *Microbial cellulose--the natural power to heal wounds.* Biomaterials, 2006. **27**(2): p. 145-51.

18. Eichhorn, S.J., et al., *Review: current international research into cellulose nanofibres and nanocomposites.* Journal of Materials Science, 2010. **45**(1): p. 1-33.

19. Jonas, R. and L.F. Farah, *Production and application of microbial cellulose.* Polymer Degradation and Stability, 1998. **59**(1,Äì3): p. 101-106.

20. Watanabe, K., et al., *Structural Features and Properties of Bacterial Cellulose Produced in Agitated Culture.* Cellulose, 1998. **5**(3): p. 187-200.

21. Fontana, J.D., et al., *Acetobacter cellulose pellicle as a temporary skin substitute.* Appl Biochem Biotechnol, 1990. **24-25**: p. 253-64.

22. Krystynowicz, A., et al., *The evaluation of usefulness of microbial cellulose as a wound dressing material.* MEDEDELINGEN-FACULTEIT LANDBOUWKUNDIGE EN TOEGEPASTE BIOLOGISCHE WETENSCHAPPEN, 2000. **65**(3; ISSU A): p. 213-220.

23. Helenius, G., et al., *In vivo biocompatibility of bacterial cellulose.* Journal of Biomedical Materials Research Part A, 2006. **76A**(2): p. 431-438.

24. Solway, D.R., W.A. Clark, and D.J. Levinson, *A parallel open-label trial to evaluate microbial cellulose wound dressing in the treatment of diabetic foot ulcers.* Int Wound J, 2011. **8**(1): p. 69-73.

25. Czaja, W.K., et al., *The future prospects of microbial cellulose in biomedical applications.* Biomacromolecules, 2007. **8**(1): p. 1-12.

26. Millon, L.E., G. Guhados, and W. Wan, *Anisotropic polyvinyl alcohol—Bacterial cellulose nanocomposite for biomedical applications.* Journal of Biomedical Materials Research Part B: Applied Biomaterials, 2008. **86B**(2): p. 444-452.

27. Correa, A., et al., *Cellulose nanofibers from curaua fibers.* Cellulose, 2010. **17**(6): p. 1183-1192.

28. George, J., et al., *Bacterial cellulose nanocrystals exhibiting high thermal stability and their polymer nanocomposites.* Int J Biol Macromol, 2011. **48**(1): p. 50-7.

29. Roman, M. and W.T. Winter, *Effect of sulfate groups from sulfuric acid hydrolysis on the thermal degradation behavior of bacterial cellulose.* Biomacromolecules, 2004. **5**(5): p. 1671-7.

30. Elazzouzi-Hafraoui, S., et al., *The shape and size distribution of crystalline nanoparticles prepared by acid hydrolysis of native cellulose.* Biomacromolecules, 2008. **9**(1): p. 57-65.

31. Liu, H., et al., *Fabrication and properties of transparent polymethylmethacrylate/cellulose nanocrystals composites.* Bioresource Technology, 2010. **101**(14): p. 5685-5692.

32. Wang, N., E. Ding, and R. Cheng, *Thermal degradation behaviors of spherical cellulose nanocrystals with sulfate groups.* Polymer, 2007. **48**(12): p. 3486-3493.

33. Sadeghifar, H., et al., *Production of cellulose nanocrystals using hydrobromic acid and click reactions on their surface.* Journal of Materials Science, 2011. **46**(22): p. 7344-7355.

34. Hubbe, M.A., et al., *Cellulosic nanocomposites: a review.* BioResources, 2008. **3**(3): p. 929-980.

35. Kamel, S., et al., *Pharmaceutical significance of cellulose: a review.* Express Polymer Letters, 2008. **2**(11): p. 258-277.

36. de Nooy, A.E.J., A.C. Besemer, and H. van Bekkum, *Highly selective nitroxyl radical-mediated oxidation of primary alcohol groups in water-soluble glucans.* Carbohydrate Research, 1995. **269**(1): p. 89-98.

37. Chang, P.S. and J.F. Robyt, *Oxidation of Primary Alcohol Groups of Naturally Occurring Polysaccharides with 2,2,6,6-Tetramethyl-1-Piperidine Oxoammonium Ion.* Journal of Carbohydrate Chemistry, 1996. **15**(7): p. 819-830.

38. Saito, T. and A. Isogai, *TEMPO-mediated oxidation of native cellulose. The effect of oxidation conditions on chemical and crystal structures of the water-insoluble fractions.* Biomacromolecules, 2004. **5**(5): p. 1983-9.

39. Saito, T., et al., *Cellulose nanofibers prepared by TEMPO-mediated oxidation of native cellulose.* Biomacromolecules, 2007. **8**(8): p. 2485-91.

40. Saito, T., et al., *TEMPO-mediated oxidation of native cellulose: Microscopic analysis of fibrous fractions in the oxidized products.* Carbohydrate Polymers, 2006. **65**(4): p. 435-440.

41. Saito, T., et al., *Distribution of carboxylate groups introduced into cotton linters by the TEMPO-mediated oxidation.* Carbohydrate Polymers, 2005. **61**(4): p. 414-419.

42. Spaic, M., *Functionalized bacterial cellulose for controlled release and delivery*, in *Biomedical Engineering*2011, University of Western Ontario: London. p. 1-95.

43. Kumar, V. and G.S. Deshpande, *Noncovalent immobilization of bovine serum albumin on oxidized cellulose.* Artif Cells Blood Substit Immobil Biotechnol, 2001. **29**(3): p. 203-12.

44. Kamada, H., et al., *Design of a pH-sensitive polymeric carrier for drug release and its application in cancer therapy.* Clin Cancer Res, 2004. **10**(7): p. 2545-50.

45. Barba, A., et al., *Synthesis and characterization of P(MMA-AA) copolymers for targeted oral drug delivery.* Polymer Bulletin, 2009. **62**(5): p. 679-688.

46. Dong, S. and M. Roman, *Fluorescently labeled cellulose nanocrystals for bioimaging applications.* J Am Chem Soc, 2007. **129**(45): p. 13810-1.

47. Porath, I. and N. Fornstedt, *Group fractionation of plasma proteins on dipolar ion exchangers.* Journal of Chromatography A, 1970. **51**(0): p. 479-489.

48. Hasani, M., et al., *Cationic surface functionalization of cellulose nanocrystals.* Soft Matter, 2008. **4**(11): p. 2238-2244.

49. Ho, T.T.T., et al., *Preparation and characterization of cationic nanofibrillated cellulose from etherification and high-shear disintegration processes.* Cellulose, 2011. **18**(6): p. 1391-1406.

50. Alince, B., J. Petlicki, and T.G.M. van de Ven, *Kinetics of colloidal particle deposition on pulp fibers 1. Deposition of clay on fibers of opposite charge.* Colloids and Surfaces, 1991. **59**(0): p. 265-277.

51. de la Orden, M.U., et al., *Novel polypropylene,Äìcellulose composites using polyethylenimine as coupling agent.* Composites Part A: Applied Science and Manufacturing, 2007. **38**(9): p. 2005-2012.

52. Wagberg, L., et al., *The Build-Up of Polyelectrolyte Multilayers of Microfibrillated Cellulose and Cationic Polyelectrolytes.* Langmuir, 2008. **24**(3): p. 784-795.

53. Abbott, A.P., et al., *Cationic functionalisation of cellulose using a choline based ionic liquid analogue.* Green Chemistry, 2006. **8**(9): p. 784-786.

54. Mahmoud, K.A., et al., *Effect of surface charge on the cellular uptake and cytotoxicity of fluorescent labeled cellulose nanocrystals.* ACS Appl Mater Interfaces, 2010. **2**(10): p. 2924-32.

55. Nielsen, L.J., et al., *Dual fluorescent labelling of cellulose nanocrystals for pH sensing.* Chem Commun (Camb), 2010. **46**(47): p. 8929-31.

56. Jackson, J.K., et al., *The use of nanocrystalline cellulose for the binding and controlled release of drugs.* Int J Nanomedicine, 2011. **6**: p. 321-30.

57. Ishikawa, M., et al., *Initial evaluation of a 290-microm diameter subcutaneous glucose sensor: glucose monitoring with a biocompatible, flexible-wire, enzyme-based amperometric microsensor in diabetic and nondiabetic humans.* J Diabetes Complications, 1998. **12**(6): p. 295-301.

58. Wagstaff, K.M. and D.A. Jans, *Nuclear drug delivery to target tumour cells.* Eur J Pharmacol, 2009. **625**(1-3): p. 174-80.

59. Murthy, K.K., et al., *Verification of setup errors in external beam radiation therapy using electronic portal imaging.* J Med Phys, 2008. **33**(2): p. 49-53.

60. Wu, J., et al., *Positioning errors and prostate motion during conformal prostate radiotherapy using on-line isocentre set-up verification and implanted prostate markers.* Radiother Oncol, 2001. **61**(2): p. 127-33.

61. Liu, Y., H. Miyoshi, and M. Nakamura, *Nanomedicine for drug delivery and imaging: a promising avenue for cancer therapy and diagnosis using targeted functional nanoparticles.* Int J Cancer, 2007. **120**(12): p. 2527-37.

62. Salata, O., *Applications of nanoparticles in biology and medicine.* J Nanobiotechnology, 2004. **2**(1): p. 3.

63. Wilchek, M. and E.A. Bayer, *The avidin-biotin complex in bioanalytical applications.* Anal Biochem, 1988. **171**(1): p. 1-32.

64. Cochrane, L., et al., *Avidin self-associates with boric acid gel suspensions: preparation of an affinity boron carrier that might be developed for boron-neutron capture therapy.* Polymers for Advanced Technologies, 2005. **16**(2-3): p. 123-126.

65. Langer, K., et al., *Preparation of avidin-labeled protein nanoparticles as carriers for biotinylated peptide nucleic acid.* European Journal of Pharmaceutics and Biopharmaceutics, 2000. **49**(3): p. 303-307.

66. Balthasar, S., et al., *Preparation and characterisation of antibody modified gelatin nanoparticles as drug carrier system for uptake in lymphocytes.* Biomaterials, 2005. **26**(15): p. 2723-2732.

67. Green, N.M., *Avidin. 3. The Nature of the Biotin-Binding Site.* Biochem J, 1963. **89**: p. 599-609.

68. Wilchek, M. and E.A. Bayer, *Introduction to avidin-biotin technology.* Methods Enzymol, 1990. **184**: p. 5-13.

69. Sakahara, H. and T. Saga, *Avidin-biotin system for delivery of diagnostic agents.* Adv Drug Deliv Rev, 1999. **37**(1-3): p. 89-101.

70. Green, N.M., *Avidin*, in *Advances in Protein Chemistry*, J.T.E. C.B. Anfinsen and M.R. Frederic, Editors. 1975, Academic Press. p. 85-133.

71. Green, N.M. and M.A. Joynson, *A preliminary crystallographic investigation of avidin.* Biochem J, 1970. **118**(1): p. 71-2.

72. Michael Green, N., *[5] Avidin and streptavidin*, in *Methods in Enzymology*, W. Meir and A.B. Edward, Editors. 1990, Academic Press. p. 51-67.

73. Yao, Z., et al., *Avidin targeting of intraperitoneal tumor xenografts.* J Natl Cancer Inst, 1998. **90**(1): p. 25-9.

74. Orelma, H., et al., *Generic method for attaching biomolecules via avidin-biotin complexes immobilized on films of regenerated and nanofibrillar cellulose.* Biomacromolecules, 2012. **13**(9): p. 2802-10.

75. Laitinen, O.H., et al., *Rational Design of an Active Avidin Monomer.* Journal of Biological Chemistry, 2003. **278**(6): p. 4010-4014.

76. Wu, S.-C. and S.-L. Wong, *Engineering Soluble Monomeric Streptavidin with Reversible Biotin Binding Capability.* Journal of Biological Chemistry, 2005. **280**(24): p. 23225-23231.

77. Aslan, F.M., et al., *Engineered single-chain dimeric streptavidins with an unexpected strong preference for biotin-4-fluorescein.* Proceedings of the National Academy of Sciences of the United States of America, 2005. **102**(24): p. 8507-8512.

78. Nordlund, H.R., et al., *Construction of a Dual Chain Pseudotetrameric Chicken Avidin by Combining Two Circularly Permuted Avidins.* Journal of Biological Chemistry, 2004. **279**(35): p. 36715-36719.

79. Riihimaki, T.A., et al., *Construction of chimeric dual-chain avidin by tandem fusion of the related avidins.* PLoS One, 2011. **6**(5): p. e20535.

80. Leppiniemi, J., et al., *Bifunctional avidin with covalently modifiable ligand binding site.* PLoS One, 2011. **6**(1): p. e16576.

81. Nordlund, H.R., et al., *Enhancing the Thermal Stability of Avidin: INTRODUCTION OF DISULFIDE BRIDGES BETWEEN SUBUNIT INTERFACES.* Journal of Biological Chemistry, 2003. **278**(4): p. 2479-2483.

82. Lesch, H.P., et al., *Avidin-biotin technology in targeted therapy.* Expert Opin Drug Deliv, 2010. **7**(5): p. 551-64.

83. Paganelli, G., et al., *Intraperitoneal radio-localization of tumors pre-targeted by biotinylated monoclonal antibodies.* Int J Cancer, 1990. **45**(6): p. 1184-9.

84. Kalofonos, H.P., et al., *Imaging of tumor in patients with indium-111-labeled biotin and streptavidin-conjugated antibodies: preliminary communication.* J Nucl Med, 1990. **31**(11): p. 1791-6.

85. Paganelli, G., et al., *Two-step tumour targetting in ovarian cancer patients using biotinylated monoclonal antibodies and radioactive streptavidin.* Eur J Nucl Med, 1992. **19**(5): p. 322-9.

86. Paganelli, G., et al., *Antibody-guided three-step therapy for high grade glioma with yttrium-90 biotin.* Eur J Nucl Med, 1999. **26**(4): p. 348-57.

87. Lehtolainen, P., et al., *Cloning and characterization of Scavidin, a fusion protein for the targeted delivery of biotinylated molecules.* J Biol Chem, 2002. **277**(10): p. 8545-50.

88. Smith, J.S., et al., *Redirected infection of directly biotinylated recombinant adenovirus vectors through cell surface receptors and antigens.* Proc Natl Acad Sci U S A, 1999. **96**(16): p. 8855-60.

89. Carpenter, D.S. and R.F. Minchin, *Targeting of a cholecystokinin-DNA complex to pancreatic cells in vitro and in vivo.* Gene Ther, 1998. **5**(6): p. 848-54.

90. Wong, C.M., K.H. Wong, and X.D. Chen, *Glucose oxidase: natural occurrence, function, properties and industrial applications.* Appl Microbiol Biotechnol, 2008. **78**(6): p. 927-38.

91. Husain, Q., *Beta galactosidases and their potential applications: a review.* Critical Reviews in Biotechnology, 2010. **30**(1): p. 41-62.

92. Burn, S.F., *Detection of beta-galactosidase activity: X-gal staining.* Methods Mol Biol, 2012. **886**: p. 241-50.

93. Prevey, P.S., *The use of Pearson VII distribution functions in X-ray diffraction residual stress measurement.* Advances in X-ray Analysis, 1986. **29**: p. 103-111.

94. Klug, H.P. and L.E. Alexander, *X-ray diffraction procedures: for polycrystalline and amorphous materials.* X-Ray Diffraction Procedures: For Polycrystalline and Amorphous Materials, 2nd Edition, by Harold P. Klug, Leroy E. Alexander, pp. 992. ISBN 0-471-49369-4. Wiley-VCH, May 1974., 1974. **1**.

95. Benedetti, A., et al., *X-ray diffraction methods to determine crystallinity and preferred orientation of lithium disilicate in Li-Zn-silicate glass-ceramic fibres.* Journal of Materials Science, 1983. **18**(4): p. 1039-1048.

96. Blotny, G., *A new, mild preparation of sulfonyl chlorides.* Tetrahedron Letters, 2003. **44**(7): p. 1499-1501.

97. Bergmeyer, H.U., Gawehn, K. and Grassl, M. , *Methods of Enzymatic Analysis (Bergmeyer, H.U. ed)* Academic Press Inc., New York, NY, 1974. **1**(2): p. 457-458.

98. Miller, J.H., *Experiments in molecular genetics*. Vol. 60. 1972: Cold Spring Harbor Laboratory Cold Spring Harbor, New York.

99. Surma-Slusarska, B., S. Presler, and D. Danielewicz, *Characteristics of bacterial cellulose obtained from Acetobacter xylinum culture for application in papermaking.* Fibres & Textiles in Eastern Europe, 2008. **16**(4): p. 108-111.

100. Fox, S.C., et al., *Regioselective esterification and etherification of cellulose: a review.* Biomacromolecules, 2011. **12**(6): p. 1956-72.

101. Po, H.N. and N.M. Senozan, *The Henderson-Hasselbalch Equation: Its History and Limitations.* Journal of Chemical Education, 2001. **78**(11): p. 1499.

102. De Smedt, S.C., J. Demeester, and W.E. Hennink, *Cationic polymer based gene delivery systems.* Pharm Res, 2000. **17**(2): p. 113-26.

103. Liesiene, J., *Synthesis of water-soluble cationic cellulose derivatives with tertiary amino groups.* Cellulose, 2010. **17**(1): p. 167-172.

104. Wada, M., T. Okano, and J. Sugiyama, *Synchrotron-radiated X-ray and neutron diffraction study of native cellulose.* Cellulose, 1997. **4**(3): p. 221-232.

105. Lee, K.-Y., et al., *Surface only modification of bacterial cellulose nanofibres with organic acids.* Cellulose, 2011. **18**(3): p. 595-605.

106. Lokhande, H.T. and A.S. Salvi, *Electrokinetic studies of cellulosic fibres I. Zeta potential of fibres dyed with reactive dyes.* Colloid and Polymer Science, 1976. **254**(11): p. 1030-1041.

107. Bellmann, C., et al., *Electrokinetic properties of natural fibres.* Colloids and Surfaces A: Physicochemical and Engineering Aspects, 2005. **267**(1,Äì3): p. 19-23.

108. Nkafamiya, I., et al., *Swelling behaviour of konkoli (maesopsis eminii) galactomannan hydrogels.* International Research Journal Plant Science, 2011. **2**(3): p. 078-086.

109. Saito, T., et al., *Homogeneous suspensions of individualized microfibrils from TEMPO-catalyzed oxidation of native cellulose.* Biomacromolecules, 2006. **7**(6): p. 1687-91.

110. Okita, Y., T. Saito, and A. Isogai, *Entire surface oxidation of various cellulose microfibrils by TEMPO-mediated oxidation.* Biomacromolecules, 2010. **11**(6): p. 1696-700.

6.2 Curriculum Vitae
Justin R. Cook

EDUCATION

2011-2013 **Accelerated Masters of Engineering Science** (*Candidate*)
Department of Biomedical Engineering
The University of Western Ontario, London, Ontario, Canada
Supervisor: Dr. Wankei Wan
Thesis: "Cationic Functionalization of Bacterial Cellulose for Targeted Drug Delivery Applications"

2008-2012 **Bachelors of Engineering Science**
Department of Chemical Engineering
The University of Western Ontario, London, Ontario, Canada

POSITIONS

2013 (January-April) **Teaching Assistant**
Department of Biomedical Engineering
The University of Western Ontario, London, Ontario, Canada
Supervisor: Dr. Amin Rizkalla
Course: BME 9525B Advanced Biomaterials Engineering

2012 (September-December) **Teaching Assistant**
Department of Chemical Engineering
The University of Western Ontario, London, Ontario, Canada
Supervisor: Dr. Wankei Wan
Course: CBE 4497 Polymer Engineering

2012-2013 **Teaching Assistant**
Department of Engineering/Ivey School of Business
The University of Western Ontario, London, Ontario, Canada
Supervisor: Dr. David House
Course: BUS 2299E Business for Engineers

HONOURS & AWARDS

2012-2013 **The Canadian Institute of Health Research (CIHR) Strategic Training Program Award**
Prestigious award given to a student who displays exceptional leadership qualities while exhibiting extraordinary work ethic. Exhibits remarkable researching techniques and proficient in applying technical theories towards industrial applications
The University of Western Ontario
National

2012-2013 **Western Graduate Research Scholarship (WGRS)**
Awarded to students who attained an overall average of at least 80% throughout their undergraduate degree while displaying exceptional management and research techniques
The University of Western Ontario
Institutional

2012 **Forth Year Thesis Award Winner**
Awarded 3rd place for a comprehensive presentation regarding the innovated techniques used in researching and developing steps in creating a targeted drug delivery system using a natural biocompatible polymer
The University of Western Ontario
Institutional

2011 & 2012 **Natural Sciences and Engineering Research Council of Canada (NSERC) Undergraduate Student Research Awards Program (USRA) Industrial Scholarship**
Competitive award given to a student completing an engineering degree at an accredited university, who attained a cumulative average of at least 80% while demonstrating exceptional leadership qualities
The University of Western Ontario
National

2010-2012 **Western Engineering Dean's Honour List**
Awarded to a student who attained an overall average greater than 80% in a selected year
The University of Western Ontario
Institutional

PUBLICATIONS, PRESENTATIONS & ABSTRACTS

Publications in Progress (2)

1. **Justin R. Cook**, Darcy P. Small, Wankei Wan. "Cationic Functionalized Bacterial Cellulose for Targeted Delivery Applications". *Materials Letters*

2. Marko Spaic, Darcy P. Small, **Justin R. Cook**, Wankei Wan. "Characterization of Anionic and Cationic Functionalized Bacterial Cellulose Nanofibres for Controlled Release Applications". *Cellulose*

Publications in Preparation (2)

1. **Justin R. Cook**, Darcy P. Small, Marko Spaic, Xinsheng Li, Wankei Wan. "Characterization of Bacterial Cellulose Nanofibers Prepared by Acid Hydrolysis". *Cellulose*

2. Marko Spaic, Darcy P. Small, **Justin R. Cook**, Wankei Wan. "Synthesis and Characterization of a Bacterial Cellulose-Gold Nanoparticle Bound Nucleic Acid Delivery System". *Cellulose*

Oral Presentations *Presenter (4)

1. **Justin R. Cook**, Darcy P. Small*, Marko Spaic, Wankei Wan. "Nano-Crystalline Cellulose for Protein and Nucleic Acid Delivery". World Biomaterials Congress, Chengdu, Sichuan, China (06/12)

2. **Justin R. Cook***, Wankei Wan. "Use of Bacterial Cellulose for Targeted Delivery of Therapeutic Proteins". Forth Year Thesis Project, The University of Western Ontario, London, Ontario, Canada (03/12)

3. **Justin R. Cook***, Darcy P. Small, Wankei Wan. "Use of Bacterial Cellulose for Targeted Delivery of Therapeutic Proteins". Canadian Society for Chemical Engineering Conference, London, Ontario, Canada (10/11)

4. Darcy P. Small*, Marko Spaic, **Justin R. Cook**, Wankei Wan. "Bacterial Cellulose Surface Functionalization for Targeted Drug Delivery". Canadian Biomaterials Society Conference, Vancouver, British Columbia, Canada (06/11)

Poster Presentations *Presenter (4)

1. **Justin R. Cook***, Darcy P. Small, Wankei Wan. "Bacterial Cellulose as a Targeted Delivery System for Therapeutic Proteins" London Health and Research Day Conference, London, Ontario, Canada (03/13)

2. **Justin R. Cook***, Darcy P. Small, Marko Spaic, Wankei Wan. "Nano-Crystalline Cellulose for the Delivery of Therapeutic Proteins and Nucleic Acids" Diabetes Research Day Conference, London, Ontario, Canada (11/12)

3. **Justin R. Cook***, Darcy P. Small, Marko Spaic, Wankei Wan. "Gold Nanoparticle Studded Nano-Crystalline Cellulose for Drug Delivery" World Biomaterials Congress, Chengdu, Sichuan, China (06/12)

4. **Justin R. Cook***, Darcy P. Small, Marko Spaic, Wankei Wan. "Use of Bacterial Cellulose for Targeted Delivery of Therapeutic Proteins" London Health and Research Day Conference, London, Ontario, Canada (03/12)

RESEARCH SUPERVISION

Undergraduate and other Summer and Rotation Student Projects

2012 (May-December)	**Graduate Student Supervisor** Chemical Engineering Masters Student: Roddick Shi, 1st year Masters of Chemical Engineering, UWO *Project:* 'Hydrolysis of Bacterial Cellulose'
2011-2012 (October-March)	**Graduate Student Supervisor** Chemical Engineering Student: Olsi Hoxha, 4th year Chemical Engineering, UWO *Various Projects:* Hydrolysis of Bacterial Cellulose, Functionalization of Bacterial Cellulose
2011-2012 (September-January)	**Graduate Student Supervisor** High School Student: Clare Xu, Grade 12, Mother Teresa Catholic Secondary School *Various Projects:* Monitoring and Preparation of Bacterial Cellulose Production

COMMITTEES AND PROFESSIONAL ACTIVITIES

2012-2013 **Professional Development** **CIHR Strategic Training Program**
The University of Western Ontario, London, Ontario, Canada

- Participated in bi-weekly seminars on current issues in the biomedical engineering field